Evapotranspiration Effects on Air Flowing over Grass in a Small Glass Roofed Tunnel

Dimitra Westdyk

Thesis presented in fulfilment of the requirements for the degree of Master of Science in Mechanical and Mechatronic Engineering at the University of Stellenbosch, South Africa

Thesis supervisor: Prof. D.G. Kröger

March 2007

DECLARATION

I, Dimitra Westdyk, the undersigned, hereby declare that the work contained in this thesis is my own original work and has not previously, in its entirety or in part, been submitted for a degree.

.....1.....day of March 2007

ABSTRACT

The search for ways of utilizing solar energy for power generation in the arid areas of the world has led to the investigation of the feasibility of erecting a "solar chimney" power plant for generating electricity. There is the added possibility of combining this power generation with agricultural activities underneath the outer rim of the glass collector. In order to investigate the influence of evapotranspiration on the properties of air flowing over vegetation growing under glass, an experimental solar tunnel was built. Air was drawn over the grass surface growing in the glass roofed tunnel and the situation was investigated experimentally and analytically. The primary purpose of the study was to measure the average rate of evapotranspiration taking place, to measure the change in dry- and wetbulb temperatures of the air and hence determine the magnitude and direction of the change in air density occurring under various air inlet and weather conditions. This is necessary since the power output of the turbine in a solar chimney power plant is dependent on the volume flow rate of air through it, which is in turn dependent on the density of the air. The second was to determine a value for the effective convective heat transfer coefficient between the grass and the air flowing over it. The third was to use the inlet air state and then apply the Penman-Monteith and the conservation equations to subsequent one meter lengths of the tunnel in order to predict the exit state of the air as well as the variation in the grass temperature along the tunnel. It was found that the maximum average rate of evapotranspiration from the grass occurs at the solar noon on a cloudless, windless summer day and is about 0.76 kg/m^{2}h at the experimental site. The grass temperature increases along the tunnel length and is usually a few degrees higher than the air drybulb temperature under most test conditions. The effective convective heat transfer coefficient was found to be between 30 W/m^{2}K and 40 W/m^{2}K for an air velocity ranging from approximately 1.5 m/s to 2.5 m/s Tests show that for typical high summer temperatures (above 35 °C) the outlet drybulb temperature of the air is largely governed by the relative humidity at the inlet: the outlet drybulb temperature being lower than the inlet drybulb temperature for a relative humidity below about 40 % and for higher values of relative humidity, the drybulb temperature at the outlet is slightly higher by between 0 °C and about 3 °C. Since there is a simultaneous increase in the wetbulb temperature due to evapotranspiration, the density of the air may decrease slightly or increase slightly or remain the same. Latent heat transfer accounts for between 80 % and 90 % of the total heat transfer between the grass and the air. Predicted values of average rate of evapotranspiration, average grass temperature and the exit state of the air were in good agreement with experimentally measured values and hence validate the use of this mathematical model. In the application to the solar chimney power plant analysis in another project [07 PR 1] it was found that the annual output of the power plant would experience a reduction of approximately 30 % for a circular glass collector of 5000 m diameter with vegetation planted radially 1000 m inward from the perimeter.

Keywords: Evapotranspiration, solar chimney power plant

OPSOMMING

Die soeke na metodes om son energie te benut in die droë dele van die wêreld het gelei tot die ondersoek na die uitvoerbaarheid om 'n sontoring kragstasie op te rig. Daar bestaan die moontlikheid om kragopwekking te kombineer met die bedryf van landbou onder die buitenste dele van die glas kollektor van die sontoring. Ten einde die invloed van evapotranspirasie op die eienskappe van lug wat oor plantegroei vloei te ondersoek, is 'n eksperimentele glasdak tonnel gebou. Lug is oor die gras oppervlakte wat in die tonnel geplant is, getrek en die opset is eksperimenteel en analities ondersoek. Die hoofdoel van die ondersoek was om onder verskillende inlaat- en weerstoestande die tempo van evapotranspirasie te meet, die verandering in droëbol en natbol temperatuur te meet en daarvolgens die verandering in die lugdigtheid te bepaal. Die krag uitset van die sontoring turbien is afhanklik van die lug vloeitempo daardeur en dit word bepaal deur die lugdigtheid. Die tweede doelwit was om die waarde van die effektiewe konvektiewe warmteoordrag koëffisiënt tussen die gras en die lug te bepaal. Die derde doelwit was om die Penman-Monteith vergelyking tesame met die energie en massa behoud vergelykings op agtereenvolgende een meter lengtes van die tonnel toe te pas om sodoende die uitlaat toestand van die lug sowel as die verandering in gemiddelde gras temperatuur te voorspel. Daar is gevind dat die maksimum gemiddelde tempo van evapotranspirasie plaasvind wanneer die son op sy hoogste is op 'n windstil, wolklose somersdag en die waarde daarvan is naastenby 0.76 kg/m^{2}u vir die bepaalde toetsomgewing. Die gras temperatuur neem al langs die tonnel toe en is gewoonlik 'n paar grade hoër as die lug temperatuur onder die meeste toets toestande. Verder is daar gevind dat die waarde van die effektiewe warmteoordrag koëffisiënt tussen die gras en die lug vir 'n lugvloei snelheid van 1.5 m/s tot 2.5 m/s tussen omtrent 30 W/m^{2}K en 40 W/m^{2}K gelê het. Toetsresultate toon dat vir tipiese hoë somer temperature (bokant 35 °C) die uitlaat droëbol temperatuur deur die relatiewe vogtigheid van die lug by die inlaat bepaal word: die droëbol temperatuur by die uitlaat is laer as by die inlaat vir 'n relatiewe vogtigheid laer as 40 % en vir hoër waardes van relatiewe vogtigheid sal die uitlaat droëbol temperatuur effens toeneem of dieselfde bly. Aangesien die natbol temperatuur toeneem a.g.v. evapotranspirasie sal die lugdigtheid of effens afneem, of dieselfde bly of effens toeneem. Latent warmte oordrag is verantwoordelik vir tussen 80 % en 90 % van die totale warmte oordrag tussen die gras en die lug. Deur gemete en voorspelde waardes met mekaar te vergelyk word afgelei dat die wiskundige model die uitlaat toestand van die lug, die gemiddelde gras temperatuur en die gemiddelde tempo van evapotranspirasie binne eksperimentele limiete, voorspel. Wanneer hierdie model toegepas word in 'n ander projek [07 PR 1] op die sontoring kragstasie analise word gevind dat die netto jaarlikse kraguitset met 30 % verminder in die geval van 'n 5000 m diameter glas kollektor wat 'n afstand van 1000 m radiaal binnetoe vanaf die buiterand van die kollektor beplant word.

Sleutel woorde: Evapotranspirasie, Sontoring kragstasie

In memory of my father
Kembla Augustus Hilton Jennings,
a great engineer, who never had the opportunity of studying at a university

"We shall not cease from exploration,
and the end of all our exploring will be
to arrive where we started and know
the place for the first time" T.S. Elliot

ACKNOWLEDGEMENTS

I would like to acknowledge the valued contributions and support of the following persons:

Prof. DG Kröger for his insight, encouragement and support especially during times of despair when the grass would die at just the wrong time and yet another year was lost waiting for the grass to grow.

My long-suffering husband, Jan Westdyk who spent many hours in blazing sun watering grass, cutting grass and carrying and cleaning sheets of glass for the solar tunnel.

Mr. Cobus Zietsman, without whose technical knowledge, insight and support, the solar tunnel could not have been built and maintained. Keeping the grass alive during hot dry holidays was especially challenging. All the electronics and data collecting were possible due to Mr Zietsman's ever ready willingness and knowledge to solve the many crises that arose.

I am indebted to Mr Peter Prior for doing all the drawings for this thesis in Mechanical Desktop for me.

All my friends for their constant encouragement and confidence in my ability to complete the project despite many setbacks.

Above all, the Lord Jesus Christ for His grace in revealing His Truth, showing me the Way, giving me Life which is truly life and the ability to investigate the marvellous workings of a small portion of His intricate creation and in addition giving patience, endurance and inspiration when much needed.

TABLE OF CONTENTS

LIST OF TABLES

LIST OF FIGURES

NOMENCLATURE

Symbols

A	area, m^2
C	coefficient
C_f	surface friction coefficient
c_p	specific heat, J/kgK
d_e	hydraulic diameter, m
D	diffusion coefficient, m^2/s
EOT	equation of time, minutes
E_o	reference total evaporation, mm
E_m	minimal total evaporation, mm
E_{vm}	basal plant evaporation, mm
e	emissivity
f	Fanning friction factor defined by $\tau_w /(\rho V^2 / 2)$
f_D	Darcy friction factor defined by $4\tau_w /(\rho V^2 / 2)$
g	gravitational acceleration, m/s^2
H_C	height of canopy or roof, m
h_c	convective heat transfer coefficient, $W/m^2 K$
h_D	mass transfer coefficient, m/s
h_d	mass transfer coefficient , $kg/m^2 s$
H_L	height of foliage, m
H	height, m
I_{on}	extraterrestrial radiation, W/m^2
I_{sc}	solar constant, W/m^2
I_{sol}	solar irradiance measured on a horizontal plane, W/m^2
I_{hor}	theoretical solar irradiance on a horizontal plane, W/m^2
I_{net}	net radiation absorbed by surface, W/m^2
i	enthalpy, J/kg
K_H	diffusion coefficient for turbulent heat transfer in air
K_M	diffusion coefficient for turbulent momentum transfer in air
K_W	diffusion coefficient for turbulent water vapor transfer in air
k	thermal conductivity, W/m K or constant for solar radiation
k_m	crop coefficient
k_{vm}	basal crop coefficient
L	length, m, or longitude
m	mass flow rate, kg/s
M	thermal capacity, J/ K or molar mass, kg/kmol
n	refractive index
p	pressure, Pa
q	heat flux, W/m^2 or specific humidity, mass vapor per kg moist air
r	resistance, s/m
r_a	canopy aerodynamic resistance, s/m
r_s	bulk stomatal canopy resistance, s/m
R_u	universal gas constant, 8.314 J/mole K
T	temperature, °C, or K
v	specific volume, m^3/kg
V	velocity, m/s
w	humidity ratio, or mass vapor per kg dry air

W	width, m
Y	approach velocity factor

Greek letters

α	thermal diffusivity, $k/\rho c_p$, m^2/s, or absorptivity of glazing
α_{gb}	absorptivity of grass for beam radiation
α_{gd}	absorptivity of grass for diffuse radiation
α_λ	absorption coefficient for short wave radiation
α_s	solar altitude angle, degrees
γ	psychrometric "constant" for heat transfer only, $\rho c_{pma} / 0.622 i_{fg}$, Pa/K
γ^*	adjusted psychrometric "constant" for heat and mass transfer defined by $\gamma\, r_V / r_H$, Pa/K
Δ	differential, or slope of the saturation vapor curve, Pa/K
δ	boundary layer thickness, m or declination
ε	surface roughness
θ	angle of incidence, degrees
θ_z	zenith angle, degrees
λ	albedo
μ	dynamic viscosity, kg/ms
ν	kinematic viscosity, m^2/s,
ρ	density, kg/m^3, reflectivity
σ	Stefan-Boltzman constant, 5.669×10^{-8} $W/m^2\ K^4$
τ	shear stress, N/m^2 , or transmissivity for solar radiation
τ_{eff}	effective transmissivity for solar radiation
ϕ_g	gas expansion factor
ϕ_l	local meridian
ϕ_m	standard meridian
χ	vapor density, mass of water vapor per unit volume
ψ	hours after midnight
ω	hour angle, degrees

Dimensionless Groups

Gr	Grashof number, $g\ \rho^2\ L^3\ \beta\ \Delta T/\mu^2$, for a plate
Le	Lewis number, $k/(\rho c_p D)$, or Sc/Pr
Nu	Nusselt number, hL/k for a plate, or hd/k for a tube
Pr	Prandtl number, $\mu c_p/k$
Re	Reynolds number, $\rho VL/\mu$ for a plate, or $\rho Vd/\mu$ for a tube
Sc	Schmidt number, $\mu/(\rho D)$
Sh	Sherwood number, $h_D L/D$ for a plate, or $h_D d/D$ for a tube
St	Stanton number, $h/\rho c_p V$

Subscripts

a	dry air, or absorptive
b	beam or bottom
c	convective
d	diffuse
db	drybulb
F	fluid i.e. air flowing through tunnel
fc	forced convection
fg	liquid-vapor
g	grass, or saturated vapor
H	pertaining to heat transfer
ir	infra-red or longwave radiation
i	inlet
k	conductive
ma	moist air
n	normal, or nozzle
nc	natural convection
o	extraterrestrial radiation, or outlet
on	extraterrestrial radiation on a plane normal to the radiation
R	roof
s	soil, or saturated
S	sky
T	total
tr	transition
tus	tunnel upstream
u	upstream
V	pertaining to vapor transfer
v	vapor
w	liquid water
wb	wetbulb

Abbreviations

ADP	Adenine Phosphate
AED	atmospheric evaporative demand
ave	average
CV	control volume
DOY	day of year
db	drybulb (temperature)
del	delta
eff	effective
EOT	equation of time, minutes
EP	enthalpy potential
ir	infrared radiation
FAD	foliage area density
LAI	leaf area index
LH	latent heat
RH	relative humidity
sat	saturated
SH	sensible heat
TH	total heat
vpd	vapor pressure depression
wb	wetbulb (temperature)

CHAPTER 1
INTRODUCTION

1.0 INTRODUCTION

This thesis forms part of a greater preliminary investigation into the possibility of erecting a solar chimney power plant in the arid areas of the world. The solar chimney consists of a large circular shaped glass collector, about 7 km in diameter, which is horizontally placed about 10 m above the ground. In the centre is a vertical chimney, 1000 to 1500 m high and with a diameter of about 200 m at the base of which are one or more turbines connected to an electrical generator. The air, which is heated by solar energy under the collector flows through the turbine(s) to rise through the chimney. The solar chimney concept of converting solar energy, a renewable and sustainable source, into electrical energy has given rise to several unique questions. For example the viability of agricultural activities under the outer section of the glass solar collector is being considered. The inclusion of agricultural activities will provide employment for the local community, possibly give rise to secondary industries, and thus also attract investors. The output of a turbine is amongst other parameters dependent on the volume flow rate of the air through it. The volume flow rate in turn is determined by the density of the air. The interaction between the air and the vegetation and subsequent change in state of the air is investigated in this thesis. The influence of evapotranspiration and convective heat transfer of the plants to the air must be established in order to predict the effect of the vegetation on the power output of the solar chimney.

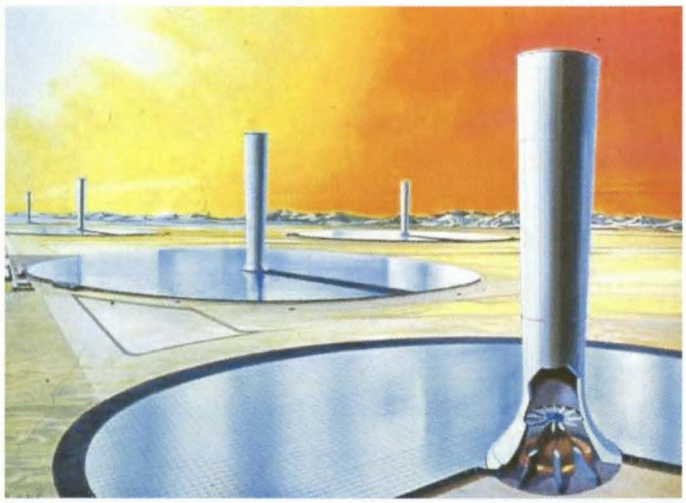

Figure 1-1: Artist's impression of several solar chimney power plants

The interaction between vegetation and atmospheric air has already been investigated. Firstly, by agriculturists from the perspective of the influence of environmental conditions on plants since vegetation is "a slave to the environment" [75MO1]. This is mainly for establishing irrigation requirements since "Atmospheric conditions create a demand for water from soil and vegetative surfaces. This demand, modified by existing surface conditions, finally determines the actual rate of water vapor exchange between the given surface and the atmosphere. This, in turn, represents the water used by the crop." [89DJ1]. Secondly, botanists are interested in the reaction of the plants to adverse atmospheric conditions. Thirdly, civil

engineers need to be able to assess water balances for near surface soil strata, landfills, tailings dams and waste dumps or for the disposal of liquid wastes on land.

In this thesis, however, the concern is vice versa, being the effect of vegetation on a fixed mass of air flowing over it. The focus is on the air itself and not the evaporating surface as such. The influence of vegetation on the properties of air has not been of primary importance and therefore very little information of relevance is available in the literature.

Data from evaporation pans are often used as the basis for assessing evaporation or evapotranspiration but the rates of evaporation from bare and vegetated soil are not the same as pan evaporation rates and empirical correction factors are often used to estimate evaporation. These empirical factors are often site-related and therefore not universally applicable. The methods for measuring evapotranspiration are usually similar to those undertaken for example by Blight [02BL1] whereby "three containers were weighed daily and the mass loss (in mm of water) has been plotted against elapsed time". The other method commonly used is the lysimeter method where water balances are used to measure evapotranspiration.

When the surface temperature is known various expressions have been established to try to predict the evaporation or evapotranspiration rate. However, as is evident in the literature [04TA1], "significant discrepancies existed between these expressions and their agreements for the prediction of water evaporation were poor". The expressions are empirical and subject to the climatic conditions under which they were derived. In the study by Tang [04TA1] it was shown that the evaporation rates from a wetted cloth surface and a free water surface differ from each other. Furthermore, the evaporation rates are not a simple and direct proportional function of the difference between the saturated vapor pressure at the surface temperature and the vapor pressure of the air with which it is in contact, but a power function of the difference. In the experimental work done by Tang the exponent was found to be 0.82 for a free water surface and 0.7 for evaporation from a wetted towel surface. The velocity of the air plays an important role too since the evaporation at very low velocities for the wetted surface was found to be greater than for the free surface, but vice versa for higher wind velocities.

The formulation of the basic equations used to represent evaporative fluxes from vegetation is difficult since the processes and mechanisms controlling transpiration are complicated, involving the interaction of abiotic factors with biotic factors; abiotic factors being the thermophysical properties of the air and soil, the radiation environment and the leaf boundary layer dynamics and biotic factors being the diffusion of water across root membranes, transport in the liquid phase through the conductive tissue, and the biochemical signals controlling the opening and closing of the stomata. Simplifying assumptions are required in order to represent this system numerically, and much of the variation between schemes is the result of different simplifications.

Evaporation of water requires relatively large amounts of energy. The evapotranspiration process is therefore governed by the energy exchange at the vegetation surface and limited by the amount of energy available. This limitation allows for a prediction of the rate of evapotranspiration given a net balance of energy fluxes.

In 1948 Penman [48PE1] developed the first of several equations in which the energy and transport equations are combined for estimating evaporation rates from climatic data alone and not from the equilibrium surface temperature. The equilibrium surface temperature (of the vegetation or any air-water interface) and the rate of evapotranspiration are determined by the net energy exchange at the surface. The

heat and mass transfers are a function of the following; the state and properties of the air flowing over the surface, the radiant, convective and conductive heat fluxes and the resistances to the transfer of both heat and water vapor at the air-water interface. An equation can be derived relating all of the above thereby eliminating the need for measurement of the surface temperature.

Several improvements to the original Penman equation were made, notably by Monteith [90MO1], who introduced terms for canopy surface resistance to account for the effects of the vegetation. These culminated in the FAO Penman-Monteith equation [FAO is the United Nations Food and Agricultural Organization].

The Penman-Monteith equation was applied by Pruitt and Doorenbos [77PR1] to develop a method of predicting reference crop evapotranspiration. Detailed procedures were presented for estimating a reference evapotranspiration rate which was defined as "the rate of evapotranspiration from an extensive surface of 8 - 15 cm tall green grass cover of uniform height, actively growing, completely shading the ground, and not short of water". Crop coefficients are then used together with values of reference evapotranspiration to estimate water use of a crop. Crop coefficients are empirical ratios of crop evapotranspiration to reference evapotranspiration and are derived from experimental data [81WR 1].

In 1986 Allen [86AL1] reviewed ten forms of the Penman evapotranspiration equation and compared with lysimeter estimates at three locations. Problems were encountered however, mainly since a "living" reference crop is difficult to reproduce over a range of locations [94AL1]. In May 1990, the FAO decided to change the concept of reference evapotranspiration and to revise calculation procedures. A hypothetical reference crop, which is described by an appropriate Penman-Monteith equation has been substituted for a living reference crop as described by Allen, Smith et al. [94 AL 1]. The evapotranspiration rate of this hypothetical canopy is referred to as the "Grass reference evapotranspiration" and together with the appropriate crop coefficients is currently applied for estimating crop water use.

The situation under the glass of the solar collector of the solar chimney is different from those normally investigated under atmospheric conditions in that firstly only the air at the inlet to the collector is at the ambient state and as the air flows inward under the glass and over the grass the effects of the mass and energy transfers and a varying velocity require a different model. Secondly, the vegetation is not directly exposed to the atmosphere but is growing under glass. The effect of the glass on the radiation and convective heat transfer needs to be taken into account.

CHAPTER 2

THE STUDY OBJECTIVE

The objective of this investigation is firstly to quantitatively establish the effect of an actively growing grass surface on the properties of atmospheric air flowing over it in a glass roofed tunnel subject to radiation and convection. This involves determining the change in state of the air and the rate of evapotranspiration of this grass surface. The grass surface is to be as close to the reference surface as defined by Doorenbos and Pruitt (1977) [89DJ1], i.e. "and extended surface of an 80 mm to 150 mm tall grass cover of uniform height actively growing, completely shading the ground and not deficient in water or nutrients".

The second objective is to obtain an expression for the effective convective heat transfer coefficient between the grass and the air flowing over it.

The third objective is to predict the following: the change in state of the air as it flows over the grass, the change in temperature of the grass along the tunnel and the average rate of evapotranspiration. This is achieved by applying the Penman-Monteith and conservation equations to subsequent one meter lengths of the tunnel. The predicted values are then compared with the measured values in order to test the applicability of the Penman-Monteith equation to this particular situation and therefore to the solar chimney in general (taking into account the difference in boundary layer profile in the much larger solar chimney).

In order to achieve this objective the following goals were set viz.

a. A literature study of biophysical plant physiology, psychrometrics, heat and mass transfer, solar radiation and viscous fluid flow as applicable to this specific set-up.

b. Designing and building an experimental set-up together with the instrumentation and the software necessary to determine relevant values using clipped grass as the representative plant.

c. Accumulating and using data in order to determine the effective convective heat transfer coefficient, to calculate the actual average rate of evapotranspiration and to establish trends or patterns.

d. Applying the Penman-Monteith and conservations equations, to predict both the leaving air state and the average rate of evapotranspiration and comparing with measured values.

The study objective is to obtain dependable experimental values in order to find parameters that can describe the heat and mass transfer for general cases and different crops, velocities, geographical positions, etc.

CHAPTER 3

APPARATUS AND EXPERIMENTAL SET-UP

3.0 INTRODUCTION

The usual method employed by micrometeorologists to determine the evapotranspiration of vegetation growing in soil is the lysimeter method. In this method water balances are determined for an isolated portion of grass, for example, in an extended grass field, and this gives an indication of the water evaporated by both the grass and the soil over that period. In this thesis the change in the humidity ratio and the mass flow rate of the air flowing over the vegetated surface is measured and the rate of evapotranspiration subsequently calculated.

3.1 APPARATUS AND EXPERIMENTAL SET-UP

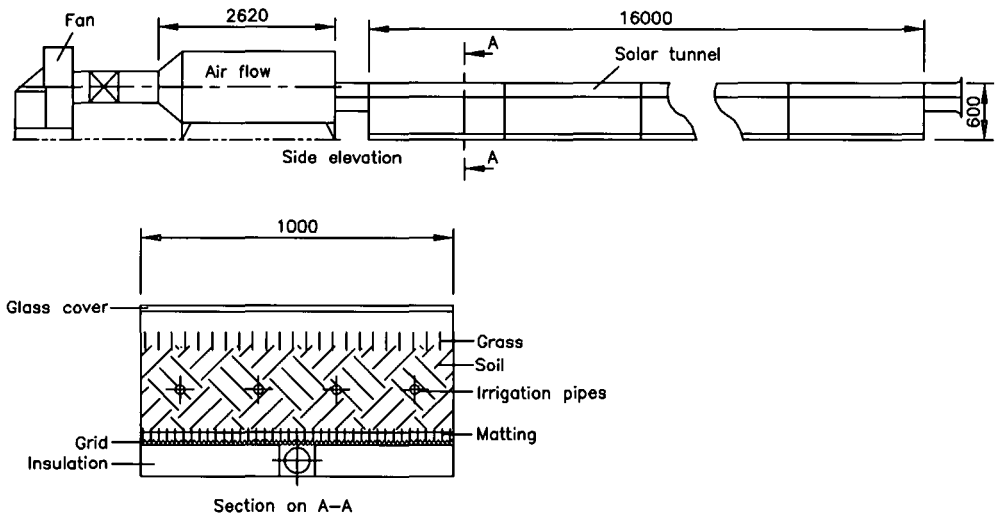

Figure 3.1: The experimental tunnel

Figure 3.1 shows a schematic of the experimental solar tunnel constructed in the Solar Energy Laboratory at the University of Stellenbosch, South Africa, located about 100 m above sea level, latitude 33.98 °S and longitude 18.85 °E. The rectangular shaped tunnel was constructed by bolting 2 m long U-shaped fibreglass sections together to a total length of 16 m. The roof was formed by covering these sections with sixteen 1 m × 1 m sheets of 4 mm green-of-edge bevelled edge glass to form an airtight tunnel. The overall dimensions of the tunnel are: 16 m long by 1 m wide and 600 mm high. The through-flow width and that of the grass is 1 m. All surfaces, except the glass roof, are thermally insulated from the environment on the outside with sheets of polystyrene 75 mm thick glued to the fibreglass. The polystyrene is protected from external damage, including wetting, by thin metal sheeting which has been painted white to reduce heat absorption by radiation.

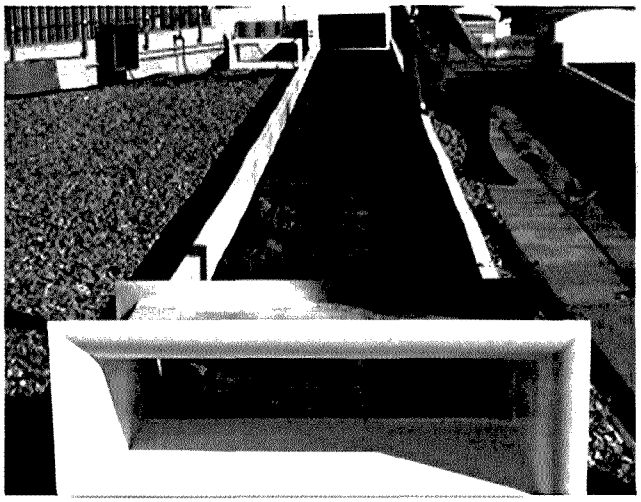

Figure 3.2 Photograph of tunnel under construction showing irrigation and drainage systems

Figure 3-2 shows the bottom of the fibreglass channel in which is a central drainage channel; a mesh layer is placed on top of the channel and on top of this nylon matting to ensure that during drainage no soil is lost. Soil to a depth of 300 mm is placed on top of the nylon matting. A dropwise point irrigation system is installed about 100 mm below the soil surface and Kikuyu grass established on top of the soil. The grass is irrigated by an automatic timing system; the duration and intervals between wetting can be set as needed. The glass "roof" is about 150 mm above the grass surface.

The inlet to the tunnel itself is aerodynamically shaped and air is drawn through the tunnel by means of a centrifugal fan placed at the outlet of the tunnel. The mass flow rate of the air through the tunnel may be varied using the bypass section of the fan. Before the inlet to the tunnel, a box-frame covered in shade cloth is placed ensuring a more even inlet airflow and therefore a more even temperature distribution.

Between the fan and the tunnel is a mixing and measuring box made of wood and which is also thermally insulated on the outside.

The air discharged from the tunnel has velocity, temperature and humidity gradients. The air therefore needs to be mixed to ensure that average values of the above quantities are measured. The mixers are a series of vanes which divide the flow into smaller streams and then diverts and deflects the streams across each other.

After going through the mixers the air is forced to flow through a venturi section in which four thermocouples are installed; two for measuring the drybulb temperature and two for measuring the wetbulb temperature. Downstream are three elliptically shaped nozzles of differing size for measuring the air mass flow rate. The nozzles are chosen, installed and used according to ASHRAE standards 33-78. On either side of the nozzles straighteners are installed as specified – these straighteners consist of perforated steel plating and ensure that the fan does not distort the air flow through the nozzles. The moist exit air is vented far from the inlet to the tunnel ensuring no possibility of short circuiting the supply air.

3.2 INSTRUMENTATION

Wet- and drybulb air temperatures are measured using copper-constantan type T thermocouples. The wetbulb temperature is attained by covering the end of the thermocouple with a cotton wick which draws water from a supply pipe. Only distilled water is to be used so that algae growth and subsequent incorrect readings are prevented. All the thermocouples are shielded to prevent any radiation effects.

Figure 3.3. Photograph showing thermocouple attached to glass roof above grass surface

The inlet dry- and wetbulb thermocouples (six in all - three for measuring the drybulb temperature and three for measuring the wetbulb temperature) are placed within the inlet section in such a way that radiation effects are eliminated.

Two shielded and insulated thermocouples for measuring the glass temperature are placed on top of the glass, at either end of the tunnel in order to establish a mean glass temperature.

The grass temperature is measured using a thin thermocouple wire placed within the grass structure ensuring that convective and radiant heat transfer effects are eliminated without affecting the transpiration process.

The soil temperature is measured at two depths, namely 20 mm and 50 mm below the grass level using thermocouples placed about midway downstream of the inlet to the tunnel.

Four thermocouples (two for drybulb and two for wetbulb temperature measurements) are placed in the airstream in a narrowed section of the mixing and measuring box; the airflow is thoroughly mixed to obtain the average wet- and drybulb temperatures.

The solar radiation above the glass is measured using a Kipp & Zonen pyranometer.

The static pressure drop over the grass surface from inlet to the exit of the tunnel is measured using measuring points and a pressure transducer. The holes for the pressure points are drilled from the inside outwards ensuring that no burrs or unevenness on the inside of the tunnel can adversely affect the reading of the static

pressure at those points. Sometimes, however it was not observed that the holes were blocked by grass seeds or dust. This only came to light after the data was being used for calculations. The pressure drop measurements are therefore not always reliable. Pressure loss measurements were taken specifically a few months later in order to determine the drop in pressure for a recently clipped grass surface. The effective convective heat transfer coefficient was based on these measurements.

Finally the pressure drop over the nozzles in the mixing box is measured using a pressure transducer in order to calculate the air mass flow rate.

The output of the twenty sensors are linked to a datalogger and a computer program "IMPVIEW" which converts the input voltage to temperature, pressure or radiation – whichever is applicable. The datalogger is capable of logging continuously as well as showing data and saving it at specified intervals. Graphs are drawn using Microsoft Excel and the data provided by the Impview converted program.

The fan is switched on and the system runs continuously. Data is also continuously collected by the data logger, during the day as well as during the night. Water is added by the irrigation system at regular intervals to ensure that the grass can freely transpire yet without being drowned.

3.3 EXPERIMENTAL PROCEDURE

The air velocity through the tunnel is kept constant at a certain value for a series of measurements and then changed to another value under similar weather conditions whenever possible. The velocity ranges from about 0.5 m/s to about 2 m/s and measurements are logged continuously during daylight hours. A few measurements were taken to verify that no evapotranspiration takes place after sunset. Of particular interest are the measurements taken during the hours of maximum solar radiation – i.e. over the period occurring at solar noon in midsummer; this is at about 13h00 local time at Stellenbosch. This is the time that the maximum transpiration is likely to occur and which will have the greatest influence on the air density as it flows through the tunnel. It was endeavoured to take measurements during periods of clear sky and maximum solar radiation, i.e. during the months of November through February.

CHAPTER 4
LITERATURE STUDY SYNOPSIS

4.0 INTRODUCTION

The literature study involved the investigation of psychrometrics, solar radiation, biophysical plant physiology, heat and mass transfer as well as viscous fluid flow. All these pertain to the Penman-Monteith equation whereby the amount of evaporation from a water surface or evapotranspiration from a vegetated surface may be predicted using climatic data alone. The following is a summary of the chief principles involved. Detailed explanations and derivations are given in the appendices.

4.1 THE PENMAN-MONTEITH EQUATION

Using psychrometric principles, Penman [48PE1] combined the energy and transport equations to estimate evaporation from a wetted surface, subject to solar radiation and in contact with unsaturated air, utilizing climatic data alone. This eliminated the need to know the temperature of the surface. In Appendix A the derivation is shown in detail and below is the equation for evaporation from a horizontal surface in which the heat and vapor transfer areas are considered equal. Monteith refined the Penman equation by including the canopy stomatal resistance in addition to the boundary layer resistance.

$$(m_v / A) i_{fg} = \frac{h_c\,(vpd) + \Delta I_{net}}{\Delta + \gamma^*} \qquad (A.69)$$

where

m_v / A is the water evaporated from the surface, kg/m^2s.

i_{fg} is the latent heat of evaporation at the surface temperature, J/kg. When the surface temperature is unknown, the average of the dry- and wetbulb temperatures of the air in contact with the surface is to be used.

Δ is the average slope of the saturation pressure line between the wetbulb temperature of the air above the surface and the surface temperatures. When the surface temperature is unknown, Δ is calculated at the average of the dry and wetbulb temperatures of the air, Pa/K.

I_{net} is the net radiation absorbed by the surface- this includes infrared radiation exchange, W/m^2. The radiation absorbed is dependent on the properties of the surface with respect to solar radiation. When the surface is vegetation, the albedo or reflectivity is the main parameter to be considered. The main surface differences between grass and open water as evaporating surfaces lies in the amounts of short wave radiation reflected and the effective heat transfer coefficients. The water surface reflects about 20 % and the grass 5 % [51PE1]. The effective heat transfer coefficient is lower for the water than for the grass surface due to roughness differences.

vpd is the vapor pressure depression i.e. the difference in actual vapor pressure of the air above the surface and the saturation vapor pressure at the same drybulb temperature, Pa, and is an indication of the driving potential for vapor transfer (This is also referred to in the literature as vapor pressure deficit).

h_c is the effective heat transfer coefficient between the surface and the air flowing over it, W/m^2K. The heat transfer coefficient is dependent on the velocity of the air, the roughness of the surface and the temperature differences between the surface and the air (see Appendix D for details).

γ^* is the "adjusted psychrometric constant" (see appendix A) for a system in which heat and vapor transfer are dominated by forced convection. The ratio of the heat and vapor transfer coefficient relationships is the controlling parameter. Monteith [75MO1] included the stomatal resistance in addition to the surface or boundary layer resistance for vapor transfer, whereas Penman [48PE1] considered only the surface or boundary layer resistance to vapor transfer. Evaporation or transpiration rates are mainly determined by the incoming energy supply and the important quantity is the projected surface on a horizontal plane; the evaporation from a piece of wet blotting paper is not increased by putting another wet piece underneath it [51PE1].

By definition

$$\gamma^* = \gamma\, r_V / r_H \qquad (A.42)$$

r_v being the boundary layer or surface resistance to vapor transfer and r_H the resistance to heat transfer.

Monteith considered the stomatal and boundary layer resistances to be in series adopting the electrical resistance analogy and defined the resistance to vapor transfer as

$$r_v = r_a + r_s \qquad (A.71)$$

where $r_a \approx r_H$ considering the boundary layer resistance to vapor transfer of the surface, r_a, to have the same value as the resistance to heat transfer, r_H [90MO1].

r_s is the stomatal resistance.

Regarding the mass, heat and momentum transfer relationships in the boundary layer according to Pruit [73PR1], "a source of uncertainty exists, especially for diabatic conditions. For example the ratio of heat to momentum transfer coefficients is $\frac{K_H}{K_M} = 1.35$ by Businger et al. (1971) as opposed to the value of 0.88 in 1959 by Priestley".

Literature on the subject of transfer coefficient relationships offers many diverse opinions [73PR1].

Using psychrometric principles and the Penman-Monteith equation an expression for the surface temperature, T_s, may be derived which gives this temperature relative to the drybulb temperature of the air, T_A.

$$T_S = T_A + \frac{1}{(\Delta + \gamma^*)}\left(\frac{\gamma^* I_{net}}{h_c} - vpd\right) \qquad (A.81)$$

4.2 THE ABSORPTION OF SOLAR RADIATION BY THE GRASS

The solar radiation reaching the grass is determined by the solar characteristics of the glass roof of the tunnel and the albedo of the grass. The albedo or reflectivity of the grass determines the amount of radiation absorbed. Since all solar characteristics

are given in terms of solar time, local time needs to be converted to solar time. There are two corrections to be made, one for the time meridian (longitude) of the country in question and the observer's meridian which may differ, and then secondly the equation of time, (EOT) which accounts for the non-uniformity of the earth's orbit around the sun. The former is a function of longitude and the latter of the day of the year.

Appendix B gives the detailed equations.

The effective transmissivity–absorptivity product, $(\tau\alpha)$ incorporates the solar characteristics of both the glass roof and the grass surface.

According to Duffie [91DU1] and referring to figure (B.2), the effective transmissivity-absorptivity product, $(\tau\alpha)$, is given by

$$(\tau\alpha) = \alpha\left[\frac{\tau}{1-(1-\alpha)\rho_d}\right] \qquad \text{(B.24)}$$

where α is the absorptivity of the lower absorbing surface (in this application it will be the grass), ρ is the reflectivity of the upper surface (the glass roof in this application), ρ_d is the diffuse reflectivity and τ the transmissivity of the glass sheet.

The absorptivity of the grass is dependent on the albedo of the grass. This is a function of the angle of the radiation striking the grass surface. The albedo of grass is given by Dong [92DO1] as

$\lambda = 0.00158\theta + 0.386\exp(-0.0188\theta)$ (B.26), where θ is the angle at which the ray strikes the grass surface.

The infrared radiation exchange between the grass surface and the upper glass roof is given by

$$q_{rgR} = \frac{\sigma\left(T_2^4 - T_1^4\right)}{\frac{1}{\varepsilon_1} + \frac{1}{\varepsilon_2} - 1} \qquad \text{(B.29)}$$

where ε_1 and ε_2 are the emissivities of the vegetated surface and glass roof respectively.

A portion of the incoming heat energy is transferred to the soil below. This varies throughout the day depending on the temperature difference between the grass surface and the soil below. The specific heat capacity of the soil is difficult to estimate as the moisture content of the soil varies depending on irrigation times, evapotranspiration, cloud cover and radiation values for the day. The FAO [04FA1] gives an approximate value of 10% of the incoming radiation lost to the soil when doing calculations over a period of a day.

4.3 PLANT PHYSIOLOGY

Chlorophylls are the pigments which create the green color in leaves and which are responsible for the absorption of solar energy in specific wave bands (absorption in the red and blue bands being slightly higher than in the green band).

Plants need to be able to transport water and various solutes throughout the plant structure. Although molecules move across cells walls by diffusion, water moves throughout the plant at a much higher rate than what is possible by diffusion. The transpiration-cohesion hypothesis [95MO1] states that water moves from the roots to

the top of the plant in an unbroken column in order to replace the water evaporating from the leaves. Cohesive forces keep the water column intact while adhesion to the cell wall prevents gravity from draining the water from the water conducting elements in the plant. Plants need to take up carbon dioxide for photosynthesis through the stomata and hereby expose the stomatal cavity to water loss by evaporation to the surrounding atmosphere (called transpiration). Stomatal control therefore links transpiration to photosynthesis. The chemical reaction of photosynthesis is light driven; so too are the light sensitive guard cells controlling the stomatal apertures. At night when no photosynthesis takes place and therefore no demand for carbon dioxide is made, the stomatal apertures are small and this prevents undue loss of water. As far as botanists can ascertain, transpiration does not seem to be essential for plant growth. Minerals can move independently of transpiration. Most botanists today regard transpiration as an "unavoidable evil - unavoidable because of leaf structure, and evil because it desiccates and often injures leaves" [95MO1]. When the stomata are open, water is transported from the soil to the atmosphere in response to physical forces namely the difference in water vapor concentration between the stomatal cavity and the external air, as well as the diffusional resistance of this pathway.

4.4 VISCOUS FLUID FLOW AND THE EFFECTIVE CONVECTIVE HEAT TRANSFER COEFFICIENT

The air flow through the tunnel can be viewed firstly as flow over a flat plate, above the grass and below the glass roof with boundary layers growing from below and above until the boundary layers merge. Thereafter the flow can be viewed as developing or fully developed pipe flow or flow between parallel plates. From calculations it was found that for the velocity range investigated the flow can be viewed without significant error as turbulent for the entire tunnel. The effective heat transfer coefficient is dependent on the surface roughness, the velocity of the air flowing over the surface and the temperature difference between the surface and the air. The Reynolds-Colburn analogy which relates the convective heat transfer to surface roughness may be applied to determine a value for the effective heat transfer coefficient. Due to the complex nature of the analysis of the air-grass interaction a single effective convective heat transfer coefficient is utilized for the entire tunnel length for a given air velocity. Pressure drop measurements made over the length of the tunnel were used to determine the friction loss and then related to the effective convective heat transfer coefficient. However it was found that the friction loss or pressure drop varied according to the length of the grass. It was therefore endeavoured to keep the grass as short as possible to exclude the effect of varying grass length.

The Burger-Kröger semi-empirical equation [06BU1] for uniform heat flux which is dependent on the surface roughness, C_f, is investigated.

$$h_{cgF}\left[\frac{\mu T}{g(T_g - T_F)c_{pma}k^2\rho^2}\right]^{1/3} = 0.2106 + v_w(C_f/2)\left[\frac{\rho T}{\mu g(T_g - T_F)}\right]^{1/3} \qquad (D.31)$$

where $(T_g - T_F) \geq 4°C$ and $C_f/2 = 0.0026$ for a smooth surface and where

h_{cgF} is the effective convective heat transfer coefficient, W/m^2K

v_w is the velocity of the air, m/s

C_f is the surface friction coefficient

T_g and T_F the surface and air temperatures respectively and T, (in K), the average of the two

When $(T_g - T_F) < 4°C$, the following equation applies:

$$h_{cgF} = 3.87 + 0.0022\left(\frac{v_w \rho c_{pma}}{Pr^{2/3}}\right) \text{ for a smooth surface} \qquad (D.33)$$

The first equation is dependent on the temperature difference between the surface and the air in contact with the surface. Temperature measurements of the grass and the air along the tunnel show that the temperature difference is close to or less than 4 °C or even negative (when the grass temperature is lower than the temperature of the air flowing over it). Calculations also show that the effective convective heat transfer coefficient utilizing both equations give values to within 0.05 % of each other. The second equation is therefore utilized incorporating an appropriate friction coefficient and not the value of 0.0022 which is applicable to a smooth surface.

4.5 PREDICTING THE OUTLET AIR STATE AND THE RATE OF EVAPOTRANSPIRATION

Data accumulated on cloudless windless days during times of maximum radiation may be utilized in two ways. The first would be to use both measured inlet and outlet state values of the air in order to determine the actual rate of evapotranspiration. The second application would be to apply the conservation equations in addition to the Penman-Monteith equation to a control volume around the fluid flow on the inside of the tunnel to subsequent one meter lengths of the tunnel in order to predict the state of the air at the outlet of the tunnel, starting off with a given inlet state. The average rate of evapotranspiration, the state of the air at the exit to the tunnel and the average grass temperature for the entire tunnel length may then be determined. This procedure involves lengthy calculations and needs to be done for every measurement time. It is recognized that the flow in the tunnel is not immediately turbulent but is so within about 1.5 m from the inlet, depending on the velocity of the air in the tunnel. Considering the tunnel to be 16 m in length and given the complexity of the calculations it was found that viewing the flow as fully turbulent from the inlet does not significantly influence the results as is evident in the graphs showing measured and predicted values. Figure 4.1 shows the control volume and mass and energy exchanges within the tunnel boundaries.

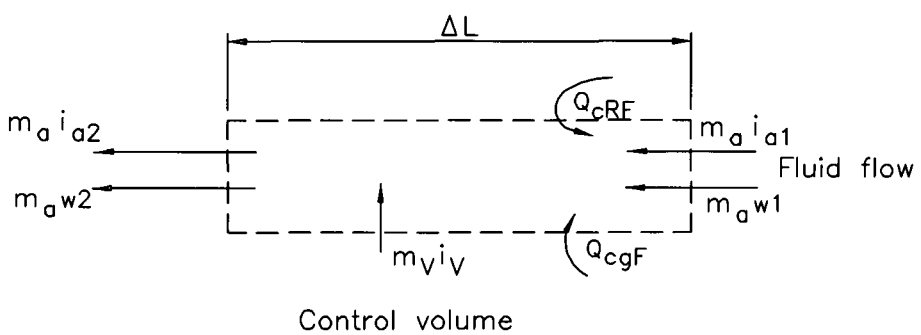

Figure 4.1 Control volume around the air or fluid flow over the grass

The succession of calculations are the following:

All properties of the entering air are calculated from the average of the measured drybulb and wetbulb temperatures at the inlet. The mass flow rate of the dry air is

constant throughout the tunnel and is also known. The radiation at that particular instant is known from the reading of the pyranometer. All values required for the Penman-Monteith equation can be determined and hence the rate of evapotranspiration for a one meter length of tunnel is known.

From the conservation of water mass, the water vapor content of the air at the end of one meter can be determined using

$$w_2 = w_1 + \frac{m_v}{m_a} \text{ kg/kg dry air} \tag{4.1}$$

The air mass flow rate and the inlet state are known. The solar radiation, I_{net}, absorbed by the grass is also known. The value of m_v is obtained from the Penman-Monteith equation where the area in question A = 1 m^2.

$$(m_v / A)i_{fg} = \frac{h_{cgF}(vpd) + \Delta I_{net}}{\Delta + \gamma^*}, \text{ J/sm}^2 \tag{A.69}$$

From the energy balance, find.

$$m_a i_{a1} + Q_{cRF} + Q_{cgF} + m_v i_v = m_a i_{a2}, \text{ J/s} \tag{4.2}$$

The effective heat transfer coefficients for determining Q_{cRF} and Q_{cgF} are known. For a one meter length of tunnel, $\Delta L = 1$, and which is one meter wide, the heat transfer area is one square meter so that

$$Q_{cRF} = h_{cRF}(T_R - T_F), \text{ J/sm}^2 \tag{4.3}$$

$$Q_{cgF} = h_{cgF}(T_g - T_F), \text{ J/sm}^2 \tag{4.4}$$

Subscripts R, F and g refer to the glass roof, fluid (air) and grass respectively.

It must be pointed out that the glass temperature was measured at the inlet and outlet of the tunnel and the values differed usually by less than 1 °C so that a constant glass temperature was used for all calculations. Glass temperatures were initially measured above and below the glass sheet and found to differ by a negligible amount from each other.

The energy conservation equation is now

$$m_a i_{a1} + [h_{cgF}(T_g - T_F) + h_{cRa}(T_R - T_F)] + m_v i_v = m_a i_{a2} \text{ J/s} \tag{4.5}$$

or

$$i_{a2} = i_{a1} + [h_{cgF}(T_g - T_F) + h_{cRF}(T_R - T_F)]/m_a + m_v i_v / m_a \text{ J/kg dry air} \tag{4.6}$$

The enthalpy of the air is dependent on the drybulb temperature as well as the water vapor content. Since the water vapor content has already been obtained from the water balance, the drybulb temperature may be obtained from the above equation since

$$i_a = c_{p\,da} T_{db} + w(2501000 + c_{p\,v} T_{db}) \text{ J/kg dry air} \tag{4.7}$$

where the enthalpy is defined relative to 0 °C and 0 % relative humidity and with T in °C.

The drybulb temperature of the air varies from T_1 to T_2 so that an average temperature needs to be used for the temperature $T_F = (T_1+T_2)/2$

From this find

$$T_2\left[c_{pa}+w_2c_{pv}+\left(\frac{h_{cRF}+h_{cgF}}{2m_a}\right)\right]=T_1\left[c_{pa}+w_1c_{pv}-\left(\frac{h_{cRF}+h_{cgF}}{2m_a}\right)\right]$$
$$+(w_2-w_1)(i_v-i_{fg@0°C})+\left[\frac{h_{cRF}T_R+h_{cgF}T_g}{m_a}\right]$$

or

$$T_2(C_2)=T_1(C_1)+(w_2-w_1)(i_v-i_{fg@0°C})+\left[\frac{h_{cRF}T_R+h_{cgF}T_g}{m_a}\right] \quad (4.8)$$

or

$$T_2=\left(\frac{C_1}{C_2}\right)T_1+\frac{(w_2-w_1)(i_v-i_{fg@0°C})}{C_2}+\left[\frac{h_{cRF}T_R+h_{cgF}T_g}{C_2m_a}\right]$$

where the coefficients C_1 and C_2 are given by

$$C_1=\left[c_{pa}+w_1c_{pv}-\left(\frac{h_{cRF}+h_{cgF}}{2m_a}\right)\right]$$

and (4.9)

$$C_2=\left[c_{pa}+w_2c_{pv}+\left(\frac{h_{cRF}+h_{cgF}}{2m_a}\right)\right]$$

The wetbulb temperature can now be obtained from the non-explicit formula for the humidity ratio, w_2, which is a function of both the wet- and drybulb temperatures. The drybulb temperature has been determined and hence the wetbulb temperature can be determined by an iterative process.

$$w_2 = \left(\frac{2501.6-2.3263(T_{wb2}-273.15)}{2501.6+1.8577(T_{db2}-273.15)-4.184(T_{wb2}-273.15)}\right)\left(\frac{0.62509p_{vwb2}}{p_{abs}-1.005p_{vwb2}}\right)$$
$$-\left(\frac{1.00416(T_{db2}-T_{wb2})}{2501.6+1.8577(T_{db2}-273.15)-4.184(T_{wb2}-273.15)}\right), \text{ kg/kg dry air}$$

(F.3.5)

with T_{wb} in °C

The grass temperature may be predicted for each subsequent meter and in the end a final average grass temperature may be determined. The grass surface temperature is given by

$$T_g=T_F+\frac{1}{(\Delta+\gamma^*)}\left(\frac{\gamma^*I_{net}}{h_{cgF}}-vpd\right), \text{ °C} \quad (A.80)$$

CHAPTER 5

SAMPLE CALCULATION – THE MEASURED RATE OF EVAPOTRANSPIRATION FROM THE GRASS

5.0 INTRODUCTION

The actual evapotranspiration rate from the grass surface is determined by measuring the increase in the water vapor content of the fixed mass flow rate of air flowing over the grass.

5.1 ATMOSPHERIC AIR PROPERTIES AT INLET AND OUTLET OF TUNNEL

To avoid confusion all atmospheric air properties are first determined before any other calculations are embarked on.

This sample calculation is for a clock hour of 14h02 or solar hour 13h36 on the 15 December.

The following temperatures were recorded.

Average air drybulb temperature at the inlet

$$T_{ai} = \left(\frac{T_{ai1} + T_{ai2} + T_{ia3}}{3}\right) = \left(\frac{29.71 + 30.18 + 29.69}{3}\right) = 29.86^{\circ}C \quad \text{or} \quad 303.01\,K$$

Average air wetbulb temperature at the inlet

$$T_{wbi} = \left(\frac{T_{wbi1} + T_{wbi2} + T_{wbi3}}{3}\right) = \left(\frac{20.60 + 19.96 + 21.11}{3}\right) = 20.56^{\circ}C \quad \text{or} \quad 293.71K$$

Average air drybulb temperature at the outlet

$$T_{ao} = \left(\frac{T_{ao1} + T_{ao2}}{2}\right) = \left(\frac{34.58 + 33.98}{2}\right) = 34.28^{\circ}C \quad \text{or} \quad 307.43\,K$$

Average air wetbulb temperature at the outlet

$$T_{wbo} = \left(\frac{T_{wbo1} + T_{wbo2}}{2}\right) = \left(\frac{29.37 + 28.73}{2}\right) = 29.05^{\circ}C \quad \text{or} \quad 302.2\,K$$

Average glass temperature

$$T_{R} = \left(\frac{T_{Ri} + T_{Ro}}{2}\right) = \left(\frac{37.28 + 37.28}{2}\right) = 37.28^{\circ}C \quad \text{or} \quad 310.43K$$

(for this experimental run only one glass temperature was recorded).

It must be stated here that the temperature of the glass roof was measured at the inlet and outlet of the tunnel both above and below the glass and the measurements were all within 1 °C to 1.3 °C of each other hence a single average constant glass temperature was used in all calculations to avoid unnecessary complications.

Grass temperature, measured halfway along the tunnel, T_g = 37.05 ºC or 310.20 K.

The average atmospheric pressure for the day = 100 000 Pa.

5.1.1 Calculation of thermophysical properties of atmospheric air at the inlet

The properties of dry air and saturated water vapor are calculated separately and thereafter the properties of the atmospheric air are determined. All the formulae require the temperature, T, to be in Kelvin.

Thermophysical properties of dry air at the inlet [04 KR 1]

The properties at the inlet and outlet states are calculated separately.

For the inlet state of the air:

Average drybulb air temperature in: 29.86 ° C or $T_{ai} = 303.01 K$

Average wetbulb air temperature in: 20.56 ° C or $T_{wbi} = 293.71 K$

The specific heat of dry air at the inlet state, c_{pai}, is given by:

$$\begin{aligned} c_{pai} &= 1.045356\times10^{3} - 3.161783\times10^{-1}T + 7.083814\times10^{-4}T^{2} \\ &\quad -2.705209\times10^{-7}T^{3} \\ &= 1.045356\times10^{3} - 3.161783\times10^{-1}(303.01) + 7.083814\times10^{-4}(303.01)^{2} \\ &\quad -2.705209\times10^{-7}(303.01)^{3} \\ &= 1005.53\ J/kgK \end{aligned} \qquad (F.1.2)$$

The dynamic viscosity, μ_{ai}, is given by

$$\begin{aligned} \mu_{ai} &= 2.287973\times10^{-6} + 6.259793\times10^{-8}T - 3.131956\times10^{-11}T^{2} \\ &\quad +8.15038\times10^{-15}T^{3} \\ &= 2.287973\times10^{-6} + 6.259793\times10^{-8}(303.01) - 3.131956\times10^{-11}(303.01)^{2} \\ &\quad +8.15038\times10^{-15}(303.01)^{3} \\ &= 1.861\times10^{-5}\ kg/sm \end{aligned} \qquad (F.1.3)$$

The thermal conductivity is given by

$$\begin{aligned} k_{ai} &= -4.937787\times10^{-4} + 1.018087\times10^{-4}\,T - 4.627937\times10^{-8}\,T^{2} \\ &\quad +1.250603\times10^{-11}\,T^{3} \\ &= -4.937787\times10^{-4} + 1.018087\times10^{-4}\,(303.01) - 4.627937\times10^{-8}\,(303.01)^{2} \\ &\quad +1.250603\times10^{-11}\,(303.01)^{3} \\ &= 0.02645\ W/mK \end{aligned} \qquad (F.1.4)$$

Thermophysical properties of saturated water vapor at the inlet

The specific heat, c_{pvi}, is given by

$$c_{pvi} = 1.3605 \times 10^3 + 2.31334T - 2.46784 \times 10^{-10}T^5 + 5.91332 \times 10^{-13}T^6 \text{ J/kgK}$$
$$= 1.3605 \times 10^3 + 2.31334(303.01) - 2.46784 \times 10^{-10}(303.01)^5 + 5.91332 \times 10^{-13}(303.01)^6$$
$$= 1875.28 \text{ J/kgK} \qquad \text{(F.2.2)}$$

The dynamic viscosity, μ_{vi}, is given by

$$\mu_{vi} = 2.562435 \times 10^{-6} + 1.816683 \times 10^{-8}T + 2.579066 \times 10^{-11}T^2 - 1.067299 \times 10^{-14}T^3$$
$$= 2.562435 \times 10^{-6} + 1.816683 \times 10^{-8}(303.01) + 2.579066 \times 10^{-11}(303.01)^2 - 1.067299 \times 10^{-14}(303.01)^3$$
$$= 1.014 \times 10^{-5} \text{kg/sm} \qquad \text{(F.2.3)}$$

The thermal conductivity, k_{vi}, is given by

$$k_{vi} = 1.3046 \times 10^{-2} - 3.756191 \times 10^{-5}T + 2.217964 \times 10^{-7}T^2 - 1.111562 \times 10^{-10}T^3$$
$$= 1.3046 \times 10^{-2} - 3.756191 \times 10^{-5}(303.01) + 2.217964 \times 10^{-7}(303.01)^2 - 1.111562 \times 10^{-10}(303.01)^3$$
$$= 0.01893 \text{ W/mK} \qquad \text{(F.2.4)}$$

The calculation of the thermophysical properties of atmospheric air at the inlet

The humidity ratio of atmospheric air, w, is given by

$$w = \left(\frac{2501.6 - 2.3263(T_{wb} - 273.15)}{2501.6 + 1.8577(T - 273.15) - 4.184(T_{wb} - 273.15)}\right)\left(\frac{0.62509p_{vwb}}{p_{abs} - 1.005p_{vwb}}\right) - \left(\frac{1.00416(T - T_{wb})}{2501.6 + 1.8577(T - 273.15) - 4.184(T_{wb} - 273.15)}\right), \text{ kg/kg da} \qquad \text{(F.3.5)}$$

The saturation pressure, p_{vwb}, at the wetbulb temperature, T_{wbi} must first be calculated.

The vapor pressure, p_v, is given by

$p_v = 10^z$, N/m^2 (F.2.1)

where z is given by

$$z = 10.79586\left(1-\frac{273.16}{T}\right)+5.02808\log10\left(\frac{273.16}{T}\right)$$
$$+1.50474\times10^{-4}\left[1-10^{-8.29692\left\{\left(\frac{273.16}{T}\right)-1\right\}}\right]$$
$$+4.2873\times10^{-4}\left[10^{4.76955\left(1-\frac{273.16}{T}\right)}-1\right]+2.786118312 \qquad \text{(F.2.2)}$$

Insert T_{wbi} = 20.56 °C or 293.71 K into the above formula and find

$$z = 10.79586\left(1-273.16\frac{273.16}{293.71}\right)+5.02808\log10\left(273.16\frac{273.16}{293.71}\right)$$
$$+1.50474\times10^{-4}\left[1-10^{-8.29692\left\{\frac{293.71}{273.16}-1\right\}}\right]]$$
$$+4.2873\times10^{-4}\left[10^{4.76955\left(1-\frac{273.16}{293.71}\right)}-1\right]+2.786118312$$
$$= 3.38$$

subsequently

$$p_{wb} = 10^{z} = 10^{3.38} = 2419.86\,\text{Pa}$$

Inserting $p_{atm} = 100000\,\text{Pa}$, $T_{wb} = 293.71\,\text{K}$, $T = 303.01\,\text{K}$, find

the humidity ratio, w_i, for the air at the inlet to be:

$$w_i = \left(\frac{2501.6-2.3263(293.71-273.15)}{2501.6+1.8577(303.01-273.15)-4.184(293.71-273.15)}\right)$$
$$\left(\frac{0.62509\times2419.86}{100000-1.005\times2419.86}\right)$$
$$\left(\frac{1.00416(303.01-293.71)}{2501.6+1.8577(303.01-273.15)-4.184(293.71-273.15)}\right)$$
$$= 0.01161\,\text{kg/kg da}$$

For atmospheric air the average specific heat is given by

$$c_{pma} = c_{pa} + wc_{pv}\ \text{J/K kg da}$$

Inserting the relevant values for the inlet state find,

$$c_{pmai} = 1005.32 + 0.01161(1875.28) = 1027.31\,\text{J/kg da} \qquad \text{(F.3.2b)}$$

In order to calculate the other properties of atmospheric air, the mass fractions X_a and X_v, must first be calculated, where

$$X_a = \frac{1}{(1+1.608\,w)}$$

$$X_v = \frac{w}{(w+0.622)}$$

Substituting w = 0.01161 find:

$$X_{ai} = \frac{1}{(1+1.608\ w)} = \frac{1}{(1+1.608\times 0.01161)} = 0.982$$

$$X_{vi} = \frac{w}{(w+0.622)} = \frac{0.01161}{(0.01161+0.622)} = 0.018$$

For atmospheric air the average dynamic viscosity, μ_{av}, is given by

$$\mu_{av} = \frac{\left(X_a \mu_a M_a^{\ 0.5} + X_v \mu_v M_v^{\ 0.5}\right)}{\left(X_a M_a^{\ 0.5} + X_v M_v^{\ 0.5}\right)}$$

Substituting the relevant values, find the dynamic viscosity of atmospheric air at the inlet state, μ_{avi}, to be

$$\mu_{avi} = \frac{\left(0.982\times 1.861\times 10^{-5}\times 28.97^{0.5} + 0.018\times 1.014\times 10^{-5}\times 18.016^{0.5}\right)}{\left(0.982\times 28.97^{0.5} + 0.018\times 18.016^{0.5}\right)}$$

$$= 1.848\times 10^{-5}\ \text{kg/sm}$$

For atmospheric air the average thermal conductivity is given by

$$k_{av} = \frac{\left(X_a k_a M_a^{\ 0.33} + X_v k_v M_v^{\ 0.33}\right)}{\left(X_a M_a^{\ 0.33} + X_v M_v^{\ 0.33}\right)}\ 4\text{W/mK} \qquad \text{(F.3.4)}$$

Substituting the relevant values, find the conductivity of atmospheric air at the inlet state, k_{avi}, to be

$$k_{avi} = \frac{\left(0.982\times 0.02645\times 28.97^{0.33} + 0.018\times 0.01893\times 18.016^{0.33}\right)}{\left(0.982\times 28.97^{0.33} + 0.018\times 18.016^{0.33}\right)}$$

$$= 0.02633\ \text{W/mK}$$

For atmospheric air the average density is given by

$$\rho_{av} = (1+w)[1-w/(w+0.62198)]p_{abs}/287.08T$$

Substituting the relevant values, find the average density of the atmospheric air at the inlet state, ρ_{avi}, to be

$$\rho_{avi} = (1+w)[1-w/(w+0.62198)]p_{abs}/287.08T$$
$$= (1+0.01161)[1-0.01161/(0.01161+0.62198)]100000/287.08\times 303.01$$
$$= 1.14\ \text{kg air} - \text{vapor}/\text{m}^3$$

The enthalpy of the air is determined by the following equation

$$i_{ma} = c_{pa}(T-273.15) + w[i_{fgw@0°C} + c_{pv}(T-273.15)] \qquad \text{(F.3.6b)}$$

Inserting the relevant values, calculate the enthalpy of the incoming air:

Previously calculated are:

c_{pai} = 1005.53 J/kg/kg dry air

w_i = 0.01161 kg/kg dry air

c_{pvi} = 1875.28 J/kg K

The enthalpy of evaporation at 0°C

$i_{fgw@0°C} = 2.5016 \times 10^6$ J/kg

Substitute into equation (F3.6b) and find

$$i_{mai} = c_{pai}(T - 273.15) + w[i_{fgw@0°C} + c_{pvi}(T - 273.15)]$$
$$= 1005.321(303.01 - 273.15) + 0.01161[2.5016 \times 10^6 + 1875.28(303.01 - 273.15]$$
$$= 59737.44 \text{ J/kg dry air}$$

Vapor pressure depression of atmospheric air at the inlet state

Calculate the saturated vapor pressure, $p_{sat,T_{db}}$ of the drybulb temperature at the inlet state:

Since $p_v = 10^z$, N/m^2 (F.2.1)

$$z = 10.79586(1 - 273.16/T) + 5.02808 \log_{10}(27316/T)$$
$$+ 1.50474 \times 10^{-4} [1 - 10^{-8.29692\{(T/273.16) - 1\}}]$$
$$+ 4.2873 \times 10^{-4} [10^{4.76955(1-273.16/T)} - 1] + 2.786118312$$

Insert T = 303.01 K into the above formula and find

$$z = 10.79586(1 - 273.16/303.01) + 5.02808 \log_{10}(27316/303.01)$$
$$+ 1.50474 \times 10^{-4} [1 - 10^{-8.29692\{(303.01/273.16) - 1\}}]$$
$$+ 4.2873 \times 10^{-4} [10^{4.76955(1-273.16/303.01)} - 1] + 2.786118312 = 3.624$$

and subsequently

$p_{sat,T_{db}} = 10^{3.624} = 4210.03$ Pa

The partial vapor pressure of the atmospheric air, p_{vap}, is calculated from the wetbulb and drybulb temperatures

$$p_{vap} = p_{sat,wb} - \frac{(T_{db} - T_{wb})(p_{atm} - p_{sat,wb})}{1550 - 1.44T_{wb}} \quad \text{(F.3.7)}$$

where

$p_{sat,wb}$ is the saturation pressure at the wetbulb temperature.

For the inlet state where the average wetbulb temperature is 293.71 K

Find

$$z = 10.79586(1 - 273.16/303.01) + 5.02808 \log_{10}(27316/303.01)$$
$$+ 1.50474 \times 10^{-4} [1 - 10^{-8.29692\{(293.71/273.16) - 1\}}]$$
$$+ 4.2873 \times 10^{-4} [10^{4.76955(1-273.16/293.71)} - 1] + 2.786118312$$
$$= 3.3838$$

$p_{sat,wb} = 2419.86$ Pa

The measured atmospheric pressure = 100000 Pa

At the inlet to the tunnel where the drybulb temperature is 303.01 K and the wetbulb temperature is 293.71 K, find

$$p_{vap} = p_{sat,wb} - \frac{(T_{db} - T_{wb})(p_{atm} - p_{sat,wb})}{1550 - 1.44T_{wb}}$$

$$= 2419.86 - \frac{(303.01 - 293.71)(100000 - 2419.86)}{1550 - 1.44(293.71 - 273.15)}$$

$$= 1822.85 \text{Pa}$$

$$p_{vap\ inlet} = 1822.85 \text{ Pa}$$

The vapor pressure depression at the inlet state is

$$\text{vpd} = p_{sat,T_{db}} - p_{vap} = 4210.03 - 1822.85 = 2387.18 \text{ Pa}$$

5.1.2 Calculation of thermophysical properties of atmospheric air at the outlet

The properties of dry air and saturated water vapor are calculated separately and thereafter the properties of the atmospheric air are determined. All the formulae require the temperature, T, to be in Kelvin.

Thermophysical properties of dry air:

Average drybulb air temperature out: 34.28 °C or $T_{ao} = 307.43$ K

Average wetbulb air temperature out 29.05 °C or $T_{wbo} = 302.20$ K

The specific heat of dry air at the outlet state, c_{pao}, is given by:

$$c_{pao} = 1.045356 \times 10^3 - 3.161783 \times 10^{-1} T + 7.083814 \times 10^{-4} T^2 - 2.705209 \times 10^{-7} T^3$$

$$= 1.045356 \times 10^3 - 3.161783 \times 10^{-1}(307.43) + 7.083814 \times 10^{-4}(307.43)^2 - 2.705209 \times 10^{-7}(307.43)^3$$

$$= 1006.64 \text{ J/kgK} \qquad \text{(F.1.2)}$$

The dynamic viscosity, μ_{ao}, is given by

$$\mu_{ao} = 2.287973 \times 10^{-6} + 6.259793 \times 10^{-8} T - 3.131956 \times 10^{-11} T^2 + 8.15038 \times 10^{-15} T^3$$

$$= 2.287973 \times 10^{-6} + 6.259793 \times 10^{-8}(307.43) - 3.131956 \times 10^{-11}(307.43)^2 + 8.15038 \times 10^{-15}(307.43)^3$$

$$= 1.881 \times 10^{-5} \text{kg/sm} \qquad \text{(F.1.3)}$$

The thermal conductivity, k_{ao} is given

$$k_{ao} = -4.937787 \times 10^{-4} + 1.018087 \times 10^{-4} T - 4.627937 \times 10^{-8} T^2 + 1.250603 \times 10^{-11} T^3$$
$$= -4.937787 \times 10^{-4} + 1.018087 \times 10^{-4} (307.43) - 4.627937 \times 10^{-8} (307.43)^2 + 1.250603 \times 10^{-11} (307.43)^3$$
$$= 0.02679 \text{ W/mK} \quad \text{(F.1.4)}$$

Thermophysical properties of saturated water vapor at the outlet state

The specific heat , c_{pvo} ,is given by

$$c_{pvo} = 1.3605 \times 10^3 + 2.31334T - 2.46784 \times 10^{-10} T^5 + 5.91332 \times 10^{-13} T^6 \text{ J/kgK}$$
$$= 1.3605 \times 10^3 + 2.31334(307.43) - 2.46784 \times 10^{-10} (307.43)^5 + 5.91332 \times 10^{-13} (307.43)^6$$
$$= 1877.17 \text{ J/kgK} \quad \text{(F.2.2)}$$

The dynamic viscosity , μ_{vo} , is given by

$$\mu_{vo} = 2.562435 \times 10^{-6} + 1.816683 \times 10^{-8} T + 2.579066 \times 10^{-11} T^2 - 1.067299 \times 10^{-14} T^3$$
$$= 2.562435 \times 10^{-6} + 1.816683 \times 10^{-8} (307.43) + 2.579066 \times 10^{-11} (307.43)^2 - 1.067299 \times 10^{-14} (307.43)^3$$
$$= 1.027 \times 10^{-5} \text{ kg/sm} \quad \text{(F.2.3)}$$

The thermal conductivity, k_{vo} , is given by

$$k_{vo} = 1.3046 \times 10^{-2} - 3.756191 \times 10^{-5} T + 2.217964 \times 10^{-7} T^2 - 1.111562 \times 10^{-10} T^3$$
$$= 1.3046 \times 10^{-2} - 3.756191 \times 10^{-5} (307.43) + 2.217964 \times 10^{-7} (307.43)^2 - 1.111562 \times 10^{-10} (307.43)^3$$
$$= 0.01923 \text{ W/mK} \quad \text{(F.2.4)}$$

The calculation of the thermophysical properties of atmospheric air at the outlet

The humidity ratio of atmospheric air, w, is given by

$$w = \left(\frac{2501.6 - 2.3263(T_{wb} - 273.15)}{2501.6 + 1.8577(T - 273.15) - 4.184(T_{wb} - 273.15)} \right) \left(\frac{0.62509 p_{vwb}}{p_{abs} - 1.005 p_{vwb}} \right) - \left(\frac{1.00416(T - T_{wb})}{2501.6 + 1.8577(T - 273.15) - 4.184(T_{wb} - 273.15)} \right), \text{kg/kg da} \quad \text{(F.3.5)}$$

The saturation pressure, p_{vwb} , at the wetbulb temperature, T_{wbo} must first be calculated.

The vapor pressure, p_v, is given by

$$p_v = 10^z, \text{ N/m}^2 \qquad \text{(F.2.1)}$$

where z is given by

$$z = 10.79586(1 - 273.16/T) + 5.02808\log10(27316/T) + 1.50474 \times 10^{-4}\left[1 - 10^{-8.29692\{(T/273.16)-1\}}\right] + 4.2873 \times 10^{-4}\left[10^{4.76955(1-273.16/T)} - 1\right] + 2.786118312 \qquad \text{(F.2.2)}$$

Insert T_{wbo} = 29.05 °C or 302.20 K into the above formula and find

$$z = 10.79586(1 - 273.16/302.20) + 5.02808\log10(273.16/302.20) + 1.50474 \times 10^{-4}\left[1 - 10^{-8.29692\{(302.20/273.16)-1\}}\right] + 4.2873 \times 10^{-4}\left[10^{4.76955(1-273.16/302.20)} - 1\right] + 2.786118312 = 3.604$$

subsequently

$$p_{wb} = 10^z = 10^{3.604} = 4018.31\,\text{Pa}$$

Inserting $p_{atm} = 100000$ Pa, $T_{wb} = 302.20$ K, T = 307.43 K, find

the humidity ratio, w_o, for the air at the outlet to be:

$$w_o = \left(\frac{2501.6 - 2.3263(302.20 - 273.15)}{2501.6 + 1.8577(307.43 - 273.15) - 4.184(302.20 - 273.15)}\right)\left(\frac{0.62509 \times 4018.31}{100000 - 1.005 \times 4018.31}\right) - \left(\frac{1.00416(307.43 - 302.20)}{2501.6 + 1.8577(307.43 - 273.15) - 4.184(302.20 - 273.15)}\right) = 0.02392 \text{ kg/kg da}$$

For atmospheric air the average specific heat is given by

$$c_{pma} = c_{pa} + wc_{pv} \text{ J/K kg da}$$

inserting the relevant values for the outlet state find, (F.3.2b)

$$c_{pmao} = 1006.64 + 0.02392(1877.17) = 1051.56 \text{ J/kg da}$$

In order to calculate the other properties of atmospheric air, the mass fractions X_a and X_v, must first be calculated, where

$$X_a = \frac{1}{(1 + 1.608\ w)}$$

$$X_v = \frac{w}{(w + 0.622)}$$

Substituting w = 0.02392 kg/kg da find:

$$X_{ao} = \frac{1}{(1+1.608\ w)} = \frac{1}{(1+1.608\times 0.02392)} = 0.963$$

$$X_{vo} = \frac{w}{(w+0.622)} = \frac{0.02392}{(0.02392+0.622)} = 0.037$$

For atmospheric air the average dynamic viscosity, μ_{av}, is given by

$$\mu_{av} = \frac{\left(X_a \mu_a M_a^{\ 0.5} + X_v \mu_v M_v^{\ 0.5}\right)}{\left(X_a M_a^{\ 0.5} + X_v M_v^{\ 0.5}\right)} \qquad \text{(F.3.3)}$$

Substituting the relevant values, find the dynamic viscosity of atmospheric air at the outlet state, μ_{avo}, to be

$$\mu_{avo} = \frac{\left(0.963\times 1.881\times 10^{-5}\times 28.97^{0.5} + 0.037\times 1.027\times 10^{-5}\times 18.016^{0.5}\right)}{\left(0.963\times 28.97^{0.5} + 0.037\times 18.016^{0.5}\right)}$$

$$= 1.856\times 10^{-5}\ \text{kg/sm}$$

For atmospheric air the average thermal conductivity is given by

$$k_{av} = \frac{X_a k_a M_a^{\ 0.33} + X_v k_v M_v^{\ 0.33}}{\left(X_a M_a^{\ 0.33} + X_v M_v^{\ 0.33}\right)}\ \text{W/mK} \qquad \text{(F.3.4)}$$

Substituting the relevant values, find the conductivity of atmospheric air at the outlet state, k_{avo}, to be

$$k_{avo} = \frac{\left(0.963\times 0.02679\times 28.97^{0.33} + 0.037\times 0.01923\times 18.016^{0.33}\right)}{\left(0.963\times 28.97^{0.33} + 0.037\times 18.016^{0.33}\right)}$$

$$= 0.02655\ \text{W/mK}$$

For atmospheric air the average density is given by

$$\rho_{av} = (1+w)[1-w/(w+0.62198)]p_{abs}/287.08T \qquad \text{(F.3.1)}$$

Substituting the relevant values, find the average density of the atmospheric air at the outlet state, ρ_{avo}, to be

$$\rho_{avo} = (1+w)[1-w/(w+0.62198)]p_{abs}/287.08T$$

$$= (1+0.02392)[1-0.02392/(0.02392+0.62198)]100000/287.08\times 307.43$$

$$= 1.1172\ \text{kg air} - \text{vapor}/\text{m}^3$$

The enthalpy of the air is determined by the following equation

$$i_{ma} = c_{pa}(T-273.15) + w\left[i_{fgw@0°C} + c_{pv}(T-273.15)\right] \qquad \text{(F.3.6b)}$$

inserting the relevant values, calculate the enthalpy of the incoming air:

Previously calculated are

c_{pao} = 1006.64 J/kgK dry air

w_o = 0.02392 kg/kg dry air

c_{pvo} = 1877.17 J/kg K vapor

$i_{fgw@0°C}$ = 2.5016 x 10^6 J/kg

Substitute and find

$$i_{mao} = c_{pa}(T - 273.15) + w[i_{fgw@°C} + c_{pv}(T - 273.15)]$$
$$= 1006.64(307.43 - 273.15)$$
$$+ 0.02392[2.5016 \times 10^6 + 1877.17(307.43 - 273.15]$$
$$= 95898.32 \text{ J/kg dry air}$$

Vapor pressure depression of air at the outlet state

For the outlet state where T = 307.43 K, find

$$z = 10.79586(1 - 273.16/307.43) + 5.02808 \log_{10}(27316/307.43)$$
$$+ 1.50474 \times 10^{-4} [1 - 10^{-8.29692\{(307.43/273.16) - 1\}}]$$
$$+ 4.2873 \times 10^{-4} [10^{4.76955(1-273.16/307.43)} - 1] + 2.786118312 = 3.733$$

$$p_{sat,T_{db}} = 10^{3.733} = 5403.28 \text{ Pa}$$

The partial vapor pressure of the atmospheric air, p_{vap}, is calculated from the wetbulb and drybulb temperatures

$$p_{vap} = p_{sat,wb} - \frac{(T_{db} - T_{wb})(p_{atm} - p_{sat,wb})}{1550 - 1.44T_{wb}} \qquad (F.3.7)$$

where

$p_{sat,wb}$ is the saturation pressure at the wetbulb temperature.

For the outlet state where the average wetbulb temperature is 302.2 K

Find

$$z = 10.79586(1 - 273.16/T) + 5.02808 \log_{10}(27316/T)$$
$$+ 1.50474 \times 10^{-4} [1 - 10^{-8.29692\{(T/273.16) - 1\}}]$$
$$+ 4.2873 \times 10^{-4} [10^{4.76955(1-273.16/T)} - 1] + 2.786118312$$

$$z = 3.604$$

$$p_{sat,wb} = 4018.31 \text{ Pa}$$

The measured atmospheric pressure = 100000 Pa

At the outlet of the tunnel where the drybulb temperature is 307.43 K and the wetbulb temperature is 302.2 K, find

$$p_{vap} = p_{sat,wb} - \frac{(T_{db} - T_{wb})(p_{atm} - p_{sat,wb})}{1550 - 1.44T_{wb}}$$
$$= 4018.31 - \frac{(307.43 - 302.2)(100000 - 4018.31)}{1550 - 1.44(302.2 - 273.15)}$$
$$= 3685.87 \text{ Pa}$$

$$p_{vap\ outlet} = 3685.87 \text{ Pa}$$

The vapor pressure depression at the outlet state is

$$vpd = p_{sat,T_{db}} - p_{vap} = 5403.28 - 3685.87 = 1717.41 \text{Pa}$$

The log mean vapor pressure depression, LMvpd, can now be calculated for the inlet and outlet states:

$$\text{LMvpd} = \frac{2387.18 - 1717.41}{\ln[2387.18/1717.41]} = 2215.52.\,\text{Pa}$$

This value is useful when considering the tunnel in its entirety (similar to the LMTD for heat transfer in heat exchangers).

5.2 MASS FLOW RATE OF AIR

The air mass flow rate drawn through the tunnel is determined by measuring the pressure drop over 2 elliptically shaped nozzles mounted in a plate in the measuring box at the outlet of the tunnel.

The mass flow rate is given by the following equation [04KR1]

$$m = C_n \Phi_g Y A_n (2\rho_n \Delta p_n)^{0.5}$$

C_n, the nozzle coefficient of discharge is a function of the Reynolds number. The following apply:

$30\,000 < Re_n < 100\,000$

$$C_n = 0.954803 + 6.37817 \times 10^{-7} Re_n - 4.65394 \times 10^{-12} Re_n^{\,2} + 1.33514 \times 10^{-17} Re_n^{\,3}$$

$100\,000 < Re_n < 350\,000$

$$C_n = 0.9758 + 1.08 \times 10^{-7} Re_n - 1.6 \times 10^{-13} Re_n^{\,2}$$

$Re_n > 350\,000,\ C_n = 0.994$

The gas expansion factor, Φ_g, is given by

$$\Phi_g = 1 - \frac{3\Delta p_n}{4 p_u c_p / c_v}$$

where $c_p / c_v = 1.4$ for air

p_u is the upstream pressure

Y, the approach velocity factor is given by

$$Y = 1 + 0.5(A_{up}/A_{tus})^2 + 2(A_n/A_{tus})^2 \frac{\Delta p_n}{p_u c_p / c_v}$$

where A_n and A_{tus} are the nozzle and upstream tunnel areas respectively.

Each nozzle must be viewed independently and the mass flow rates added together to obtain the total mass flow rate. The pressure drop over each nozzle is the same, but since the nozzle throughflow areas differ, so will the mass flow rates. A provisional mass flow rate is calculated by setting the coefficient of discharge equal to one. The Reynolds number through the nozzle may now be determined; the coefficient of discharge calculated and an improved Reynolds number obtained.

Calculate values for nozzle number 1 which has a diameter of 0.05 m. The nozzle area is

$$A_{n1} = \frac{\pi}{4} d_1^{\,2} = 0.001963 \text{ m}^2$$

Setting $C_n = 1$

$$m_{provisional} = \Phi_g Y A_n (2\rho_n \Delta p_n)^{0.5}$$

Calculate the gas expansion factor Φ_g

$$\Phi_g = 1 - \frac{3\Delta p_n}{4 p_u c_p / c_v}$$

where

$p_u \approx p_{atm}$ since the pressure drop over the grass surface is negligible (about 10 Pa)

The pressure drop over the nozzle is 821.30 Pa

$$\Phi_g = 1 - \frac{3 \times 821.31}{4 \times 100000 \times 1.4}$$
$$= 0.995600$$

Calculate Y, the approach velocity factor for the values

$A_{n1} = 0.001963 \text{ m}^2$

$A_{tus} = 0.62 \text{ m}^2$

$\Delta p_{n1} = 821.31 \text{Pa}$

$p_u = 100000 \text{ Pa}$

$c_p / c_v = 1.4$

$$Y = 1 + 0.5(A_{up} / A_{tus})^2 + 2(A_n / A_{tus})^2 \frac{\Delta p_n}{p_u c_p / c_v}$$

Substituting the above find

$$Y = 1 + 0.5(0.001963 / 0.62)^2 + 2(0.001963 / 0.62)^2 \frac{821.31}{100000 \text{x} 1.4}$$

$$= 1{,}000005$$

For the calculation of the provisional mass flow rate, the density of the atmospheric air through the nozzle is needed: this value will be the density of the air calculated at the outlet state since the air that flows through the nozzles is assumed to be at the same state as the air at the outlet of the tunnel: i.e. $\rho_{ave,o} = 1.1172 \text{ kg/m}^3$.

$$m_{1\,provisional} = 1 \times 0.995600 \times 1.000005 \times 0.001963 \times (2 \times 1.1172 \times 821.31)^{0.5}$$
$$= 0.0837 \quad \text{kg/s}$$

A similar calculation for nozzle number 2 which has a diameter of 0.075 m follows.

The nozzle area

$$A_{n2} = \frac{\pi}{4} d_2^{\,2}$$
$$= 0.004418 \text{ m}^2$$

Setting $C_n = 1$

$$m_{provisional} = \Phi_g Y A_n (2\rho_n \Delta p_n)^{0.5}$$

The gas expansion factor Φ_g will be the same as for nozzle 1 since all relevant values remain the same.

calculate Y, the approach velocity factor for the values

$A_{n1} = 0.004418\ m^2$

$A_{tus} = 0.62\ m^2$

$\Delta p_{n2} = 821.31 Pa$

$p_u = 100000$

$c_p / c_v = 1.4$

$$Y = 1 + 0.5(A_{up} / A_{tus})^2 + 2(A_n / A_{tus})^2 \frac{\Delta p_n}{p_u c_p / c_v}$$

Substituting the above find

$$Y = 1 + 0.5(0.004418 / 0.62)^2 + 2(0.004418 / 0.62)^2 \frac{821.31}{100000 x 1.4}$$

$$= 1{,}000025$$

$$m_{2\,provisional} = 1 \times 0.995600 \times 1.000025 \times 0.004418 \times (2 \times 1.1172 \times 821.31)^{0.5}$$

$$= 0.1884 \quad kg/s$$

The Reynolds number for each nozzle may now be calculated from

$$Re_n = \frac{\rho_n d_n V_n}{\mu}$$

Since

$$m = \rho \frac{\pi}{4} d_n^{\,2} V_n$$

find

$$Re_n = \frac{4m}{\pi d_n \mu}$$

Substitute and find

$$Re_{n1} = \frac{4 \times 0.0837}{\pi \times 0.05 \times 1.856 \times 10^{-5}}$$

$$= 114910$$

Inserting this value in the equation for the nozzle coefficient for

$100000 < Re_n < 300000$

find

$$C_n = 0.9758 + 1.08\times10^{-7}\,Re_n - 1.6\times10^{-13}\,Re_n^{\,2}$$
$$= 0.9758 + 1.08\times10^{-7}\times114910 - 1.6\times10^{-13}\times114910$$
$$= 0.98642$$

The mass flow rate may now be calculated incorporating the nozzle coefficient i.e.

$$m_1 = C_n\Phi_g Y\, A_n(2\rho_n\ \Delta p_n)^{0.5}$$

$$= 0.98642\times0.995600\times1.000005\times0.001963(2\times1.1172\times821.31)^{00.5}$$

$$= 0.0826\ \text{kg/s}$$

From this an improved Reynolds number may be calculated and an improved nozzle coefficient calculated until the same value for the mass flow rate is found in at least two subsequent calculations. One further calculation confirmed the mass flow rate to be the same value.

The final mass flow rate for nozzle 1 is found to be

m_1 = 0.0826 kg/s

Similarly for nozzle 2,

Find the provisional Reynold's Number

$$Re_{n2} = \frac{4\times0.1884}{\pi\times0.075\times1.856\times10^{-5}}$$
$$= 172368$$

The nozzle coefficient, C_n, is calculated to be

C_{n2} = 0.99002

The mass flow rate may now be calculated incorporating the nozzle coefficient i.e.

$$m_2 = C_n\Phi_g Y\, A_n(2\rho_n\ \Delta p_n)^{0.5}$$
$$= 0.99002\times0.995600\times1.000026\times0.004418(2\times1.1172\times821.31)^{0.5}$$
$$= 0.1865\ \text{kg/s}$$

This is also found to be the final mass flow rate through nozzle 2

The total mass flow rate through the tunnel is therefore:

$$m = m_1 + m_2 = 0.0832 + 0.1865$$

$$= 0.2691\ \text{kg/s atmospheric air}$$

This must be converted to an air flow rate of kg/s dry air.

$$m_{\text{dry air}} = \frac{m_{\text{atmospheric air}}}{1+w_{\text{outlet}}} = \frac{0.2691}{1+0.02392}$$

$$= 0.2628\ \text{kg/s da}$$

5.3 MEASURED RATE OF EVAPOTRANSPIRATION IN THE TUNNEL

The specific humidity ratio at the inlet and the outlet of the tunnel has already been determined, as has the dry air mass flow rate. From this the actual average rate of evapotranspiration may be calculated.

$$m_v / A = \frac{m_{dry\ air}(w_{outlet} - w_{inlet})}{A} = \frac{0.2628\ (0.02392 - 0.01161)}{16}$$

$$= 0.2022 \times 10^{-3}\ kg/m^2s$$

where A is the projected horizontal area of the grass surface in the tunnel.

CHAPTER 6

SAMPLE CALCULATION: INVESTIGATING THE EFFECTIVE CONVECTIVE HEAT TRANSFER COEFFICIENT

6.0 INTRODUCTION

Apart from atmospheric data, the Penman equation is dependent on the heat transfer coefficient between the evaporating surface and the air flowing over it. The heat transfer coefficient is always problematic as is shown by the large amount of research on the subject. [48PE1], [51PE1], [68WA1], [75TH1], [83FR1], [86AL1], [89DJ1], [90MO1], [92RA1], [94AL1], [94AL2], [00SA1], [04FA1]. Various options are investigated and the one chosen which best agrees with the measured data. It was found that the predicted grass temperature which corresponds closest to the measured grass temperature is the parameter to be scrutinized when determining the most suitable effective convective heat transfer coefficient.

The pressure drop over the tunnel is measured for various air velocities and the Darcy friction factor determined. This is not strictly accurate since the flow is not adiabatic but is the best under the circumstances. Nobel [74NO1] gives a value of between 30 s/m and 100 s/m as the boundary layer resistance for a leaf under outdoor conditions: it is expected that the boundary layer values calculated from the effective convective heat transfer coefficient should fall within this range, the velocities being within the same limits as outdoor conditions.

It must be stated here that in the application of this research to the solar chimney power plant, provision must be made for the boundary layer and accompanying transfer coefficient differences between the smaller experimental tunnel and the larger system.

6.1 EXPERIMENTAL VALUES FOR THE FRICTION COEFFICIENT

The drop in static pressure over the tunnel, at different velocities, was measured on a day that the grass was cut, and shown in Figure 6.1 below.

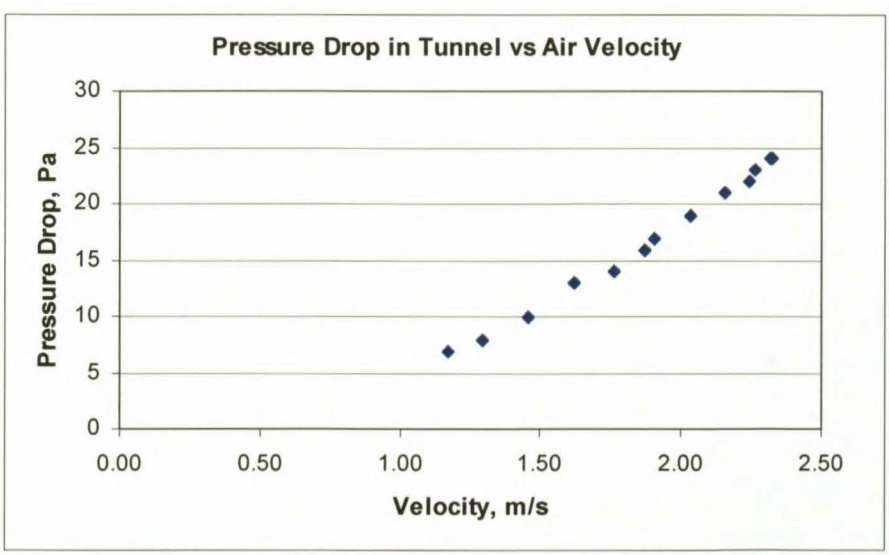

Figure 6.1: Pressure drop over tunnel vs. air velocity

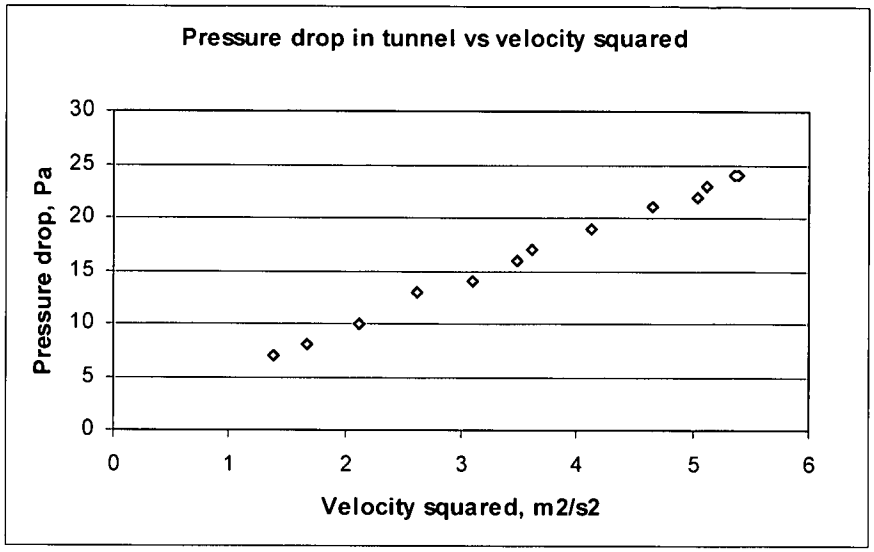

Figure 6.2: Pressure drop over tunnel vs. air velocity[2]

The pressure drop over the tunnel may be utilized to determine the Darcy friction factor. Considering equation (D.34) and rewriting, find

$$f_D = \frac{\Delta p}{\frac{\rho V^2}{2}\frac{L}{d}}$$

For duct flow of a non-circular section the Reynolds number is based on the hydraulic diameter defined as

$$d_e = \frac{4 \times \text{flow area}}{\text{wetted perimeter}}$$

For turbulent flow the friction factor is most accurately predicted when an effective diameter, D_{eff}, equal to 0.64 times the hydraulic diameter, d_e is employed [83HA1].

The distance between the grass surface and the glass roof is about 0.15 m, and the tunnel is 1 m wide, so that an effective diameter can be calculated:

$$D_{eff} = 0.64\left(\frac{4 \times 0.15 \times 1}{2.3}\right) = 0.167\text{m}$$

Utilizing this approach, find L/d = 16/0.167 = 95.833 and from this the Darcy friction factor was calculated and then tabulated in Table 6.1.

Table 6.1: Darcy friction factor from pressure drop measurements

Velocity in tunnel, m/s	Pressure drop in tunnel, Pa	Darcy friction factor
1.175	7	0.105633
1.292	8	0.099848
1.456	10	0.098277
1.616	13	0.103714
4	14	0.09427
1.867	16	0.095633
1.902	17	0.097905
2.031	19	0.095964
2.156	21	0.094123
2.244	22	0.091023
2.261	23	0.093735
2.314	24	0.093381
2.322	24	0.092739

The average Darcy friction factor was found to be $f_D = 0.095885$

From this the Fanning friction factor is found

$f_{fanning} = f_D / 4 = 0.095885 / 4 = 0.02397$

so that

$f_{fanning} / 2 = 0.011986$

6.2 VARYING PRESSURE DROP OVER GRASS ON CONSECUTIVE DAYS

Measurements were made of the pressure drop over the grass tunnel on consecutive days during the month of February and are tabulated below. It must be pointed out that although the entering air temperatures varied due to varying weather conditions on the different days, the entering air temperatures did not differ by more than 5 °C from each other.

Table 6.2: Pressure drop over grass for different lengths

Pressure Drop Readings Over Tunnel During the Month of February				
	Pressure Drop over grass	Pressure Drop over nozzle	Velocity of air over grass	Darcy friction
February	del p tunnel	del p nozzle	approx vel	factor
6	5	1262	2	0.0300
7	6	1300	2.05	0.0343
8	8	1276	2.04	0.0462
9	8.3	1248	2	0.0498
10	8.8	1286	2.04	0.0508
11	10	1300	2.05	0.0571
12	11.3	1269	2.03	0.0658
13	13.7	1294	2.04	0.0790
14	13	1244	2	0.0780
15	12.6	1214	1.95	0.0796
16	13.8	1250	2	0.0828
17	14.7	1258	2	0.0882
18	22	1703	2.35	0.0956
19	23	1729	2.36	0.0991
20	24	1735	2.36	0.1035

From the table above it is evident that as the grass grows so does the friction loss. The Darcy friction factor increases from 0.03 to 0.088 for similar air velocities since the pressure drop over the grass increased from 5 Pa to 14.7 Pa. This has implications for the effective heat transfer coefficient.

It is to be noted from pressure drop measurements made on a day the grass was cut (refer to Table 6.1), that the pressure drop for a similar velocity was higher, viz. 17 Pa, implying that newly cut grass seems to represent a rougher surface than longer grass where the blades of grass have more flexibility and yet where the friction loss increases with increasing grass length.

Investigating what the pressure drop would be if the entire tunnel surface were smooth, for turbulent flow in smooth pipes, Filonenko [04KR1] gives

$f_D = (1.82 \log_{10} Re - 1.64)^{-2}$

Utilizing the following average values for the properties of air as it flows through the tunnel:

$\rho = 1.1286\,\text{kg air} - \text{vapor}/\text{m}^3$

$\mu = 1.852 \times 10^{-5}\,\text{kg}/\text{ms}$

$V = 2\,\text{m}/\text{s}$

$D_e = 0.26$

$$Re = \frac{1.1286 \times 0.26 \times 2}{1.852 \times 10^{-5}} = 31689, \text{ find}$$

$$f_D = \left(1.82 \log_{10} 31689 - 1.64\right)^{-2} = 0.0233$$

$$f = f_D / 4 = 0.0058$$

Calculating the pressure loss over the tunnel, find

$$\Delta p = f_D \left(\frac{L}{D_e}\right) \frac{\rho V^2}{2} = 0.0233 \left(\frac{16}{0.26}\right) \frac{1.1286 \times 2^2}{2} = 3.236\ \text{Pa}$$

The influence of the state of the grass was not investigated thoroughly as part of this thesis since it was endeavoured to keep as close as possible to the "reference" grass, i.e. to keep the grass as short as possible and hence for calculation purposes a constant Fanning friction factor of 0.02397 will be used. This implies an unchaging roughness and it is recognized that this may influence the accuracy of calculations and it is suggested that further research be done in this regard. The implications of different values for the friction loss and hence the effective convective heat transfer coefficient, will be more fully discussed further on in the chapter.

6.3 THE CONVECTIVE HEAT TRANSFER COEFFICIENT BETWEEN THE GRASS AND THE AIR

6.3.1 The Reynolds-Colburn Analogy

The Reynolds-Colburn analogy can be applied to determine the convective heat transfer coefficient using various empirical and semi-empirical equations.

The Reynolds-Colburn analogy states that $St\ \ \text{Pr}^{2/3} \approx \frac{f}{2}$ (D.17)

Where f is the Fanning friction factor.

It is recognized that this equation applies to laminar and turbulent flow over a flat plate. The flow in the tunnel starts off as flow over a flat plate until the boundary layers above the grass and below the glass meet each other and thereafter it can be viewed as flow in a pipe or between parallel plates.

If the surface of the tunnel were smooth, the distance from the entrance to the tunnel may be determined where the upper and lower boundary layers meet if the flow were to be viewed as flow between parallel plates.

The thickness of the boundary layer for laminar flow is given by

$$\frac{\delta}{x} = \frac{5}{Re_x^{0.5}} \qquad (D.2)$$

For

$$\delta = H/2 = 0.15/2 = 0.075m$$

$$Re = \frac{\rho V x}{\mu}, \text{ find}$$

$$x = 5.24m$$

For turbulent flow, the thickness of the boundary layer is given by

$$\frac{\delta}{x} \approx \frac{0.16}{Re_x^{1/7}} \qquad (D.21)$$

find

x = 2.9 m

Since the grass surface is very rough, the laminar flow should become turbulent between 1 to 2 m from the inlet. The tunnel is 16 m long and since the growth of the boundary layer above the grass is complex and beyond the scope of this thesis, the flow will be viewed as fully turbulent for the entire tunnel and modelled accordingly.

Applying the Reynolds-Colburn analogy to determine the effective convective heat transfer coefficient, find

$$St_x\, Pr^{2/3} = (h_{cgF}/\rho c_{pma} V)Pr^{2/3} \approx \frac{f}{2} \quad \text{or}$$

$$h_{cgF} = \frac{f/2}{Pr^{2/3}} \rho c_{pma} V$$

From sample calculations done in Chapter 5, the average specific heat capacity and density of the air are the following

$$c_{pma,ave} = (c_{pmai} + c_{pmao})/2 = (1027.31 + 1051.56)/2 = 1039.44 J/kgK$$

$$\rho_{ave} = (\rho_i + \rho_o)/2 = (1.1400 + 1.1172)/2 = 1.1286 kg/m^3 \text{atmospheric air}$$

$$Pr_{ave} = \frac{\mu_{ave} c_{pma,ave}}{k_{ave}} = \frac{(1.848 + 1.856)\times 10^{-5}/2 \times 1039.44}{(0.02633 + 0.02655)/2} = 0.7281$$

For the average value of the velocity of the air in the tunnel, find

$$V_{ave} = m_{atm\,air}/\rho_{ave} A = 0.2691/(1.1286 \times (1 \times 0.15)) = 1.5896\ m/s$$

For a friction coefficient f/2 = 0.023971/2 = 0.011986, find

$$h_{cgF} = \frac{0.011986}{0.7281^{2/3}} \times 1.1286 \times 1039.44 \times 1.5896 = 27.645 \text{ W/m}^2$$

For uniform heat flux the Nusselt number is about 4% higher than for a constant temperature [04KR1] so that the convective heat transfer coefficient would be

$$h_{cgF,\text{uniform heat flux}} = 1.04 \times h_{cgF} = 27.645 \times 1.04 = 28.751 \text{W/m}^2\text{K}$$

The boundary layer resistance can now be calculated since

$$r_H \equiv \frac{c_{pma} \times \rho}{h_{cgF}} \text{ s/m, find therefore} \qquad \text{(A.27)}$$

$$r_H = \frac{1039.44 \times 1.1286}{28.751} = 40.8 \text{ s/m}$$

This value does indeed lie in the range given by Nobel [74NO1] of between 30 and 100 s/m.

Monteith [81MO1] states a value of about 40 s/m for the boundary layer resistance for one side of a leaf with a characteristic dimension of 5 cm for a wind speed of 0.5 m/s.

6.3.2 The Burger-Kröger Convective Heat Transfer Coefficient (Approach A)

This convective heat transfer coefficient may be applied to upward facing surfaces where the temperature of the fluid above the surface is lower than the surface temperature. For a smooth surface with a surface friction factor $C_f/2$ subject to uniform heat flux the Burger-Kröger equation [06BU1] gives

$$h_{cgF}\left[\frac{\mu T_m}{g(T_g - T_F)c_p k^2 \rho^2}\right]^{1/3} = 0.2106 + C_f/2 v_w \left[\frac{\rho T_m}{\mu g(T_g - T_F)}\right]^{1/3} \qquad \text{(D.31)}$$

where T_m is the average temperature between the grass surface at temperature T_g and the air with which it is in contact at T_F.

The equation is applicable for an air velocity, 0 m/s < v_w < 4 m/s and where

$$0 < v_w \left[\frac{\rho T_m}{\mu g(T_g - T_a)}\right]^{1/3} < 160 \text{ and for } \Delta T \geq 4 \text{ °C}$$

This equation has been obtained for a flat plate with the friction factor $C_f/2 = 0.0026$. A Fanning friction factor of $f/2 = f_D/8 = 0.011986$ will be used for the grass surface.

The measured grass temperature, T_g= 37.05 °C (310.20 K)

The average air temperature, T_F = (303.01+307.43)/2 = 305.22 K

The mean temperature, T_m is the average of the surface and air temperatures

$$T_m = (305.22 + 310.20)/2$$
$$= 307.71 \text{ K}$$

$$h_{cgF}\left[\frac{1.848x10^{-5}x307.71}{9.81(310.20-305.22)1039.43(0.026445)^2(1.129)^2}\right]^{1/3}$$

$$=0.2106+0.011986x1.59\left[\frac{1.129x307.71}{1.848x10^{-5}x9.81(310.20-305.22)}\right]^{1/3}$$

$$=4.2+27.62=31.82\ W/m^2K$$

The first term in the above equation is the influence of the temperature difference between the grass and the air and the second term is that due to the surface roughness and the velocity. This value is close to that found in the Reynolds-Colburn analogy.

Inserting this value into (A.27), find the boundary layer resistance to be

$$r_H=\frac{1039.44\times1.1286}{31.82}=36.87\,s/m$$

When the temperature difference is less than 4 °C, for a smooth surface, Kröger suggests

$$h_{cgF}=3.87+0.0022\left(\frac{V\rho c_p}{Pr^{2/3}}\right)\ W/m^2K \qquad (D.4)$$

Inserting a value of 0.011986 in the place of the smooth surface friction factor of 0.0022, find

$$h_{cgF}=3.87+0.011986\left(\frac{V\rho c_p}{Pr^{2/3}}\right)=3.87+0.011986\left(\frac{1.59\times1.129\times1039.43}{0.7281^{2/3}}\right)$$

$$=3.87+27.63=31.5\,W/m^2K$$

and

$$r_H=\frac{1039.44\times1.1286}{31.5}=37.24\,s/m$$

The temperature difference between the grass surface and the air flowing over it is usually about 4 °C and lower so that this equation will be used. It is seen that the two values are very similar since the temperature difference for this particular time of day is about 5 °C.

6.3.3 The FAO Penman-Monteith equation (Approach B)

The FAO Penman-Monteith equation for a hypothetical grass surface gives the boundary layer resistance as

$$r_H=208/u_z\ \ s/m \qquad (D.38)$$

where the velocity is measured at 2 m above the grass surface. The convective heat transfer coefficient is given by

$$h_{cgF}=\frac{c_{pma}\rho}{r_H}=\frac{c_{pma}\rho}{208/u_z}\ W/m^2K \qquad (A.27)$$

Using average values for the air flowing through the tunnel where

$\rho_{ave} = 1.129\ kg/m^3$

$c_{pma} = 1039.437\ J/kgK$

$u_z = 1.589\ m/s$

Inserting, find

$$h_{cgF} = \frac{1039.437x1.129}{208/1.589} = 8.965\ W/m^2K$$

and

$$r_H = 208/1.589 = 130.89\ s/m$$

This value for the effective convective heat transfer coefficient is a great deal lower than the ones previously obtained. However, it must be stressed that the circumstances under which the FAO equation was empirically derived and being applied is very different from the flow situation in the tunnel and a difference is to be expected. The implication of this difference is discussed below.

6.3.4 Comparing the Burger-Kröger convective heat transfer coefficient (Approach A) and the FAO Penman-Monteith approach (Approach B)

Consider the following equations all related to the Penman-Monteith equation

$$(m_v/A)_{total} i_{fg} = \frac{h_{cgF}(vpd) + \Delta I_{net}}{\Delta + \gamma^*}\ J/m^2s \qquad (A.69)$$

$$\gamma^* = \left(\frac{r_s + r_H}{r_H}\right)\gamma = (1 + r_s/r_H)\gamma\ Pa/K \qquad (A.72)$$

and

$$T_g = T_F + \frac{1}{(\Delta + \gamma^*)}\left(\frac{\gamma^* I_{net}}{h_{cgF}} - vpd\right)\ °C \qquad (A.81)$$

Consider the relationship between the effective convective heat transfer coefficient, h_{cgF} and γ^*.

$$\text{Since } r_H \equiv \frac{c_{pma} \times \rho}{h_{cgF}}\ s/m \qquad (A.27)$$

$\gamma^* = \gamma(1 + r_s h_{cgF}/c_{pma}\rho)$ Pa/K, therefore

$$(m_v/A)_{total} i_{fg} = \frac{h_{cgF}(vpd) + \Delta I_{net}}{[\Delta + \gamma(1 + r_s h_{cgF}/c_{pma}\rho)]}\ J/m^2s$$

The above equation shows that the effective convective heat transfer coefficient appears twice in the equation neutralizing the effect somewhat. However, considering equation (A.81), for the surface temperature, the same does not apply: The effective convective heat transfer coefficient appears only once and shows that the lower the coefficient, the higher will be the predicted surface temperature. A numerical example serves to illustrate these influences.

Keeping the following values constant for both approaches, viz.

vpd = 2216 Pa

$I_{net} = 628.91\ W/m^2$

$\Delta = 187.72\ Pa/K$

$\gamma = 68\ Pa/K$

The stomatal resistance is 70 s/m and $\gamma^* = \gamma(1 + r_s / r_H) = 68(1 + 70/r_H)$ Pa/K

For approach A, find

$\gamma^* = 68(1 + 70/37.24) = 195.81\ Pa/K$

$$(m_v / A)_{total} i_{fg} = \frac{31.5 \times (2216) + (195.81 \times 628.91)}{187.72 + 195.81} = 503.09\ J/sm^2$$

This is the energy associated with the water evaporated.

$$T_g = T_F + \frac{1}{(187.72 + 195.81)}\left(\frac{195.81 \times 628.91}{31.5} - 2216\right) = T_F + \frac{3909.42 - 2216}{383.53}$$
$$= T_F + 10.19 - 5.78 = T_F + 4.41\ °C$$

This implies that the grass surface temperature is about 4.41 °C above the air temperature.

For approach B:

$\gamma^* = 68(1 + 70/130.89) = 104.36 Pa/K$

$$(m_v / A)_{total} i_{fg} = \frac{8.965 \times (2216) + 187.72 \times 628.91}{187.72 + 104.36} = 472.22\ J/sm^2$$

This value of the energy associated with the water evaporated differs from that in approach A by about 6 %. This serves to illustrate that reducing the effective convective heat transfer coefficient from 31.5 W/m^2K to 8.96 W/m^2K results in a 6 % decrease in predicting the rate of evapotranspiration under similar conditions.

However, considering the surface temperature:

$$T_g = T_F + \frac{1}{(187.72 + 104.36)}\left(\frac{104.36 \times 628.91}{8.965} - 2216\right) = T_F + \frac{7322.911 - 2216}{292.1068}$$
$$= T_F + 25.069 - 7.5863 = T_F + 17.483\ °C$$

The above calculation implies that the grass surface temperature is predicted to be 17.4 °C higher than the surrounding air temperature. This is where error will be detected when using the incorrect effective convective heat transfer coefficient. It must be pointed out however, that the higher the predicted grass temperature above the air temperature, the higher the infrared radiation between the grass and the glass (glass temperature usually lower than the grass temperature during periods of maximum radiation) and the convective heat transfer from the grass to the air. The two facts together imply that the net radiation absorbed by the grass in situation B is not quite as high as calculated and the predicted grass temperature will therefore also be lower. The infrared radiation exchange varies to the fourth power and a calculation needs to be done to see the effect of this surface temperature.

Consider for example a constant glass temperature of 37.73 °C and an average air drybulb temperature of

$T_{A,ave} = (T_{dbin} + T_{dbout})/2 = (29.866 + 34.28)/2 = 32.073\ °C$, find

$$T_g = 37.073 + 17.483 = 54.55\ °C$$

This is much higher than the grass can survive!

The infrared radiation exchange for these values given by equation (A.83)

$$I_{ir}/A = \frac{\sigma(T_g^4 - T_R^4)}{\frac{1}{\varepsilon_g} + \frac{1}{\varepsilon_R} - 1} = \frac{5.669 \times 10^{-8}(273.15 + 54.55)^4 - (273.15 + 37.73)^4}{\frac{1}{0.96} + \frac{1}{0.88} - 1} = 105.5\ W/m^2$$

The net radiation can now be determined as

$$I_{net} = 628.91 - 105.5 = 523.41\ W/m^2$$

For this net radiation value, calculate the surface temperature to be

$$T_g = T_F + \frac{1}{(187.72 + 104.3868)}\left(\frac{104.3868 \times 523.4}{8.965} - 2216\right) = T_F + \frac{6094.47 - 2216}{292.1068}$$

$$= T_F + 20.8636 - 7.5863 = 37.073 + 13.34 = 50.41\ °C$$

This is still a very high temperature.

It was found that the measured grass temperatures are closer to the value predicted using approach A. The calculations to predict the exit state of the air from the inlet state will be based on the higher convective heat transfer coefficient determined by the empirical Burger-Kröger equation.

6.4 THE CANOPY OR STOMATAL RESISTANCE

During experimentation it was endeavoured to keep as close to the "reference" grass state, i.e. "an extended surface of an 80 mm to 150 mm tall grass cover of uniform height actively growing, completely shading the ground and not deficient in water or nutrients" [77PR1]. This implies a canopy resistance of 70 s/m [94AL1] provided all requirements are met. However, the canopy resistance will increase due to stomatal closure by the plant under stressed situations, be it excessively high air temperatures or any problem in the plumbing system of the plant. Water depletion in the soil will increase the canopy resistance since there is an added resistance at root level and the plant will not be able to obtain sufficient water to keep pace with the transpiration. This will lead to higher grass temperatures and the stomata may even close in order to counteract the water loss. The above will result in a predicted value of evapo-transpiration being higher than the measured value and an average grass temperature lower than the measured value. This was especially noticeable in the afternoons when the soil water content would have been much lower than in the morning. Test results confirmed this theory.

6.5 THE CONVECTIVE HEAT TRANSFER COEFFICIENT BETWEEN THE GLASS ROOF AND THE AIR

The glass roof is a downward facing surface and for this Kröger [06BU1] suggests for a smooth surface the following empirical equation.

$$h_{cRF} = 3.87 + 0.0022\left(\frac{V\rho c_p}{Pr^{2/3}}\right) = 3.87 + 0.0022\left(\frac{1.589 \times 1.129 \times 1039.437}{0.7281^{2/3}}\right) = 8.944\ W/m^2K$$

CHAPTER 7

SAMPLE CALCULATION: PREDICTING THE EXIT STATE OF THE AIR

7.0 INTRODUCTION

The application of the Penman-Monteith equation for determining the amount of evapotranspiration taking place, as well as the conservation equations to subsequent one meter lengths of the tunnel, make it possible to predict the exit state of the air leaving the tunnel when starting off with the measured and known inlet state of the air and the measured radiation. The mass flow rate of the air is also known. It must be stated that the glass roof temperature varied by a maximum of 1.5 °C from inlet to outlet and consequently a constant average glass temperature was used for the entire tunnel. The measured grass temperature was used as an initial value in determining the infrared radiation exchange between grass and roof and the final value determined iteratively. Alternately, from experience, an initial grass temperature of about 4 °C higher than the air temperature could have been used.

The average rate of evapotranspiration, the average grass temperature as well as the exit state of the air can be determined and these values compared with measured values. The exit state of the air determines the density and hence the change in density can be calculated and compared with the situation where no vegetation would be present and given similar atmospheric and other conditions.

The Penman-Monteith equation is given by

$$(m_v / A)_{total}\, i_{fg} = \frac{h_{cgF}(vpd) + \Delta I_{nett}}{\Delta + \gamma^*} \ J/m^2s \qquad (A.69)$$

Where h_{cgF} is the convective heat transfer coefficient between the surface (grass) and the air (fluid) flowing over it, W/m^2K.

The calculation is done for a single hour viz. solar hour 13h36 using values obtained from the overall calculation spreadsheet for a beginning value as well as values which are viewed as constants for the entire calculation for this hour. The specific heat of the dry air varies slightly with temperature but since the temperature varies by a maximum of 5 °C this is ignored. In order to have an average value of the temperatures involved at this specific hour, accumulated average values were used i.e. the average of readings 5 minutes before, on the hour and 5 minutes after the specific hour.

The following properties are viewed as constant:

Convective heat transfer coefficient between the grass surface and the free stream air, h_{cgF}=31.83 W/m^2K

Convective heat transfer coefficient between the glass roof and the free stream air, h_{cRF} = 8.94 W/m^2K

Constant pressure specific heat of dry air c_{pda} = 1005.534 J/kgK

Constant pressure specific heat of water vapor c_{pv} = 1875.280 J/kgK

Latent heat of evaporation at the inlet wetbulb temperature i_{fg} = 2413819 J/kgK

Average temperature of the glass roof T_R = 37.73 °C

Atmospheric pressure p_{atm} = 100000 Pa

Mass flow rate of dry air m_a = 0.2635 kg/s dry air

Nett radiation absorbed by grass I_{net} = 624.79 W/m^2

γ^* = 197.06 Pa/K

Average velocity of air through tunnel = 1.589 m/s

For the evapotranspiration, a distinction is made between the sunlit and shaded grass areas. The area of the control volume is 1 m^2.

7.1 CALCULATION OF THE VALUES NEEDED FOR THE PENMAN-MONTEITH EQUATION

The following accumulated average values for 15 December, solar hour 13.36h, are used for this sample calculation.

Average drybulb temperature at tunnel inlet T_{ai} = 29.86 °C

Average wetbulb temperature at tunnel inlet T_{wbi} = 20.56 °C

Average drybulb temperature at tunnel outlet T_{ao} = 34.28 °C

Average wetbulb temperature at tunnel outlet T_{wbo} = 29.05 °C

Average temperature of the glass roof T_R = 37.28 °C

Average temperature of the grass surface T_g = 37.05 °C

Atmospheric pressure p_{atm} = 100000 Pa.

7.1.1 Net radiation through the glass roof

The solar energy, both beam and diffuse, reaching the horizontal glass roof is measured by a Kipp & Zonen pyranometer. This was found to be I_{b+d} = 1006.36 W/m^2 from the pyranometer.

The glass transmissivity must be calculated in order to determine the amount of direct and diffuse radiation transmitted through the glass.

In order to calculate this, several other conversions and calculations are required, viz.

Conversion of clock time to solar time

Calculation of the solar angles

Calculation of the radiative properties of glass.

7.1.1.1 Conversion of local time to solar time

All solar angles are dependent on the solar hour and therefore require that the local time be converted to the solar time. Firstly a correction for the difference in longitude between the observer's meridian, $L\phi_l$, and the meridian (or longitude) on which the local standard time is based, $L\phi_m$, and secondly the Equation of Time, EOT, which accounts for the daily variation in the sun's orbit and which is a function of the day of the year.

In South Africa the standard meridian longitude, $L\phi_m$=30 ° E, and for Stellenbosch the meridian, $L\phi_l$ = 18.85 ° E.

The time correction for this geographical position is given by [52NB1]

$$\text{Time correction} = 4(L\phi_m - L\phi_l) = 4(30 - 18.85) = 44.6 \text{ minutes}$$

Solar time = Local time –44.6 + EOT

The Equation of Time, EOT [52NB1]

EOT = 2.292 (0.0075 + 0.18 cos B – 3.2077 sin B – 1.4615 cos 2B – 4.089 sin 2B) minutes

where $B = (n-1)\frac{360}{365}$ and

n = day of the year (table B.1)

For December 15, the value of n is 349. Substituting into the above equation find

$$EOT = 2.292\ (0.0075 + 0.18\ \cos\left[(n-1)\frac{360}{365}\right] - 3.2077\ \sin\left[(n-1)\frac{360}{365}\right] - 1.4615$$

$$\cos 2\left[(n-1)\frac{360}{365}\right] - 4.089\ \sin 2\left[(n-1)\frac{360}{365}\right]) \text{ minutes} = 4.5 \text{ minutes}$$

Local time of 14h02 (i.e. 14.03hrs) results in a solar hour of

Solar time = local time – 44.6/60 + 4.5/60 = 14.03-0.6683 = 13.36 h

7.1.1.2 Calculation of the solar angles

Calculation of the zenith angle, θ_z for a horizontal surface is given by

$$\cos\theta_z = \cos\phi\cos\delta\cos\omega + \sin\phi\sin\delta \qquad \text{(B.2)}$$

ϕ is the latitude angle. For Stellenbosch ϕ = 33.93 ° S

δ is the declination, the angular position of the sun at solar noon with respect to the plane of the equator, South negative.

$$\delta = -\left[23.45\sin(360\times\frac{284+DOY}{368}\right]^\circ \qquad \text{(B.3)}$$

where the Day of the Year (DOY) is 349. The declination is found to be

$$\delta = -\left[23.45\ \sin(360\times\frac{284+349}{368}\right]^\circ = -23.34^\circ$$

ω, the hour angle is given by

$$\omega = 15\left[\psi - 12 - \frac{4(L\phi_m - L\phi_l) - EOT}{60}\right]^\circ \qquad \text{(B.4)}$$

where ψ is the decimal hour after midnight (local time)

$L\phi_m$ the standard meridian for the time zone applicable (30 °E for South Africa)

$L\phi_l$ the longitude angle of the geographical location (18.85 °E for Stellenbosch)

$$\omega = 15\left[14.03 - 12 - \frac{4(30\ -18.85) - 4.5}{60}\right] = 20.11^\circ \text{ (0.351 radians)}$$

Substituting these values find the azimuth angle to be

$\cos\theta_z = \cos(-33.93)\cos(-23.34)\cos(20.11) + \sin(-33.93)\sin(-23.34) = 0.9365$ or

$\theta_z = 20.53\,°$

7.1.1.3 Calculation of the radiative properties of glass

Calculation of the reflectivity, transmissivity and absorptivity of a glass slab.

For radiation passing from one medium with refractive index n_1 to medium two with refractive index n_2 the following applies:

$$\frac{n_1}{n_2} = \frac{\sin\theta_2}{\sin\theta_1} \tag{B.9}$$

where θ_1 and θ_2 are the angles of incidence and refraction respectively.

For a horizontal surface receiving beam radiation the angle of incidence is also equal to the zenith angle, i.e.

$\theta_1 = \theta_z = 20.53°$

For air the refraction index is nearly unity, and for glass the index is 1.526

$n_1 = 1$ if medium one is air and

$n_2 = 1.526$ for glass as the second medium

so that

$$\sin\theta_2 = \frac{\sin\theta_1}{1.526} = 0.6553\sin\theta_1 \tag{B.10}$$

inserting the value of 20.53° for θ_z find

$\theta_2 = 13.29°$

$$r_\perp = \frac{\sin^2(\theta_2 - \theta_1)}{\sin^2(\theta_2 + \theta_1)} = \frac{\sin^2(13.29 - 20.11)}{\sin^2(13.29 + 20.11)} = 0.051 \tag{B.11}$$

and

$$r_{11} = \frac{\tan^2(\theta_2 - \theta_1)}{\tan^2(\theta_2 + \theta_1)} = \frac{\tan^2(13.29 - 20.11)}{\tan^2(13.29 + 20.11)} = 0.036 \tag{B.12}$$

The reflectivity of unpolarized light is given by the average of the two viz.

$$\rho = \frac{I_r}{I_i} = 1/2(r_\perp + r_{11}) = 1/2(0.051 + 0.036) = 0.0437 \tag{B.13}$$

Expressions for the reflectivity, transmissivity and absorptivity of glass for beam radiation and which has air on both sides and derived in appendix B.

$$\rho_{glass} = \rho\left[1 + \frac{(1-\rho)^2\tau_a{}^2}{1-\rho^2\tau_a{}^2}\right] \tag{B.17}$$

$$\tau_{glass} = \frac{(1-\rho)^2\tau_a}{1-\rho^2\tau_a{}^2} \tag{B.16}$$

and

$$\alpha_{glass} = \frac{(1-\rho)(1-\tau)}{1-\rho\tau} \qquad (B.19)$$

where the transmissivity of the wave is through the glass is given by

$$\tau_a = e^{\frac{-kL}{\cos\theta_2}} \qquad (B.15)$$

L being the thickness of the glass.

Similar expressions are applicable for diffuse radiation where an angle of incidence of 60° is to be used for all hours.

Calculation for beam radiation

The thickness of the glass used is 0.004 m and the value of k is found by Lombard [02LO1] to be 13.

$$\tau_{a,b} = e^{\frac{-13(0.004)}{COS(13.29)}} = 0.948$$

Insert the values for the reflectivity and transmissivity into the appropriate equations and find the following values for beam radiation for the glass roof:

$$\rho_{glass,b} = 0.0437\left[1+\frac{(1-0.0437)^2\times 0.948^2}{1-0.0437^2\times 0.948^2}\right] = 0.0797$$

$$\tau_{glass,b} = \frac{(1-0.0437)^2\times 0.948}{1-0.0437^2\times 0.948^2} = 0.8685$$

$$\alpha_{glass,b} = 1-0.8685-0.0797 = 0.0519$$

Calculation for diffuse radiation

Beam radiation incident at an angle of 60° has the same transmittance as isotropic diffuse radiation [91DU1] and the equations in the previous paragraph may be applied to diffuse radiation by inserting an angle of 60° for θ_1.

Referring to the previous section, the transmittance for diffuse radiation through single glazing is calculated

$$\sin\theta_2 = \frac{\sin\theta_1}{1.526} = 0.6553\sin\theta_1 = \frac{\sin 60}{1.526} = 0.567513$$

$$\theta_2 = 34.57^\circ$$

The other values may be determined utilizing this value of θ_2:

$$r_\perp = \frac{\sin^2(34.57-60)}{\sin^2(34.57+60)} = 0.18547$$

$$r_{11} = \frac{\tan^2(34.57-60)}{\tan^2(34.57+60)} = 0.00144$$

$$\rho_d = 0.5(0.18547+0.00144) = 0.09346$$

$$\tau_a = e^{\frac{-13(0.004)}{\cos 34.577}} = 0.93879$$

$$\rho_{glass,d} = 0.093463\left[1+\frac{(1-0.09346)^2(0.93879)^2}{1-0.09346^2(0.93879)^2}\right] = 0.16168$$

$$\tau_{glass,d} = \frac{(1-0.09346)^2 0.93879}{1-(0.09346)^2(0.93879)^2} = 0.7775$$

Experimental data shows that the diffuse component on a clear day in Stellenbosch is between 7 % and 10 % of the total radiation. A value of 10 % will be used throughout.

For the test done on 15 December at the stated hour, the total radiation measured by the pyranometer was 1006.36 W/m^2

Find therefore the diffuse component to be 100.636 W/m^2

The direct or beam radiation is 905.714 W/m^2

The Penman-Monteith equation requires a value for the net radiant energy, I_{net} absorbed by the vegetation. The grass re-radiates infrared radiation towards the glass roof in addition to reflecting the solar radiation transmitted through the glass roof. The combined effect of transmittance, reflectance and reradiation in addition to absorption is dealt with in the transmittance-absorptance product [93MO1]. There is also a loss of heat energy to the soil below and according to the FAO this is found to be of the order of 10% each of beam and diffuse radiation [04FA1].

Absorption of radiation by grass: the transmittance - absorptance product $(\tau\alpha_g)$

Part of the radiation reaching the grass surface is reflected back to the glass roof and there it is in turn reflected back to the grass. Referring to Appendix B, the transmittance-absorptance product for the transmitted beam radiation is given by

$$(\tau\alpha_g) = \frac{\alpha_g \tau}{[1-\rho_d(1-\alpha_g)]} \qquad (B.24)$$

where α_g, the absorptivity, is related to the albedo, λ, of the grass which in turn is determined by the altitude angle, θ. The albedo is given by

$$\lambda = 0.00158\theta + 0.386\exp(-0.0188\theta) \qquad (B.26)$$

It is recognized that the albedo given by Dong [92DO1] is given for total radiation and not for beam and diffusion separately. The diffuse part of the radiation is only 10 % of the total and since all other calculations are done separating the radiation into beam and diffuse, it is convenient to do the same with the equation for the albedo without compromising the result. Considering the grass to be opaque to radiation, the absorptivity of the grass is given by

$$\alpha_g = 1-\lambda$$

The altitude angle, θ, is related to the zenith angle θ_z

$$\theta = (90-\theta_z)$$

For the zenith angle = 20.53 °, find the altitude angle

$\theta = 90 - 20.53 = 69.47°$ so that

λ_b = 0.00158(69.47)+0.386exp(-0.0188(69.47)) =0.214 and

$\alpha_{g,b} = 1 - 0.214 = 0.786$

For diffuse radiation, the angle of incidence is (90 ° - 60 °) or 30 °

λ_d = 0.00158(30) + 0.386exp(-0.0188(30)) = 0.267

$\alpha_{g,d} = 1 - 0.2670 = 0.733$

For beam radiation, calculate the transmittance-absorptance product

$$(\tau\alpha_g)_b = \frac{0.786 \times 0.8685}{[1 - 0.09346(1 - 0.786)]} = 0.6963$$

Similarly for diffuse radiation

$$(\tau\alpha_g)_d = \frac{0.733 \times 0.7775}{[1 - 0.09346(1 - 0.733)]} = 0.6265$$

For the net energy absorbed by the grass surface, the heat loss to the soil and shadows on the grass surface need to be taken into account. The loss to the soil is of the order of 10 % of the radiation absorbed when the Penman-Monteith equation is applied for daily calculations [04FA1]. The presence of the inlet diffusor and the measuring box at the outlet as well as the sides of the tunnel on the northern side cause some of the grass to be in the shade. This is dependent on the zenith angle. The area in shade is that from the northern side of the tunnel plus the shadow caused by either the inlet or outlet boxes depending on whether the time considered is before or after the solar noon.

Shade from north side of tunnel = 0.01 x 1 6 m = 0.16 m^2 (measured to be 10 mm wide)

Shadow at outlet = $0.2\tan\theta_z$ for a height of 0.2 m at the outlet side of the tunnel which is causing a shadow at this hour.

The total area covered by grass is 16 m^2 so that

Area in sun = $16 - 0.16 - (2x0.2\tan 20.53) = 15.79\ m^2$

Applying this to the equation, find

$$\begin{aligned} I_{absorbed} &= (\tau\alpha_g)_b \times 0.9 \times I_{beam,} A_{sunlit}/A_{tot\,grass\,area} + (\tau\alpha_g)_d \times (1 - 0.9) \times I_{diffuse} \\ &= 0.6963 \times 0.9 \times 905.72\,(15.79/16) + 0.6265 \times (1 - 0.9) \times 100.64 \\ &= 559.95 + 56.74 = 616.7\ W/m^2 \end{aligned}$$

There is still the infrared radiation exchange between the glass roof and the grass to be considered. Before this can be done, a provisional value of the net radiation must be determined from the measured average grass temperature. Thereafter a local grass temperature can be calculated and from there the actual infrared radiation exchange between the glass roof and the grass. It was found that after two iterations the grass temperature and net radiation could be determined. In order to apply the grass temperature equation (A.81), the "adjusted" psychrometric constant and the slope of the saturation line needs to be determined.

7.1.2 The psychrometric constant, γ and the "adjusted" psychrometric constant, γ^*

The psychrometric constant gives the slope of the wetbulb temperature line on the psychrometric chart and is calculated as follows

$$\gamma = \frac{c_{pma} p_{atm}}{0.622\, i_{fg_2}} \text{ Pa/K} \qquad \text{(A.22)}$$

This requires the latent heat of evaporation at the wetbulb temperature

At the inlet state

$$i_{fgw} = 3.4831814 \times 10^6 - 5.8627703 \times 10^3 T + 12.139568 T^2 - 1.40290431 \times 10^{-2} T^3 \text{ J/kg} \qquad \text{(F.4.5)}$$

$T_{wb} = 293.71$

$$i_{fgwi} = 3.4831814 \times 10^6 - 5.8627703 \times 10^3 (293.71) + 12.139568 (293.71)^2 - 1.40290431 \times 10^{-2} (293.71) = 2452.990 \times 10^3 \text{ J/kg}$$

Similarly for the air at the outlet, $T_{wb} = 302.20$K

$$i_{fgwo} = 3.4831814 \times 10^6 - 5.8627703 \times 10^3 T + 12.139568 T^2 - 1.40290431 \times 10^{-2} T^3 \text{ J/kg}$$

$$i_{fgwo} = 3.4831814 \times 10^6 - 5.8627703 \times 10^3 (302.20) + 12.139568 (302.20)^2 - 1.40290431 \times 10^{-2} (302.20)^3 = 2432.901 \times 10^3 \text{ J/kg}$$

From previously calculated values of the specific heat capacities

$c_{pmai} = 1027.31 \times 10^3$ J/kgK

$c_{pmao} = 1051.56 \times 10^3$ J/kgK

Measured p_{atm}=100000 Pa

$$\gamma_{inlet} = \frac{1027.31 \times 10^3 \times 100000}{0.622 \times 2452.990 \times 10^3} = 67.33 \text{ Pa/K}$$

$$\gamma_{outlet} = \frac{1051.56 \times 10^3 \times 100000}{0.622 \times 2432.901 \times 10^3} = 69.49 \text{ Pa/K}$$

The above shows that the psychrometric constant is negligibly temperature dependent.

The average psychrometric constant

$$\gamma_{ave} = \frac{67.33 + 69.49}{2} = 68.41 \text{ Pa/K}$$

and the "adjusted" psychrometric constant, γ^*

$$\gamma^* = \left(\frac{r_s + r_H}{r_H}\right) 68.41 = \left(1 + \frac{r_s}{r_H}\right) 68.41 \text{ Pa/K} \qquad \text{(A.72)}$$

For an entering effective convective heat transfer coefficient of 31.83 W/m^{2}K, find

r_H =36.86 s/m, r_s=70s/m and

$$\gamma^* = \left(1+\frac{70}{36.86}\right)68.16 = 197.6 \text{ Pa/K}$$

7.1.3 The slope of the saturated vapor pressure line, Δ

By the application of the Clausius-Clapeyron equation [85VA1] to the water vapor in the atmospheric air and where the water vapor is considered an ideal gas, find the slope of the saturated vapor pressure line, Δ, as a function of temperature

$$\left(\frac{dp}{dT}\right)_{sat} \sim \frac{i_{fg}p_{sat}(T)}{T^2R_v} \equiv \Delta \text{ Pa/K} \qquad (A.11)$$

Calculate the slope of the saturated vapor pressure line at the average of the wet- and drybulb temperatures.

$T_{ave} = (T_{wb}+T_{db})/2$

$T_{ave} = (20.56+29.86)/2 = 25.21$ °C (298.36 K)

The latent heat of evaporation at this temperature is given by

$i_{fg} = 3.4831814 \times 10^6 - 5.8627703 \times 10^3 T + 12.139568T^2$
$-1.40290431\times10^{-2}T^3$ J/kg (F.4.5)

for T = 298.36, find

$i_{fg} = 3.4831814 \times 10^6 - 5.8627703 \times 10^3(298.36) + 12.139568(298.36)^2$
$-1.40290431\times10^{-2}(298.36)^3$
$= 2442.66\times10^3$ J/kg

Calculate the saturated vapor pressure at this average temperature

Vapor pressure is given by

$p_{sat}(T) = 10^z$, N/m^2 where (F.2.1)

$z = 10.79586(1 - 273.16/T) + 5.02808 \log_{10}(27316/T)$
$+ 1.50474 \times 10^{-4} [1 - 10^{-8.29692\{(T/273.16)-1\}}]$
$+ 4.2873 \times 10^{-4} [10^{4.76955(1-273.16/T)} -1] + 2.786118312$

For T = 298.36 K, find

$z = 10.79586(1 - 273.16/298.36) + 5.02808 \log_{10}(27316/298.36)$
$+ 1.50474 \times 10^{-4} [1 - 10^{-8.29692\{(298.36/273.16)-1\}}]$
$+ 4.2873 \times 10^{-4} [10^{4.76955(1-273.16/298.36)} -1] + 2.786118312 = 3.499$

$p_{sat}(T) = 10^z = 10^{3.499} = 3153.97$ Pa

and therefore

Utilizing the above values, find the slope of the saturation curve at this average temperature to be

$$\Delta_{average} = \frac{2442.66\times10^3\times3153.97}{298.36^2\times461.889} = 187.72 \text{ Pa/K}$$

7.1.4 The heat transfer by infrared radiation from the glass roof to the grass, Q_{rRg}

The radiant heat or infrared radiation exchanged between the glass roof and the grass surface below is calculated by viewing the surfaces as gray bodies. The infrared radiation exchanged from the glass to the grass is given by equation (B.29) in terms of the emissivities ε_R and ε_g of the surfaces

$$Q_{rRg} = \sigma \times A_R \left[\frac{(T_R^4 - T_g^4)}{1/\varepsilon_R + 1/\varepsilon_g - 1} \right]$$

The emissivity of the glass roof is 0.90 and that of the grass is 0.98 [63 HS 1].

The area A_R is the roof area.

The grass temperature is given by the following equation

$$T_g = T_F + \frac{1}{(\Delta + \gamma^*)} \left(\frac{\gamma^* I_{net}}{h_{cgF}} - vpd \right) \qquad (A.81)$$

where T_F is the drybulb temperature of the air.

This equation needs I_{net} which is not known yet. From the calculations done using the average measured grass temperature, an initial value for I_{net} may be determined. Firstly utilizing the measured grass temperature find,

$$Q_{rRg} = 5.67 \times 10^{-8} \times 16 \times \left[\frac{(37.28 + 273.15)^4 - (37.05 + 273.15)^4}{1/0.90 + 1/0.98 - 1} \right] = 20.89 \text{ W} \quad \text{or}$$

$$Q_{rRg} / A = \frac{20.89}{16} = 1.30 \text{ W/m}^2$$

This is transferred from the glass at the higher temperature to the grass at the lower temperature.

Thus the net radiation absorbed by the grass will be

$$I_{net} = I_{beam+diffuse\ absorbed} + I_{infrared\ exchange\ roof-grass} = 616.7 + 1.3 = 618.0 \text{ W/m}^2$$

The average grass temperature may now be determined for this first meter:

$$T_g = 29.86 + \frac{1}{(187.72 + 197.06)} \left(\frac{197.06 \times 618}{31.83} - 2387 \right) °C$$

$$= 29.86 + 12.065 - 6.724 = 33.60°C$$

Repeating the calculation with the new grass temperature, find

$$Q_{rRg} / A = \frac{393.48}{16} = 24.5 \text{ W/m}^2.$$

Inserting this value, find I_{net} to be

$$I_{net} = I_{beam+diffuse\ absorbed} - I_{infrared\ exchange\ grass-roof} = 616.7 + 24.5 = 641 \text{ W/m}^2$$

The new grass temperature will now be

$$T_g = 29.86 + \frac{1}{(187.72 + 197.06)}\left(\frac{197.06 \times 641}{31.83} - 2387\right)$$
$$= 29.86 + 4.1147 = 33.97\ ^\circ C$$

Further iterations give $I_{net} = 624.79\ W/m^2$ and a grass temperature of 33.59 °C

7.2 APPLICATION OF THE PENMAN-MONTEITH EQUATION TO ESTIMATE THE EXIT STATE OF THE AIR LEAVING THE TUNNEL

The conservation equations and the Penman-Monteith equation for determining the amount of evapotranspiration taking place, are applied to subsequent one meter lengths of the tunnel, making it possible to estimate the exit state of the air leaving the tunnel. The average rate of evapotranspiration taking place as well as the state of the air at the exit and the average grass temperature may be determined and these values compared to experimentally determined values.

From previously calculated values:

Convective heat transfer coefficient for the grass to air

h_{cgF} = 31.83 W/m^{2}K

Convective heat transfer coefficient for the glass roof to air

h_{cRF} = 8.94 W/m^{2}K

Constant pressure specific heat of dry air

c_{pda} = 1005.534 J/kgK

Constant pressure specific heat of water vapor

c_{pv} = 1875.280 J/kgK

At the inlet air drybulb and wetbulb temperatures the following were calculated

Enthalpy of air at inlet

i_1 = 58906.99 J/kg da

Humidity ratio of air at inlet

w_1 = 0.0112952 kg/kg da

The grass temperature, slope of the saturation curve, vapor pressure depression, latent heat of evaporation and the enthalpy of saturated water vapor at the grass temperature are re-evaluated at each step since all temperatures vary along the tunnel length.

Mass flow rate of dry air m_a = 0.2635 kg/s dry air

First value for net radiation absorbed by grass

I_{net} = 624.79 W/m^2. This value will vary since the infrared radiation exchange between the grass and the roof will vary as the grass temperature varies.

The "adjusted" psychrometric constant

$\gamma^* = 197.6$ Pa/K

The Penman-Monteith-Monteith equation is as follows

$$(m_v / A)\, i_{fg} = \frac{\Delta_{ave} I_{net} + h_{cgF}(vpd)}{\Delta_{ave} + \gamma^*}\ kg/m^2s$$

Consider the control volume around the air flowing through the tunnel as shown in Figure 7.1.

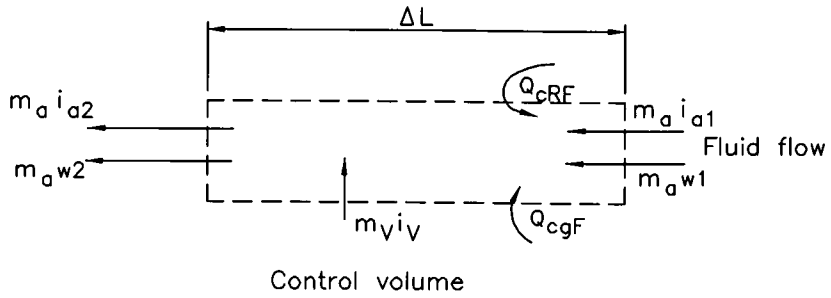

Figure 7.1: Control volume around the air or fluid flow over the grass.

The following conservation equations apply:

Water balance

$$m_a w_1 + m_v = m_a w_2 \text{ kg/s}$$

Energy balance.

$$m_a i_{a1} + Q_{cRF} + Q_{cgF} + m_v i_v = m_a i_{a2} \text{ J/s}$$

For a one meter length of tunnel, $\Delta L = 1$, and which is one meter wide, the heat transfer area is one square meter so that

$$Q_{cRF} = h_{cRF}(T_R - T_F) \text{ J/m}^2\text{s}$$

$$Q_{cgF} = h_{cgF}(T_g - T_F) \text{ J/m}^2\text{s}$$

First determine the slope of the saturation line at the average of the inlet wet and drybulb temperatures of the air

$$\left(\frac{dp}{dT}\right)_{sat} = \frac{i_{fg} p_{sat}(T)}{T^2 R_v} \equiv \Delta = 187.72 \text{ Pa/K}$$ (for the inlet state, this has already been calculated in chapter 5)

Calculate the vapor pressure depression. (This too has already been calculated for the inlet state of the air)

vpd = 2387.18 Pa

The grass temperature needs to be determined in order to calculate the enthalpy of evaporation at the grass temperature for use in the Penman-Monteith equation.

$$T_g = T_F + \frac{1}{(\Delta + \gamma^*)}\left(\frac{\gamma^* I_{net}}{h_{cgF}} - \text{vpd}\right) \qquad \text{(A.81)}$$

$T_S = 33.59$ °C (from previous calculation)

The enthalpy of evaporation at this temperature is calculated to be 2442148 J/kg

The rate of evapotranspiration can now be predicted from

$$(m_v / A)2442148 = \frac{187.72 \times 624.79 + 31.83 \times 2387}{(187.72 + 197.6)} \text{ J/m}^2\text{s}$$

or

$$m_v / A = 0.0002089 \text{ kg/m}^2\text{s}$$

Calculate the specific humidity of the air leaving the control volume.

$$m_a w_1 + m_v = m_a w_2 \ \text{kg/s}$$

$$0.2635(0.0112952) + 0.0002089 = 0.2635 w_2$$

$$w_2 = 0.0120881 \ \text{kg/kg da}$$

The drybulb temperature of the exiting air can now be determined using equation (4.8)

Inserting values, find

$$T_2\left[1005.53 + 0.0120881 \times 1875.28 + \left(\frac{8.94 + 31.83}{2 \times 0.2635}\right)\right]$$

$$= 29.86\left[1005.53 + 0.0112952 \times 1875.28 - \left(\frac{8.94 + 31.83}{2 \times 0.2635}\right)\right]$$

$$+ (0.0120881 - 0.0112952)(2562468 - 2501000) + \left[\frac{8.94 \times 37.73 + 31.83 \times 33.59}{0.2628}\right]$$

$$T_2(1106) = 29.86(949) + 49 + 5338$$

$$T_2 = 25.64 + 0.04408 + 4.828 = 30.51°C$$

From the known humidity ratio and drybulb temperature the wetbulb temperature may be solved using an iterative method: the "solver" function in Microsoft Excel.

$$w = \left(\frac{2501.6 - 2.3263(T_{wb} - 273.15)}{2501.6 + 1.8577(30.61) - 4.184(T_{wb} - 273.15)}\right)\left(\frac{0.62509 p_{vwb}}{100000 - 1.005 p_{vwb}}\right)$$

$$- \left(\frac{1.00416(30.61 - T_{wb})}{2501.6 + 1.8577(30.64) - 4.184(T_{wb} - 273.15)}\right), \ \text{kg/kg dry air}$$

From "solver" function, find the wetbulb temperature to be 21.09 °C

From these values calculate all required parameters for the second meter i.e. $\Delta, \gamma^*, \text{vpd}$. The net radiation also needs to be determined: in order to do this, an initial value for the grass temperature of 4 °C above the exit drybulb temperature is chosen and the infrared radiation calculated. From this the net radiation is determined and hence an improved value for the grass temperature.

The solar radiation alone = 616.7 W/m^2 (This is a constant for the entire length of the tunnel for this particular time slot).

Grass temperature = (30.51+4) = 34.51 °C

Average constant glass temperature = 37.73 °C

$$q_{rRg} = \sigma\left(\frac{(T_R^4 - T_g^4)}{1/\varepsilon_R + 1/\varepsilon_g - 1}\right)$$

$$= 5.67 \times 10^{-8}\left(\frac{(37.73 + 273.15)^4 - (34.51 + 273.15)^4}{1/0.9 + 1/0.98 - 1}\right) = 19.09 \ \text{W/m}^2$$

Total radiation absorbed by the grass is then

$$q_{total} = q_{solar} + q_{ir} = 616.7 + 19.09$$
$$= 635.79\,W/m^2$$

Recalculate the grass temperature using this value until values converge. The calculations for the following meter are based on this value of total radiation absorbed by the grass. This calculation process is repeated meter by meter for the length of the tunnel until final values are obtained as shown in the spreadsheet in detail and in summary below.

Table 7.1: Predicted temperatures and evapotranspiration along the tunnel length, solar hour 13h36

meters	Drybulb Temperature	Wetbulb Temperature, °C	Grass Temperature	Humidity Ratio kg/kgda	Penman-Monteith Evapotranspiration kg/sqm s
1	29.86	20.33	33.59	0.01130	0.000208932
2	30.51	21.09	34.36	0.01209	0.000214263
3	31.16	21.85	34.84	0.01290	0.000216548
4	31.76	22.57	35.24	0.01372	0.000217571
5	32.33	23.27	35.64	0.01455	0.000218616
6	32.86	23.94	36.03	0.01538	0.000219492
7	33.35	24.58	36.42	0.01621	0.000220115
8	33.82	25.20	36.78	0.01705	0.000220534
9	34.26	25.80	37.14	0.01788	0.000220781
10	34.68	26.38	37.49	0.01872	0.000220877
11	35.08	26.94	37.83	0.01956	0.00022084
12	35.46	27.49	38.16	0.02040	0.000220688
13	35.82	28.02	38.48	0.02124	0.000220435
14	36.17	28.53	38.80	0.02207	0.000220095
15	36.50	29.02	39.10	0.02291	0.000219679
16	36.82	29.51	39.40	0.02374	0.000219197
Measured	34.28	29.05			
	Average measured grass temperature		37.5	°C	
	Average predicted grass temperature		37.14	°C	
	Average evapotranspiration measured		0.2082	g/sqm s	
	Average evapotranspiration predicted		0.2050	g/sqm s	

In viewing the above results it must be stated that the inlet and exit wetbulb temperatures of the various thermocouples differed from each other by zero to 1.3 °C. The measured values of all the properties at the exit are determined from the values of the inlet and outlet dry and wetbulb temperatures so that the predicted values are within the experimental error range.

CHAPTER 8
RESULTS

8.0 INTRODUCTION

Collecting data during periods of cloudless skies, windless days and maximum radiation proved to be challenging since such days are few and far between in the Western Cape Province. This was in addition to using living material for experimentation. This alternatively suffered either root rot from overwatering or dried out due to underwatering during extremely hot days mainly due to human error, resulting in experiments having to wait for yet another year while the grass recovered.

The effective convective heat transfer coefficient between the grass surface and the air was determined by measuring the pressure drop over the tunnel for various velocities and thereby establishing an effective friction coefficient in order to determine the effective convective heat transfer coefficient. The friction pressure drop varied with the growth length and state of the grass and an average value was used throughout for calculation purposes. It is interesting to note that with increasing grass length the pressure drop increased but that the pressure drop over freshly mowed grass was the highest, indicating probably that the grass was less flexible and therefore presented an overall rougher surface.

The graphs shown below are obtained by beginning with the measured inlet state of the air to the solar tunnel followed by stepwise calculations for every subsequent meter until the state of the air at the exit of the tunnel is predicted. The Penman-Monteith equation is applied to each following section in order to predict both the grass temperature and the amount of evapotranspiration taking place. The conservation equations are then applied in order to predict both the dry and wetbulb temperatures at the end of each section. For the heat transfer between the glass roof and the air below it was evident from measurements of the temperature of the glass roof that this temperature did not vary more than about 1.5 °C from one end of the tunnel to the other. To facilitate calculations it was decided to use the average temperature between the inlet and the outlet without compromising on accuracy. The predicted exit dry and wetbulb temperatures together with the measured temperatures at the inlet are used to calculate the average rate of evapotranspiration for the entire tunnel and then compared with the measured values of the average rate of evapotranspiration.

8.1 PREDICTED AND MEASURED RATES OF EVAPOTRANSPIRATION

The following graphs illustrate the measured and predicted values of the rate of evapotranspiration of the grass in the solar tunnel for various dates in various years of measurement.

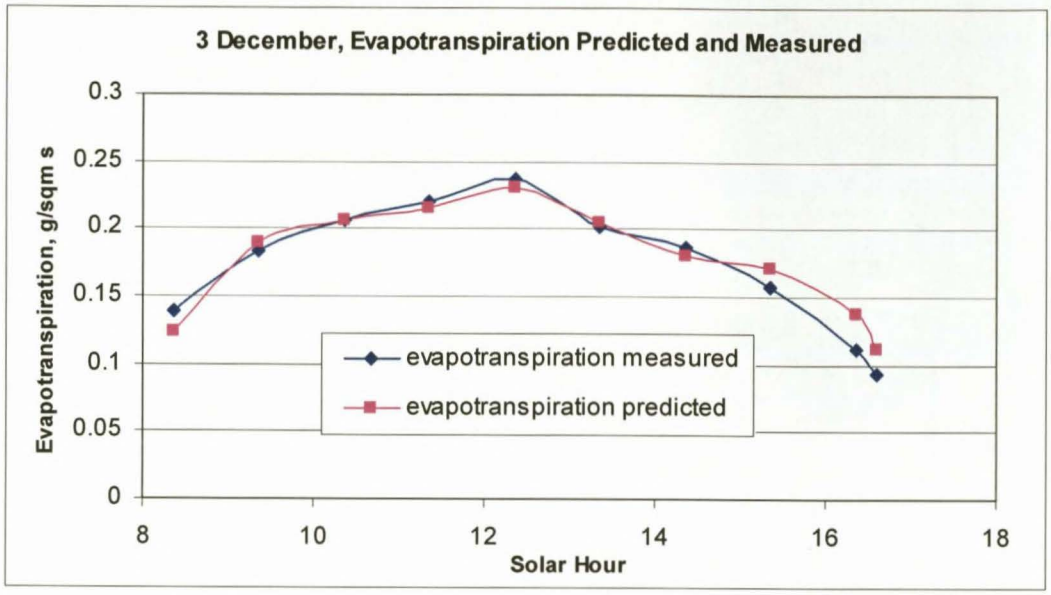

Figure 8.1: Evapotranspiration predicted and measured, 3 December

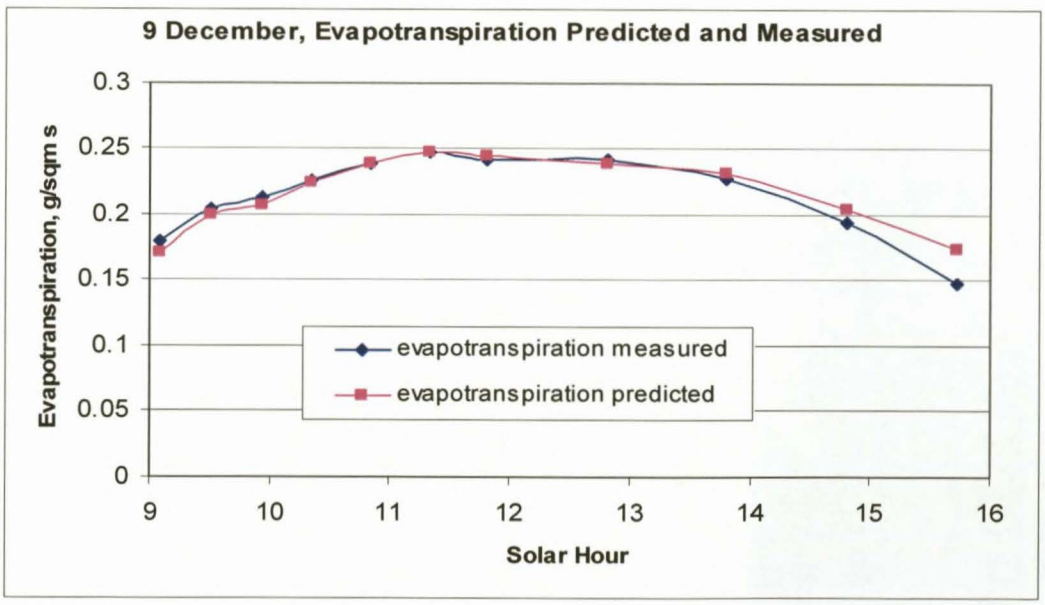

Figure 8.2: Evapotranspiration predicted and measured, 9 December

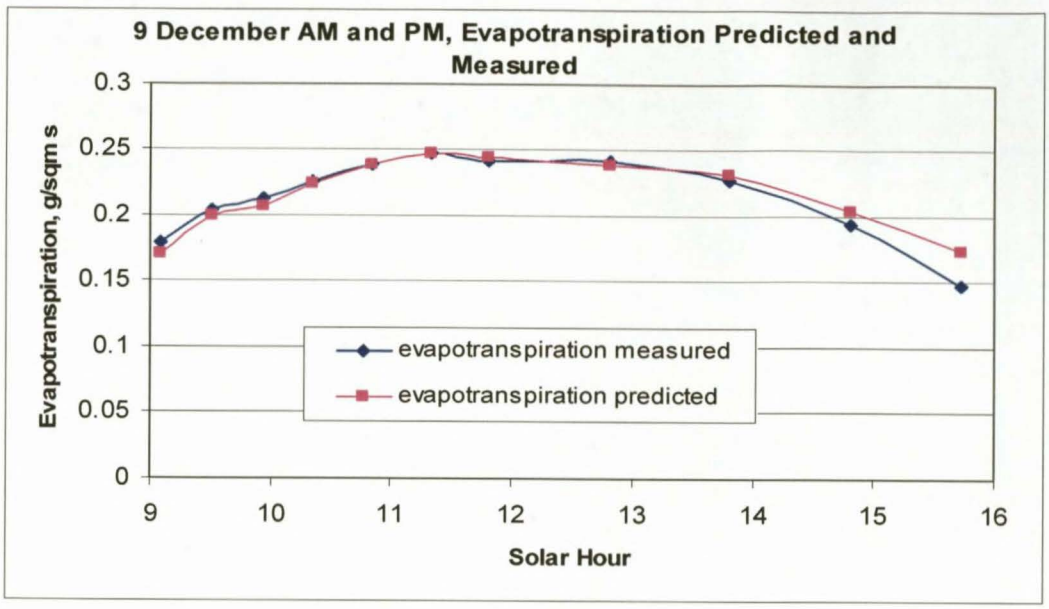

Figure 8.3: Evapotranspiration predicted and measured, 9 December AM and PM separately

(Note: Readings on the above date were interrupted for about 30 minutes between 12h00 and 13h00 due to computer error).

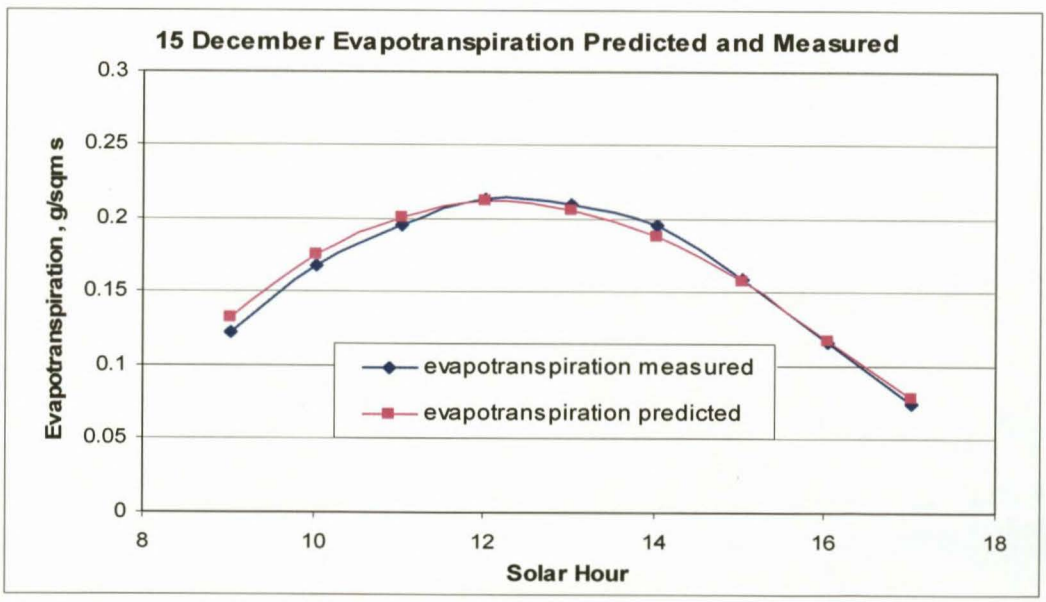

Figure 8.4: Evapotranspiration predicted and measured, 15 December

8.2 PREDICTED AND MEASURED GRASS TEMPERATURES

The following graphs show the average predicted and measured grass temperatures for the various dates. It must be pointed out that while data was being collected the researcher was unaware of the variation in grass temperature along the length of the tunnel and a single grass temperature was measured more or less in the centre of the tunnel. In addition, since the thermocouple had to be installed after the grass was cut or the glass taken off the experimental tunnel in adverse weather conditions, it was not always placed exactly in the same position each time.

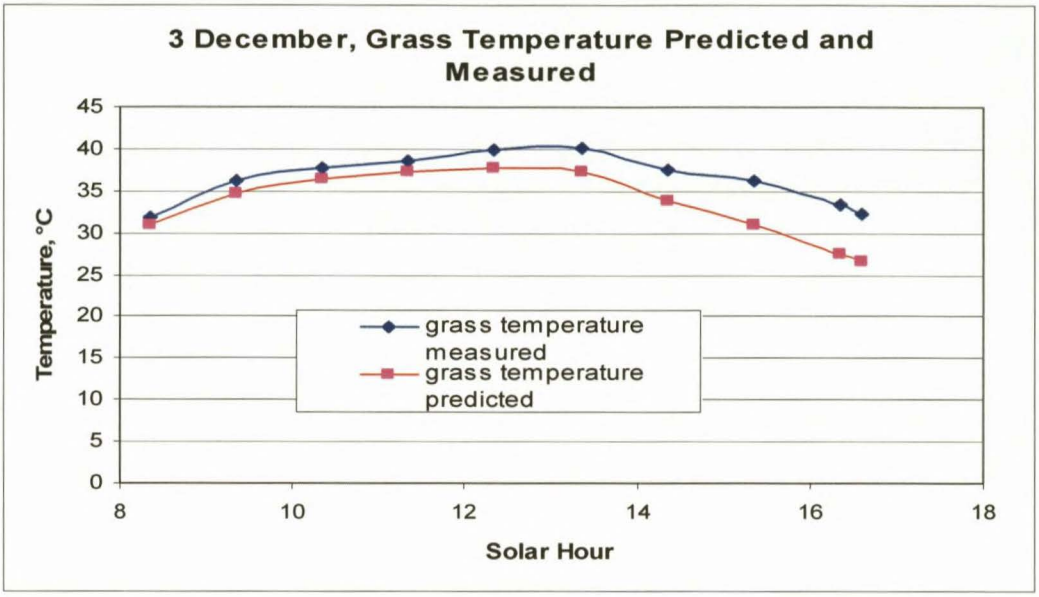

Figure 8.5: Grass temperature predicted and measured, 3 December

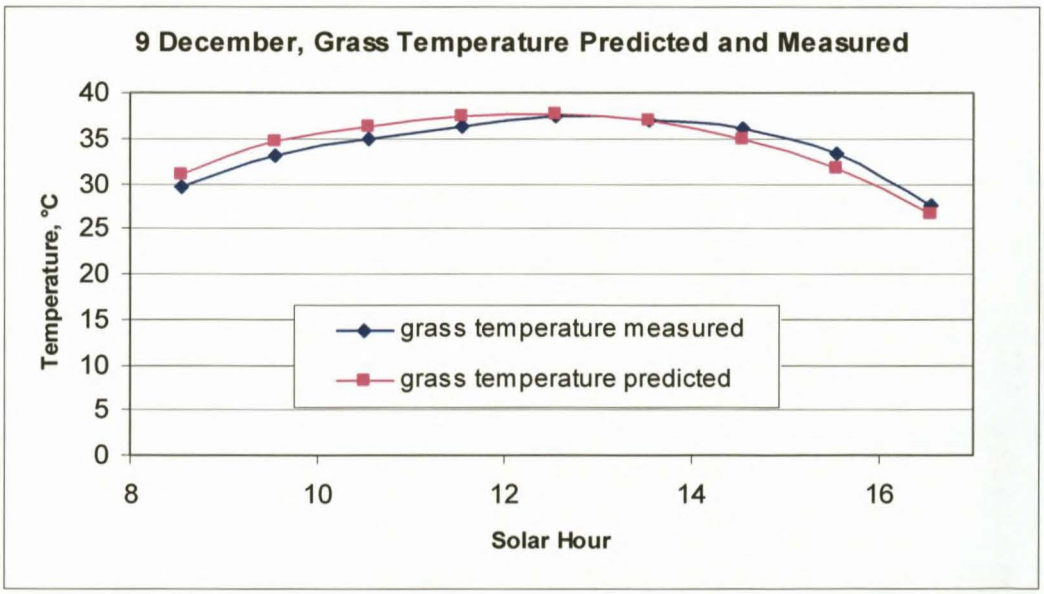

Figure 8.6: Grass temperature predicted and measured, 9 December

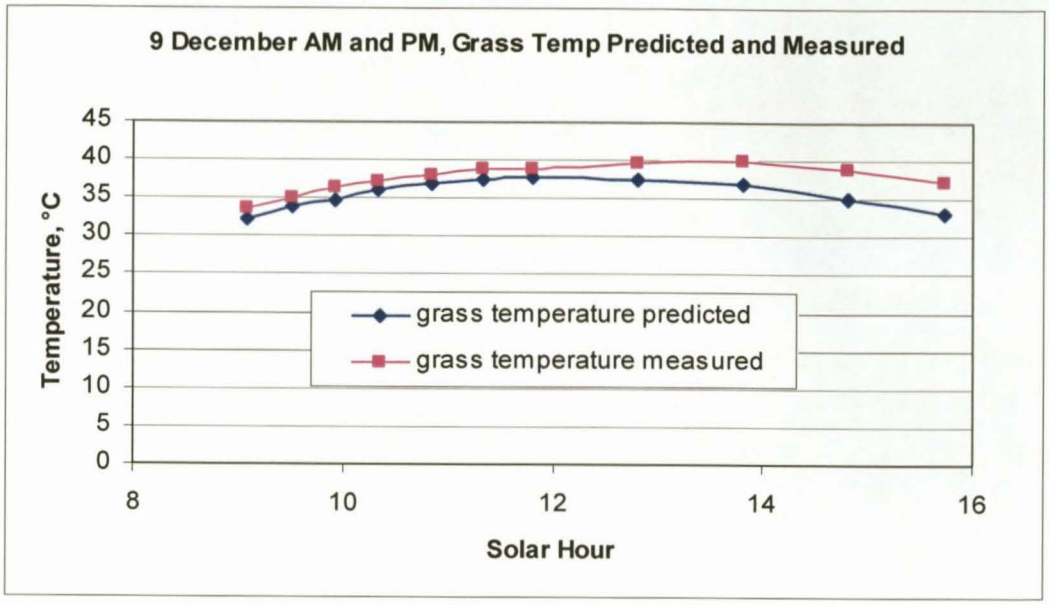

Figure 8.7: Grass temperature predicted and measured, 9 December, AM and PM

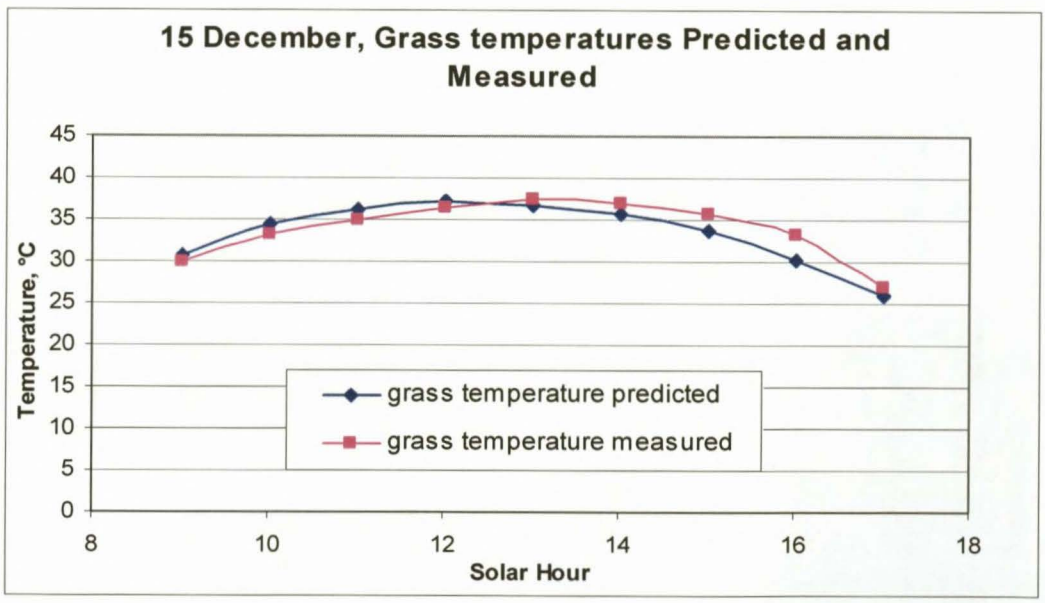

Figure 8.8: Grass temperature predicted and measured, 15 December

8.3 WETBULB TEMPERATURE OF THE AIR PREDICTED AND MEASURED AT THE EXIT OF THE TUNNEL

The following graphs show the predicted and measured wetbulb temperatures of the air as it exits the tunnel.

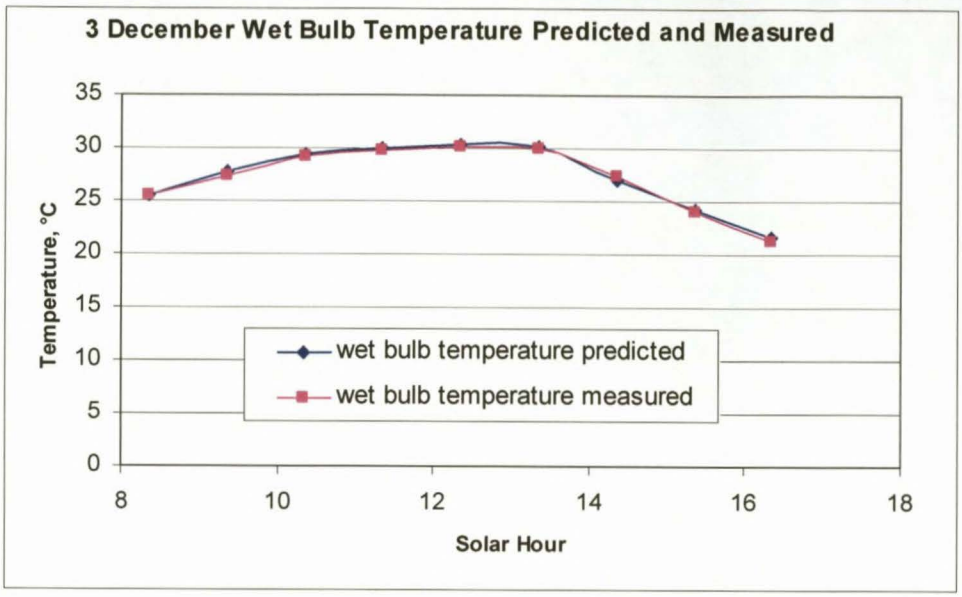

Figure 8.9: Wetbulb temperature of the air predicted and measured, 3 December

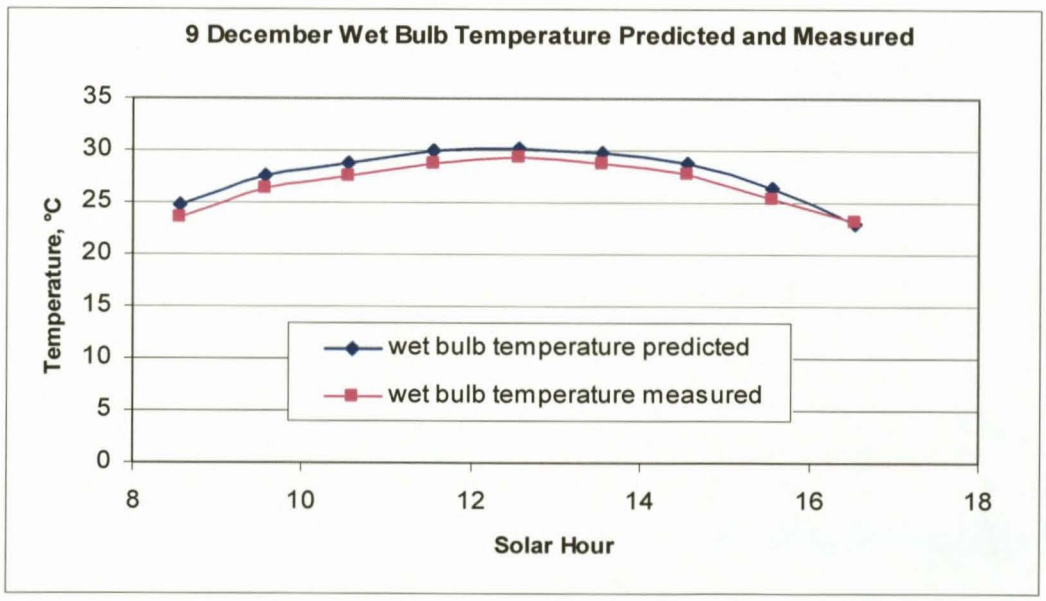

Figure 8.10: Wetbulb temperature of the air predicted and measured, 9 December

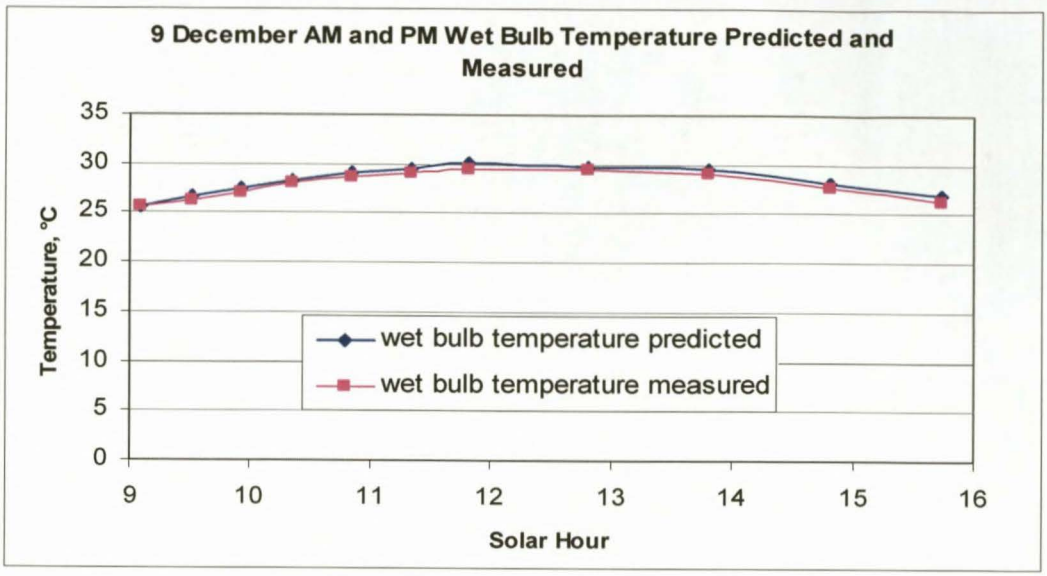

Figure 8.11: Wetbulb temperature of the air predicted and measured, 9 December, AM and PM

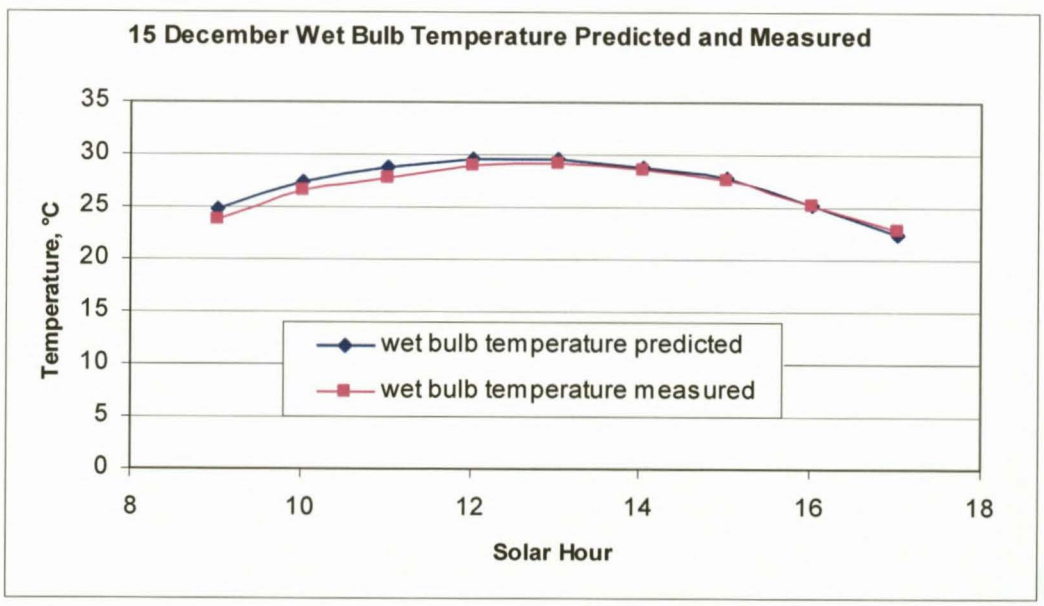

Figure 8.12: Wetbulb temperature of the air predicted and measured, 15 December

8.4 DRYBULB TEMPERATURE OF THE AIR PREDICTED AND MEASURED AT THE EXIT OF THE TUNNEL

The following graphs show the predicted and measured drybulb temperatures of the air at the exit of the tunnel.

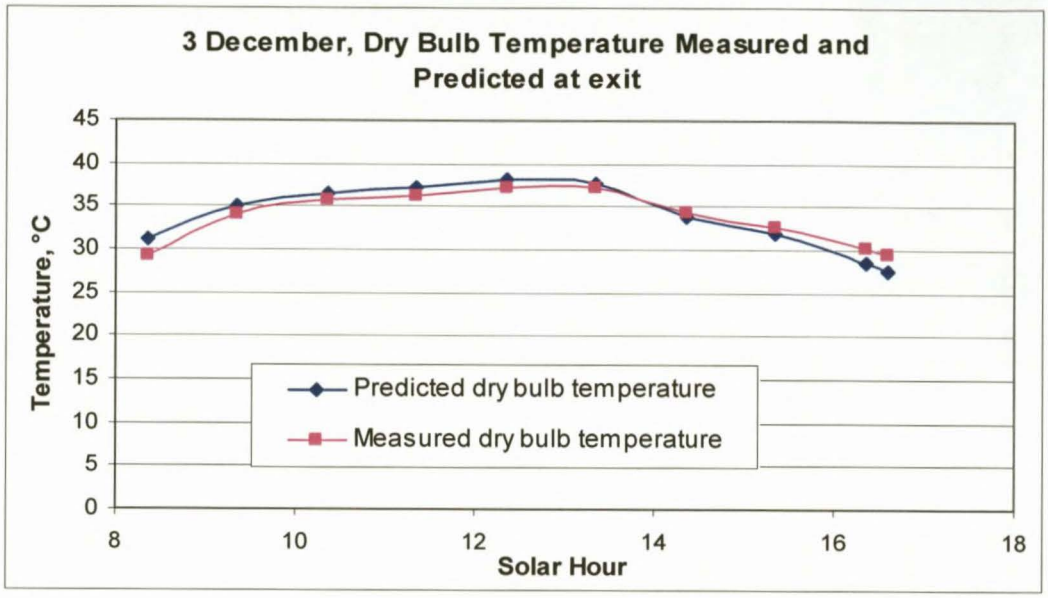

Figure 8.13: Drybulb temperature of the air predicted and measured, 3 December

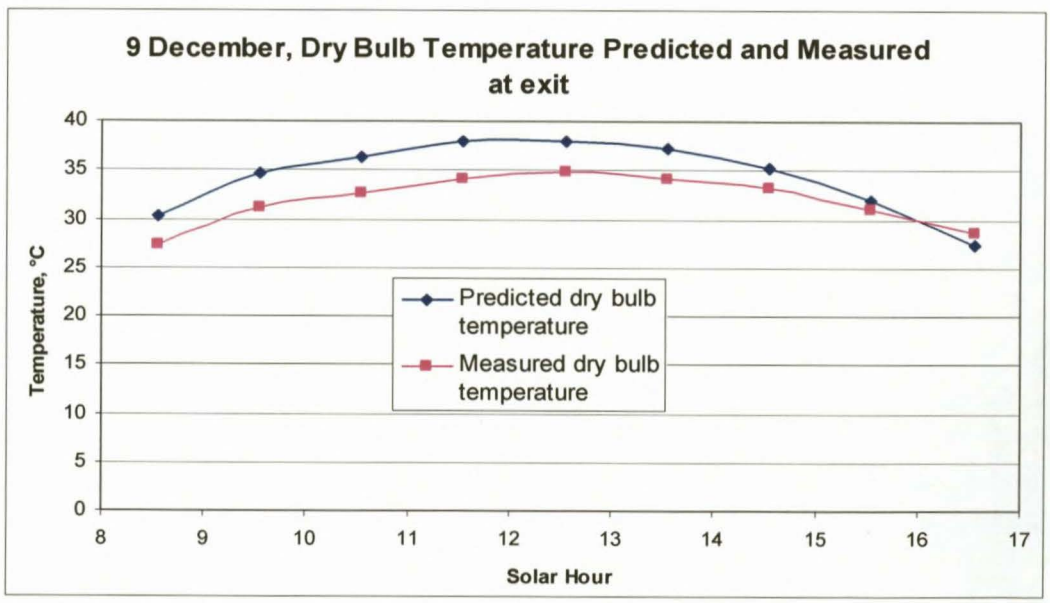

Figure 8.14: Drybulb temperature of the air predicted and measured, 9 December

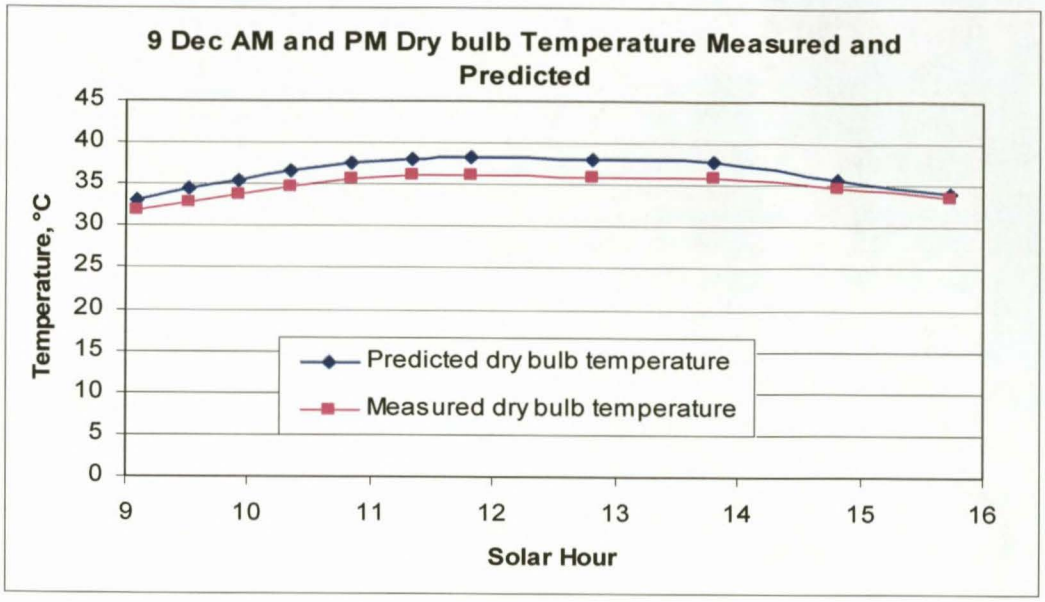

Figure 8.15: Drybulb temperature of the air predicted and measured, 9 December, AM and PM

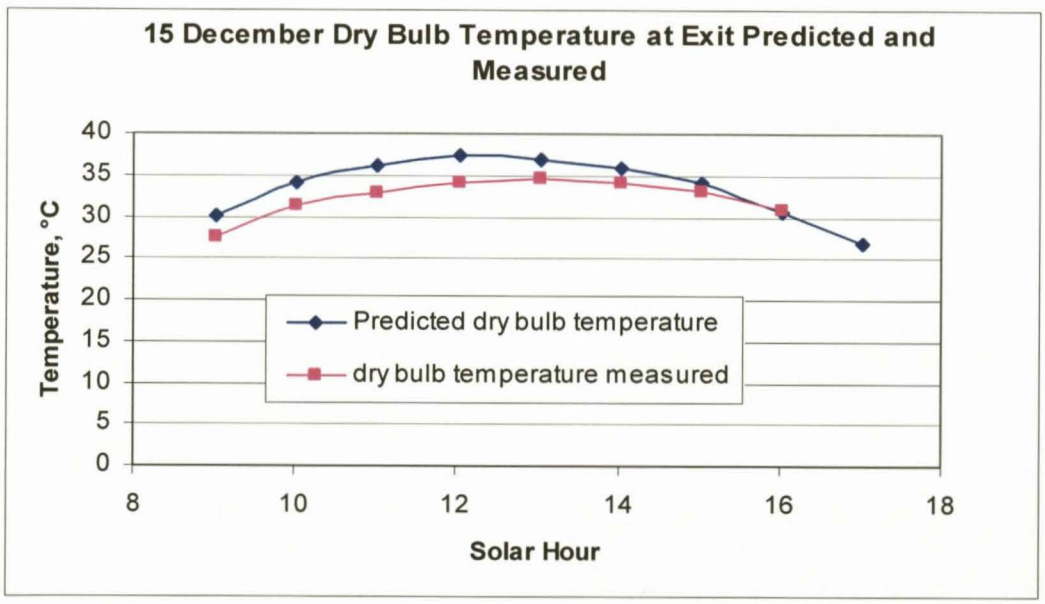

Figure 8.16: Drybulb temperature of the air predicted and measured, 15 December

The graphs for 3 December need to be viewed in the light of the graph below which show the variation in the inlet air temperature on that day.

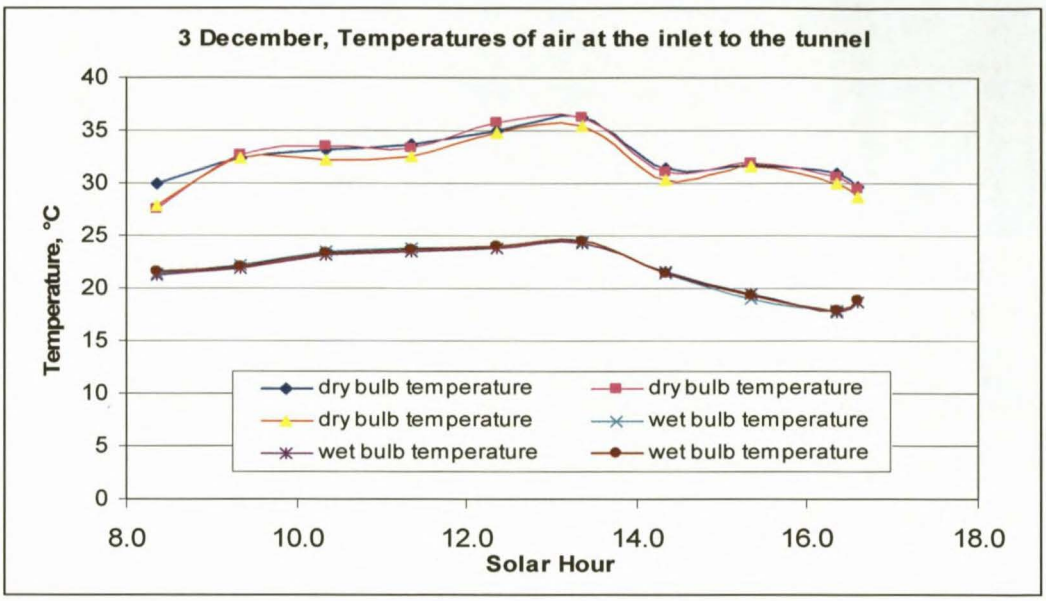

Figure 8.17: Inlet temperatures measured on 3 December

8.5 DIFFERENT EFFECTIVE CONVECTIVE HEAT TRANSFER COEFFICIENTS

From calculations done using a single set of data, the influence of varying the friction factor, and hence the effective convective heat transfer coefficient, was investigated. Calculations were done to predict the following, namely the evapotranspiration rate, the grass temperature and the dry and wetbulb temperatures at the exit of the tunnel. A series of calculations were done using the same inlet state and altering the value of the effective convective heat transfer coefficient each time. This was calculated for solar hour 13.36h on 15 December. The results are tabulated below and include the measured values of the rate of evapotranspiration, the grass temperature and the predicted dry and wetbulb temperatures at the exit of the tunnel. These predicted values are compared to the measured values and the difference given as a percentage of the measured value.

Table 8.1: The effect of various effective convective heat transfer coefficients on predicted values

THE INFLUENCE OF CHANGING THE EFFECTIVE CONVECTIVE HEAT TRANSFER COEFFICIENT ON THE PREDICTION OF THE AVERAGE RATE OF EVAPOTRANSPIRATION THE TEMPERATURE OF THE GRASS SURFACE, AND PREDICTION OF THE DRYBULB TEMPERATURE AT THE EXIT								
Heat transfer coefficient W/sqmK	Predicted rate of evapotrans-piration		Predicted grass Temperature		Predicted drybulb Temperature		Predicted wetbulb temperature	
	g/sqm s	% differ-ence	Grass °C	°C difference from measured value	Dry °C	°C difference from measured value	Wet °C	°C difference from measured value
10	0.1868	7.56	44.6	7.10 °C	37.61	3.33 °C	29.41	0.36 °C
20	0.1995	1.27	39.2	2.00 °C	37.36	3.08 °C	29.74	0.69 °C
30	0.2052	-1.52	37.06	-0.44 °C	37.09	2.81 °C	29.74	0.69 °C
40	0.2072	-2.54	36.30	-1.20 °C	36.96	2.68 °C	29.89	0.84 °C
50	0.2088	-3.32	35.70	-1.80 °C	36.83	2.55 °C	29.9	0.85 °C
60	0.2098	-3.80	35.29	-2.20 °C	36.72	2.43 °C	29.91	0.86 °C
Measured values	**0.2021**		**37.50**		**34.28**		**29.05**	

8.6 SPECIFIC VOLUME CHANGE OF THE AIR FROM THE INLET TO THE EXIT OF THE TUNNEL

Calculations show that depending on the inlet dry and wetbulb temperatures of the air, at times of maximum evapotranspiration such as occurs during the months of December, January and February, the specific volume either decreases or increases or remains the same. Figure 8.18 shows the change in air state from the inlet to the exit of the tunnel for three time instances on 15 December. The figure shows the relatively large (about 80 %) transfer of latent heat at the hour of maximum radiation in addition to the large increase in specific humidity. As expected in the afternoon the amount of evapotranspiration shows a significant decrease. For inlet air temperatures above 40 °C the dry bulb temperature decreased from inlet to exit as opposed to an increase as shown in Figure 8.18 when the inlet dry bulb temperature was below 40 °C.

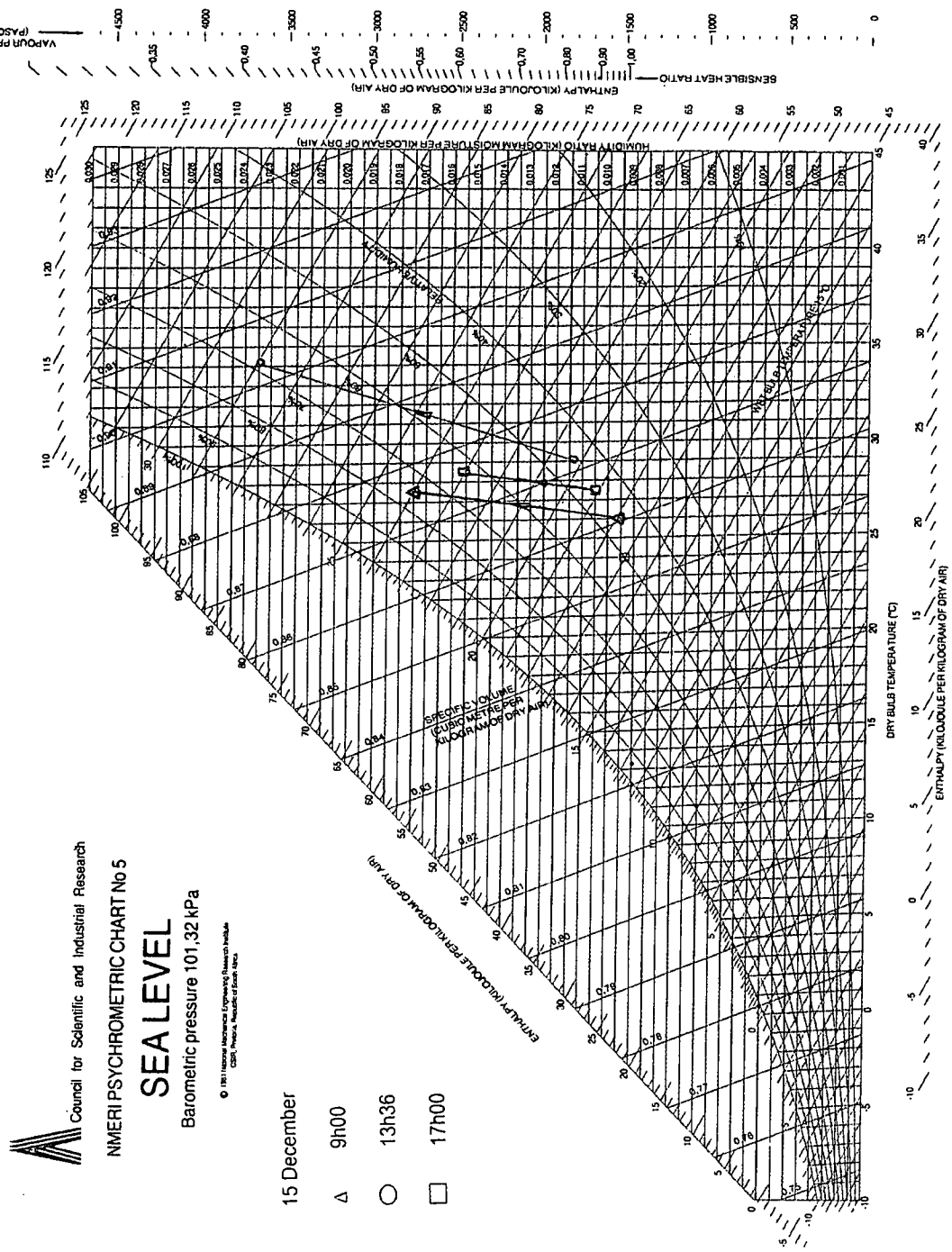

Figure 8.18: Change in measured air state from inlet to outlet at various times, 15 December

8.7 CHANGE IN GRASS TEMPERATURE ALONG TUNNEL LENGTH

The transpiring grass surface is enclosed within a tunnel and hence the grass temperature must of necessity vary along the tunnel length, contrary to what happens in an open field where there is a large quantity of free atmospheric air flowing over the field. In this situation, the ever increasing air humidity causes a decreasing potential for evapotranspiration and hence an increasing quasi equilibrium surface temperature as shown in the graph below.

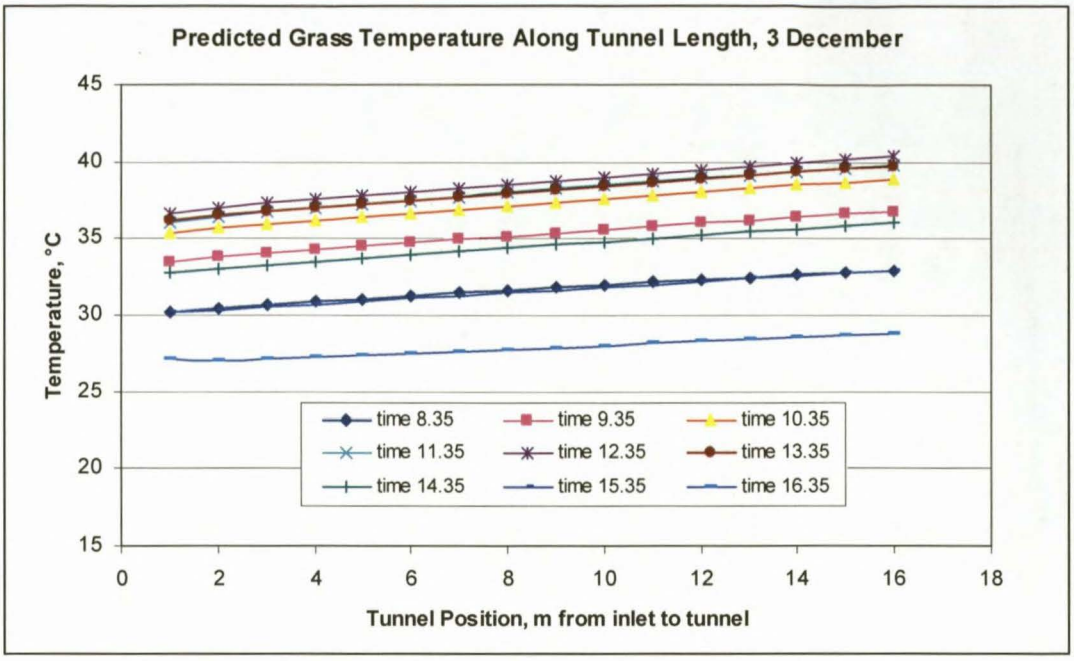

Figure 8.19: Change in grass temperature along tunnel length from inlet for various times of the day

8.8 GROUND AND AIR TEMPERATURES

Figures 8.20 and 8.21 show the change in ground temperature about 20 mm below the exposed grass surface. Also shown is the temperature of the air at the inlet to the tunnel.

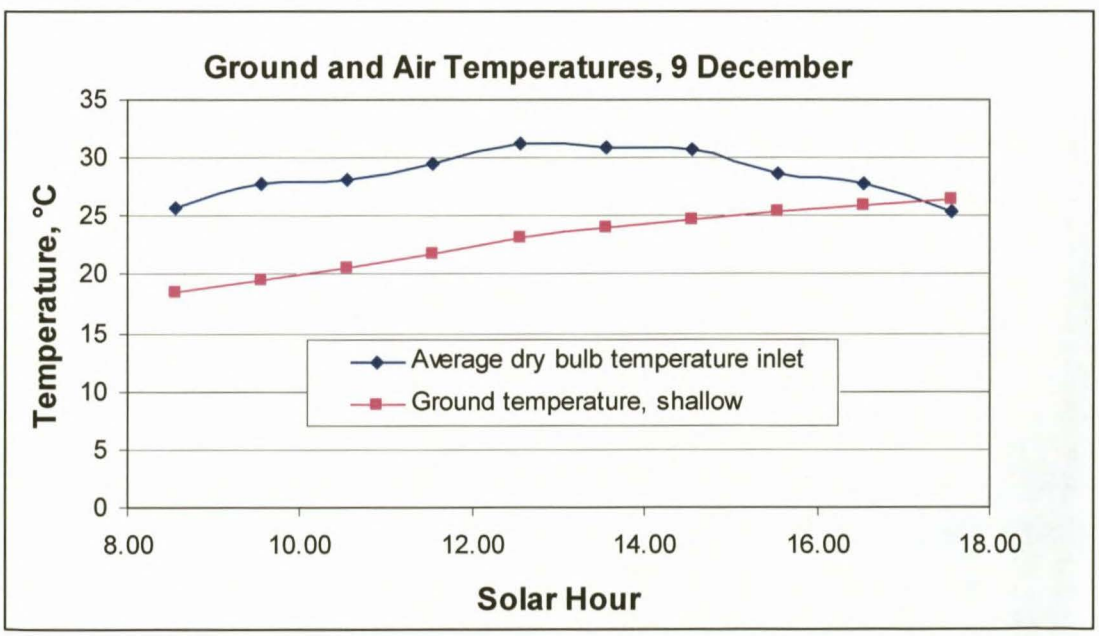

Figure 8.20: Ground and air temperatures, 9 December

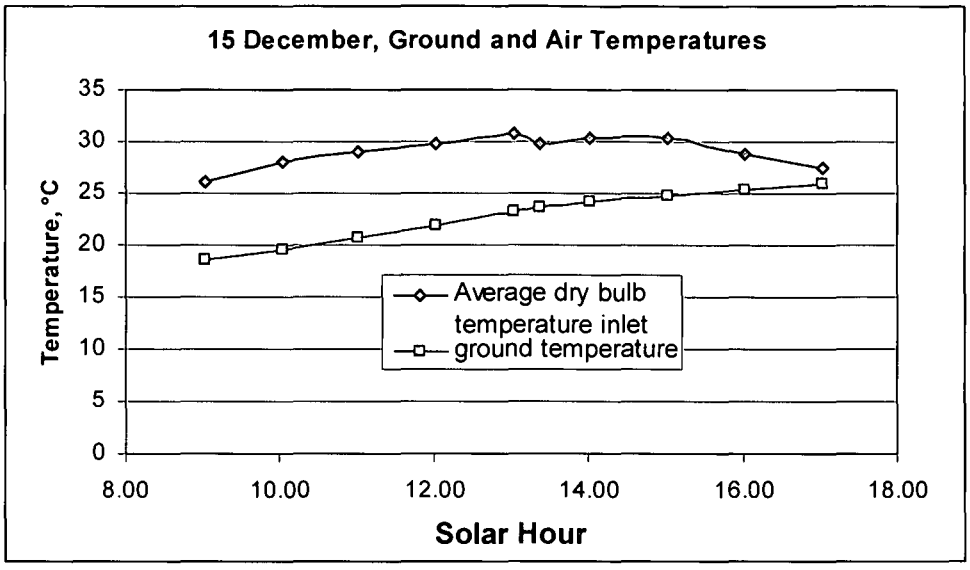

Figure 8.21: Ground and air temperatures, 15 December

8.9 FACTORS INFLUENCING THE PREDICTION OF THE EXIT DRYBULB TEMPERATURE

Table 8.2 shows the contribution of each parameter in equation 4.8 to the prediction of the exit drybulb temperature.

Table 8.2: Factors involved in predicting the exit drybulb temperature (See equation (4.8))

Contribution of each part of the equation to predict the exit drybulb temperature							
Tunnel Position Meters	Coeffi-cient C_2	(w_2-w_1) $*(i_v-if_g)$	Coeffi-cient C_1	Temperature rise due to evapotrans-piration °C	$T_1\left(\frac{C_2}{C_1}\right)$ Related to T_1	Temperature difference due to convective heat transfer	Predicted Exit Drybulb Temper-ature
1						°C	29.86
2	1106	48.74	949	0.04	25.64	4.83	30.51
3	1107	51.11	951	0.05	26.21	4.91	31.16
4	1109	52.36	952	0.05	26.77	4.95	31.76
5	1110	53.19	954	0.05	27.29	4.99	32.33
6	1112	54.05	955	0.05	27.78	5.02	32.86
7	1113	54.85	957	0.05	28.24	5.06	33.35
8	1115	55.58	959	0.05	28.68	5.09	33.82
9	1116	56.24	960	0.05	29.09	5.13	34.26
10	1118	56.84	962	0.05	29.47	5.16	34.68
11	1120	57.39	963	0.05	29.84	5.19	35.08
12	1121	57.89	965	0.05	30.19	5.22	35.46
13	1123	58.34	966	0.05	30.52	5.25	35.82
14	1124	58.76	968	0.05	30.84	5.27	36.17
15	1126	59.14	970	0.05	31.15	5.30	36.50
16	1127	59.49	971	0.05	31.44	5.33	36.82

8.10 CHANGE IN RELATIVE HUMIDITY ALONG TUNNEL LENGTH

Figure 8.22 shows the change in relative humidity of the air as it flows along the tunnel length. During experimentation the fan drawing air over the grass was accidentally switched off for about 30 minutes during the hottest time of the day. The result was that the relative humidity of the air increased to such an extent in the enclosed tunnel that the grass could not transpire and the grass temperature rose to such an extent that the grass dried and died within these 30 minutes. This unfortunate incident indicates how important the role of transpiration is in keeping the temperature of the grass below the maximum of 45 °C [98TZ1]. Figures 8.23 and 8.24 shows the grass in the tunnel before and after the incident.

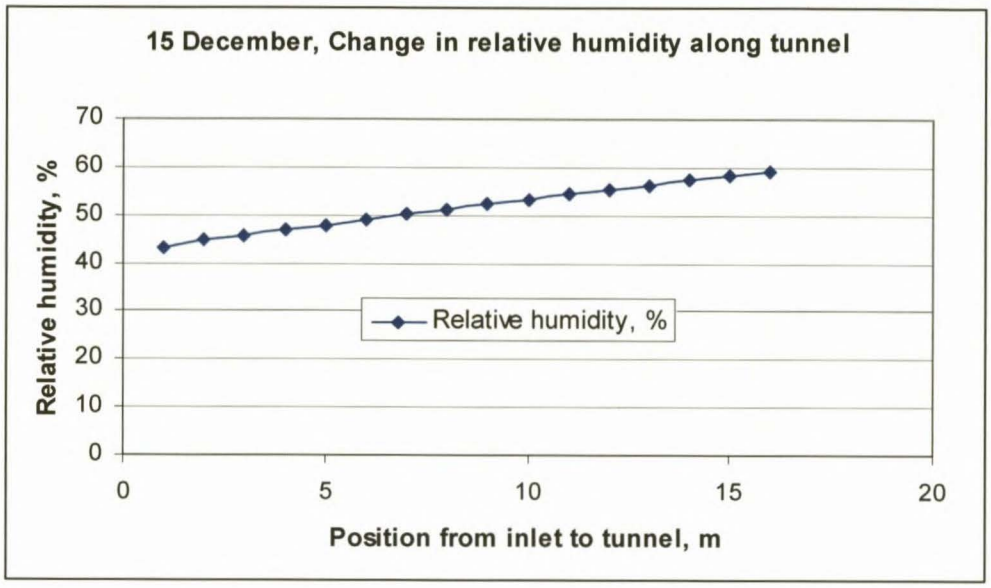

Figure 8.22: Change in relative humidity of the air as it flows along the tunnel

Figure 8.23: State of grass which was unable to transpire due to 100% relative humidity in closed glass tunnel (glass roofing sheets removed)

Figure 8.24: Healthy grass in tunnel prior to disaster (glass roofing sheets partially removed)

Figure 8.25 shows the change in predicted relative humidity and grass temperature if the experimental solar tunnel were to be extended.

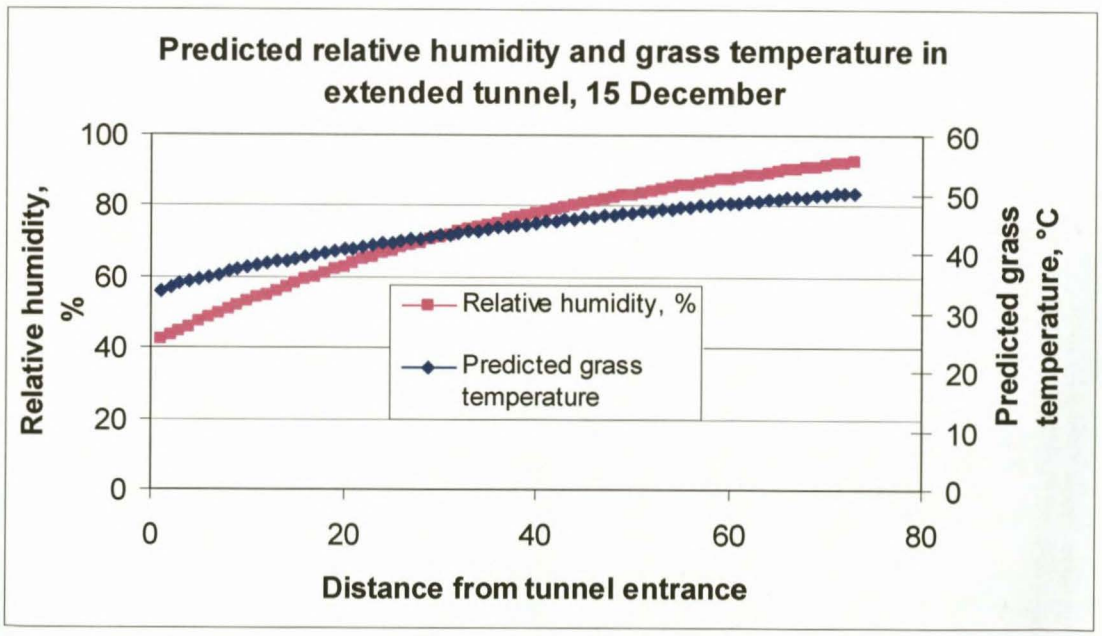

Figure 8.25: Predicted relative humidity and grass temperature if tunnel were to be extended

CHAPTER 9
DISCUSSION OF RESULTS AND CONCLUSIONS

9.0 INTRODUCTION

The objectives of this thesis were to

- determine the actual average rate of evapotranspiration of a grass surface by measuring the change in state of the air flowing over it
- estimate a value for the effective convective heat transfer coefficient between the grass surface and the air flowing over it and finally
- investigate whether the Penman-Monteith and conservation equations could be applied in the experimental set-up to predict the average rate of evapotranspiration, the grass surface temperature and the exit state of the air for a given inlet state. Upon validation of the model it will then be applied to the large-scale solar chimney power plant to ascertain the influence of vegetation on the annual power output of the plant. It is understood that a different boundary layer will apply in the large-scale model.

9.1 THE ACTUAL AVERAGE RATE OF EVAPOTRANSPIRATION

It was found that the maximum rate of evapotranspiration for days of maximum radiation varied between approximately 0.2 g/m^{2}s or 7.2 kg/m^{2}h to 0.25 g/m^{2}s or 9 kg/m^{2}h at the solar noon. Inlet air temperatures of about 40 °C accounted for the higher rate of evapotranspiration for more or less the same radiation intensity.

The calculation of the actual rate of evapotranspiration of the grass surface is dependent on the value of the dry and wetbulb temperature values at the inlet and outlet of the solar tunnel. During measurements these temperatures differed from thermocouple to thermocouple by between 0.5 °C and 1.5 °C because of the inlet air coming up from over the corner of the building, either from the north facing side (where the temperature was lower) or the east facing side (temperature higher due to solar radiation in the morning) or both, dependent on the fluctuating airflow direction. In spite of having a shade cloth cover over the inlet to try and even out the airflow, it was not always possible to have an airflow of equal temperature everywhere. In order to counteract this effect to a certain degree, all calculations are done using an average of three values over ten minute periods, i.e. a value every five minutes.

9.2 THE EFFECTIVE CONVECTIVE HEAT TRANSFER COEFFICIENT

Pressure drop measurements over freshly mowed grass were made in order establish a friction loss coefficient and hence an expression for the effective convective heat transfer coefficient. The velocity of the air in the tunnel was varied and the pressure drop over the tunnel measured. From these measurements the average Darcy friction factor was calculated and found to have a value of f_D = 0.0958. Inserting this value into the empirical equation of Burger-Kröger resulted in a value for the effective convective heat transfer coefficient of approximately 25 W/m^{2}K to 40 W/m^{2}K depending on the velocity of the air. The same Darcy friction factor was used throughout for all the calculations. However, referring to measurements taken during the month of February where conditions were not conducive to general measurements as there was cloud around, Table 6.2 shows that the pressure loss over the grass varies as the days go by. From the table it is evident that as the grass grows so does the friction loss. The Darcy friction factor increases from f_D = 0.03 to

f_D = 0.088 for the same air velocity since the pressure drop over the grass increased from 5 Pa on 6th February to 14.7 Pa on 17th February. This has implications for the effective heat transfer coefficient. However, on the day measurements were made shortly after the grass was mowed, it was found that the pressure drop was higher than for longer grass. The average Darcy friction factor had a value of 0.0958 implying that newly cut grass seems to represent a rougher surface than longer grass where the blades of grass have more flexibility and yet where the friction loss increases with increasing grass length. It is also possible though that the growth density of the grass was not the same as during previous measurements. Measurements were made over a period of several years in which the grass state varied and it was not possible to always have the same grass state. The problem with working with a living crop is that the approximate LAI as defined by Allen et al. (1989) may range between 1.9 to 3.6 between cuttings leading to a variation in canopy resistance depending on the structural characteristics and regrowth. This is evident from the variation in measured pressure drop over the grass for approximately the same air velocity.

The influence of the state of the grass as such was not investigated thoroughly as this was beyond the scope of the thesis and hence for calculation purposes a constant Darcy friction factor of 0.0958 was used. The implications of different values for the effective convective heat transfer coefficient are more fully discussed in a following section.

Utilizing the above values for the range of effective convective heat transfer coefficients applicable, the boundary layer resistance is calculated to lie between 30 s/m and 40 s/m for dependent on the velocity of the air. This is consistent with values found in the literature [81MO1].

9.3 APPLYING THE PENMAN-MONTEITH EQUATION TO PREDICT THE RATE OF EVAPOTRANSPIRATION

One of the important discoveries in this analysis was that the grass temperature changes along the solar tunnel and, by ignoring this fact, widely differing results in predicted values ensue. Conversely, the temperature of the glass roof differs only by a maximum of about 1.5 °C from inlet to outlet and in the conservation equations a single value for the entire tunnel was used for the glass temperature. From calculations it was found that the grass temperature changes by about 5 °C and this results in the infrared radiation exchange changing from about 25 W/m^2 at the inlet to about – 5 W/m^2 at the outlet which makes a difference of about 30 W/m^2 over the tunnel length. The maximum radiation absorbed by the grass was about 600 W/m^2 and the variation in infrared radiation will influence the rate of evapotranspiration by about 5 %. During periods of maximum insolation, i.e. during the summer months, latent heat transfer due to evapotranspiration accounted for about 80 % to 90 % of the total heat transfer to the air and is therefore the controlling parameter.

Referring to Figures 8.1, up to and including Figure 8.4, it is evident that the difference between the measured and predicted values of average rates of evapo-transpiration are within experimental limits. However, there is a tendency on some days to overprediction mainly in the afternoon. A possible explanation could be a difference in the availability of water in the soil as the day progressed. This would lead to a higher canopy resistance and hence lower rate of evapotranspiration. Then too it was not always possible to have the same moisture content of soil for all measurement days as the weather is variable and perfect measuring days not always predictable. During a series of tests the grass was watered every day in order to try

and keep the soil saturated and thus eliminate this variable but this resulted in the roots rotting due to lack of oxygen in the ground and the grass died. Further experiments were delayed for yet another year. During another series of tests where the surrounding air temperatures were in excess of 40 °C the measured value of evapotranspiration was about 15 % lower than the predicted value possibly indicating stomatal closure. When considering predicted and measured average evapotranspiration rates, it was found that for a lower measured evapotranspiration rate compared to the predicted rate the measured grass temperature (compared to the predicted temperature) was higher. This should be so since less evapotranspiration implies less evaporative cooling for the leaves, hence higher leaf temperatures. The predicted rate of evapotranspiration was based on a canopy or stomatal resistance of 70 s/m which is not always the case.

For the canopy or stomatal resistance, a constant value of 70 s/m was used: this being the value used by the FAO when considering reference grass evapotranspiration. The canopy resistance may, however, vary due either to an increasing resistance due to stomatal closure or an increasing resistance due to soil water depletion adding a resistance at root level. In a specific calculation it was found that for a canopy or stomatal resistance of 70 s/m the predicted latent heat transfer for the entire tunnel was 7550 W. Doubling the canopy resistance to 140 s/m leads to a latent heat transfer of 6720 W, being an 11 % decrease in evapotranspiration predicted when referred to the reference resistance. Furthermore the canopy or stomatal resistance is also dependent on the growth state of the grass: i.e. the LAI or otherwise stated, the grass length and grass density. Further research is called for in this area. The link between soil water content and canopy resistance also needs more thorough investigation.

In addition it was found that in the calculation of the rate of evapotranspiration that a difference in 1 °C higher or lower in the wetbulb temperature, for the same drybulb temperature, leads to a change in predicted value of the rate of evapotranspiration from about - 5 % to about + 5 % compared to the measured value. Considering that the measured values of the drybulb and wetbulb temperatures from the thermocouples used, themselves differed by about 0.5 °C to about 1.5 °C, the predicted values compared well within experimental limits with the measured values of average evapotranspiration rates.

9.4 APPLICATION OF THE PENMAN-MONTEITH EQUATION TO PREDICT THE GRASS SURFACE TEMPERATURE

Considering Figure 8.5 and Figure 8.7 there is a tendency for the measured grass temperature to be lower in the morning and higher in the afternoon than the predicted temperature. Referring to Figures 8.20 and 8.21 where the ground and air temperatures are shown, it is possible that over prediction of the grass temperature in the morning and under prediction in the afternoon when compared to measured values could be due to a greater loss of heat to the soil in the morning and less in the afternoon as the day progresses since the temperature difference is large in the morning and very much smaller in the afternoon. A constant value for the entire day of heat loss to the soil of 10 % of the heat reaching the grass was used in all calculations. This is in accordance with suggestions by the FAO. The grass temperature is dependent also on the net radiation absorbed by the grass. This is in turn affected by the amount of infrared radiation exchanged between the glass roof and the grass surface. These are all linked to each other so that a small error in one parameter will result in errors in all the dependent parameters.

Considering the complexity of the energy exchanges and many interdependent parameters it can be concluded that the Penman-Monteith approach gives a reasonable estimate of the surface temperature within experimental limits. It must also be borne in mind that in the deduction of the Penman-Monteith equation several approximations were made which exacerbate any abberations.

9.5 PREDICTING THE EXIT DRYBULB TEMPERATURE

Table 8.1 shows the influence of changing the effective convective heat transfer coefficient on the prediction of the various parameters. These values are for 15 December at solar hour 13.36 h and show that the effective convective heat transfer coefficient most consistent with experimental data has a value of about 30 W/m^2K. The average grass surface temperature and the rate of evapotranspiration are closest to those measured and show percentage wise the greatest deviation in value from the measured value for the various convective heat transfer coefficients. The prediction of the exit dry- and wetbulb temperatures does not vary very much with the effective convective heat transfer coefficient although there is an overprediction in the value of the drybulb temperature. This seems to suggest that the effective convective heat transfer coefficient would be that which most accurately predicts the grass surface temperature and rate of evapotranspiration. The effective convective heat transfer coefficient of about 30 W/m^2K for the relevant velocity is also consistent with the value calculated from pressure drop measurements over the grass surface. This leads to confidence in the value of the effective convective heat transfer coefficient used in the calculations.

9.6 EXTENDING THE TUNNEL THEORETICALLY

Figure 8.25 shows the predicted increase in relative humidity and grass temperature if the tunnel were to be extended. In applying this model to the large-scale model one would be able to ascertain how far inward vegetation could be planted before a critical vegetation temperature of 45 °C is reached. The graph shows that the air is below saturation when the critical vegetation temperature is reached thus showing that the vegetation temperature is the controlling parameter.

9.7 RECOMMENDATIONS AND SUGGESTIONS FOR FURTHER RESEARCH

- Considering that the accurate determination of the dry- and wetbulb temperatures at the inlet and the outlet of the tunnel is critical, it is suggested that a special mixing box also be placed at the inlet to the tunnel to ensure a thorough mixing of the air before entering the tunnel.

- Furthermore it is suggested that many more thermocouples be used at either end of the tunnel for a more accurate average value to be determined.

- The grass temperature needs to be measured at more points along the tunnel to have a better measured temperature profile of the grass surface along the length of the tunnel in. In this thesis only one and sometimes two measuring points were used.

- The water content of the soil was not measured and therefore only the FAO estimate of a heat loss to the soil of 10 % of the energy absorbed by the grass was used in all calculations. The specific heat capacity of soil is greatly affected by the water content and this will affect the heat transfer. This should be

measured and taken into account. The soil water content also affects the canopy resistance at root level: the resistance will increase if soil water is not freely available as could happen towards the end of a day of continuous measurement during periods of high dry bulb temperatures.

- The state of the grass or growth density and grass length need to be investigated more thoroughly so that the effective convective heat transfer coefficient can be determined as a function of grass length at least as a first approximation.

- The canopy or stomatal resistance variation due to changing growth density as well as the high air temperature (higher than 40 °C) influence on stomatal closure needs to be investigated in order to determine more accurately the value of γ^* in the Penman – Monteith equation.

- The heat loss to the soil needs to be refined also in terms of the temperature difference between the grass and the soil and is not viewed as the constant value of 10 % of the energy absorbed by the grass throughout the day.

REFERENCES

[48 PE 1] Penman, H., Natural Evaporation from Open Water, Bare Soil and Grass. Proceedings of the Royal Society of London, A, Vol. 194, pp. 120 – 145, 1948.

[51 PE 1] Penman, H.L. and Schofield, R.K., Some Physical Aspects of Assimilation and Transpiration. Symposium of the Society of Experimental Biology, Vol. 5, pp. 115 - 129, 1951.

[52 NB 1] National Building Research Institute, 1952. Pretoria, South Africa.

[61 RO 1] Rohsenow, W.M., and Choi, H., Heat, Mass and Momentum Transfer. Prentice-Hall, 1961.

[63 HS 1] Hsu, Shao Ti, Engineering Heat Transfer. D. Van Nostrand Company, Princeton, New Jersey, 1963.

[68 GA 1] Gates, D. E., Transpiration and Leaf Temperature. Annual Review of Plant Physiology, Vol. 19, pp. 211 - 238, 1968.

[68 ME 1] Meidner, H. and Mansfield, T., Physiology of Stomata. McGraw-Hill, 1968.

[68 WA 1] Waggoner, P.E. and Reifsnyder, W.E., Simulation of the Temperature, Humidity and Evaporation Profiles in a Leaf Canopy. Jnl. of Applied Meteorology, Vol. 7, pp. 400 – 409, 1968.

[71 GA 1] Gates, D.M., Atlas of Energy Budgets of Plant Leaves. Academic Press, 1971.

[72 LI 1] Linacre, E.T., Leaf Temperature, Diffusion Resistances, and Transpiration. Agricultural Meteorology, Vol. 10, pp. 365 – 382, 1972.

[72 TH 1] Thom, A.S., Momentum, Mass and Heat Exchange of Vegetation, Quart. Jnl. of the Royal Met. Soc., 98, pp. 124 – 134, 1972.

[73 MO 1] Monteith, J.L., Principles of Environmental Physics. Arnold, 1973.

[73 PR 1] Pruit, W.O. and Morgan, D.L., Momentum and Mass Transfers in the Surface boundary layer. Quart. Jnl. of the Royal Met. Soc. 99, pp. 370 – 386, 1973.

[74 NO 1] Nobel, Park S., Introduction to Biophysical Plant Physiology. W.H. Freeman and Company, 1974.

[75 MO 1] Monteith, J.L., Editor, Vegetation and the Atmosphere. Academic Press, 1975.

[75 TH 1] Thom, A.S., Momentum, Mass, and Heat Exchange of Plant Communities. Vegetation and the Atmosphere, 1, Principles, ed. Monteith, J.L., pp. 57 - 109, Academic Press, London, 1975.

[77 PR 1] Pruitt, W.O., Doorenbos, G., "Background and Development of Methods to Predict Reference Crop Evapotranspiration", Guidelines for predicting crop

water requirements (FAO Irrigation and Drainage Paper 24), Food and Agric. Organization of the United Nations, Rome, Italy, pp. 108 - 119, 1977.

[81 MO 1] Monteith, J.L., Evaporation and surface temperature. Quart. Jnl. of the Royal Met. Soc. Vol. 107, pp. 1 – 27, 1981.

[81 WR 1] Wright, J.L., Crop coefficients for Estimates of Daily Crop Evapotranspiration, Irrigation, Scheduling for Water and Energy Conservation in the 80's. Proc. Irrig. Scheduling Conference. A.S.M.E., Chicago. pp. 18 – 26, 1981.

[82 ST 1] Stoecker, W.F. and Jones, J.W., Refrigeration and Air Conditioning, McGraw Hill, 1982.

[83 FR 1] Frevert, D.K, Hill, R.W. and Traaten, B.C., Estimation of FAO Evapotranspiration coefficients. Jnl. Irrig. And Drainage Eng., ASCE, Vol. 109, pp. 265 – 270, 1983.

[83 HA 1] Haaland, S.E., Simple and Explicit Formulas for the Friction Factor in Turbulent Pipe Flow, Jnl. of Fluids Engineering, Vol. 105, pp. 89 - 90, March 1983.

[85 VA 1] Van Wylen, G., Fundamentals of Classical Thermodynamics, 3rd Edition. Wiley, 1985.

[86 AL 1] Allen, R.G., A Penman for all Seasons, Jnl. of Irrig. and Drainage Eng., ASCE, Vol. 112, no 4, pp. 348 - 368, 1986

[89 CO 1] Conradie, P.J., Psigrometrie. Unpublished notes, University of Stellenbosch, South Africa, 1989.

[89 DJ 1] De Jager, J.M. and van Zyl, W.H., Atmospheric Evaporative Demand and Evaporation Coefficient Concepts, Water SA, Vol. 15, No 2. April 1989.

[89 HO 1] Holman, J.P., Heat Transfer. McGraw Hill, 1989.

[90 MO 1] Monteith, J.L. and Unsworth, M.H., Principles of Environmental Physics, 2nd ed. Arnold, 1989.

[91 AL 1] Allen, R.G. and Pruitt, W.O., FAO-24 reference evapotranspiration factors. J. Irrig. And Drainage Eng., ASCE, Vol. 117 no. 5, pp. 758 – 773, 1991.

[91 DU 1] Duffie, J. and Beckman, W.A., Solar Engineering of Thermal Process, 2nd ed. Wiley, 1991.

[91 WH 1] White, F.M., Viscous Fluid Flow, 2nd ed. McGraw-Hill, 1991.

[92 AS 1] ASHRAE Handbook. HVAC Systems and Equipment, ASHRAE, 1992.

[92 DO 1] Dong, A., Grattan, S.R., Carroll, J.J. and Prashar, C.R.K., Estimation of Daytime Net Radiation over Well-Watered Grass, J. Irrig. and Drainage Eng., Vol. 118, No. 3, 1992.

[92 RA 1] Raupach, M.R., Drag and Partition on Rough Surfaces, Boundary-Layer Meteorology Vol. 60, pp. 375 - 395, 1992.

[93 MO 1] Modest, M.F., Radiative Heat Transfer, McGraw-Hill, Inc.,1993.

[94 AL 1] Allen, R.G., Smith, M. and Pereira, L.S., An Update for the Definition of Reference Evapotranspiration, ICID Bulletin, Vol. 43, No. 2 , pp. 1 - 34, 1994.

[94 AL 2] Allen, R.G., Smith, M. and Pereira, L.S., An Update for the Definition of Reference Evapotranspiration, ICID Bulletin, Vol. 43, No. 2 , pp. 35-61, 1994.

[94 WH 1] White, W.H., Fluid Mechanics, 3rd Ed., McGraw-Hill, Inc., 1994.

[95 MO 1] Moore, R. et al. Botany,. Wm. C. Brown Communications Inc., Dubuque, IA 52001., 1995.

[97 WI 1] Winterton, R.H.S., Where did the Dittus and Boelter Equation Come From?, Technical Notes, Int. Jnl. Heat Mass Transfer. Vol. 41, Nos. 4 - 5, pp. 809 - 810, 1997.

[98 TZ 1] Taiz, L. and Zeiger, E., Plant Physiology, 2nd. Ed., Sinauer, Assoc. Inc., 1998.

[00 SA 1] Sartori, E., A Critical Review on Equations Employed for the Calculation of the Evaporation Rate from Free Water Surfaces. Solar Energy, Vol. 68, No. 1, pp. 77 - 89, 2000

[02 BL 1] Blight, G.E., Measuring Evaporation from Soil Surfaces for Environmental and Geotechnical Purposes, Water SA, Vol. 28, No 4. October 2002.

[02 CE 1] Cengel, Y. and Boles, M.A., Thermodynamics, an Engineering Approach, 4th Ed., Mc Graw-Hill, 2002.

[02 KR 1] Kröger D.G., Convection Heat Transfer Between a Horizontal Suface and The Natural Environment, South African Institution Of Mechanical Engineering, R & D Journal, Vol. 18, No. 3, pp. 49 – 53, November 2002.

[02 LO 1] Lombaard, F., Performance of a Solar Air Heater Incorporating Thermal Storage, Master's thesis, University of Stellenbosch, Stellenbosch, South Africa, 2002

[04 TA 1] Tang, R., Etzion, Y., Comparative studies on the water evaporation rate from a wetted surface and that from a free water surface. Building and Environment, Vol. 39, pp. 77 - 86, 2004.

[04 FA1] http://www.fao.org/docrep/X0490E/x490e07.htm, 13/10/2004

[04 KR 1] Kröger, D.G., Air-cooled Heat Exchangers and Cooling Towers, Penwell Corp., Tulsa, OK, USA, 2004

[06 BU 1] Burger, M., Kröger, D.G.: Experimental Convection Heat Transfer Coefficient Between a Horizontal Surface and the Natural Environment,

Proc. 17th International Congress of Chemical and Process Engineering, Prague, Czech Rep., Lecture J6.04, Summary: pp. 1523 - 1524, 27 – 31 Aug. 2006.

[06 PR 1] Pretorius, H.P., Optimization and Control of a Large-scale Solar Chimney Power Plant, PhD thesis, University of Stellenbosch, South Africa, 2006.

APPENDIX A

BACKGROUND HISTORY TO THE PENMAN AND PENMAN MONTEITH EQUATIONS

A.0 INTRODUCTION

In the area of agriculture, accurate and consistent estimates of daily evapotranspiration are vitally important for irrigation planning and scheduling. Penman [48PE1] developed the first of several equations in which the energy and transport equations are combined for estimating evapotranspiration rates from climatic data. From this the rate of evapotranspiration and therefore crop water requirement may be estimated. In the application to the solar tunnel, the influence of the water vapor added on the properties of the air flow may be predicted.

Monteith improved the original Penman equation by introducing terms for surface resistance to account for the effects of the vegetation. This culminated in the United Nations Food and Agricultural Organization, FOA, Penman-Monteith equation.

This equation was applied by Doorenbos and Pruitt [77PR1] to evaluate a reference crop evapotranspiration rate. Detailed procedures for estimating a reference evapotranspiration rate were presented, defined as "the rate of evapotranspiration from an extensive surface of 8-15 cm tall green grass cover of uniform height, actively growing, completely shading the ground, and not short of water" as quoted by Wright, J.L. [81WR1]. Crop coefficients are then used together with values of reference evapotranspiration to estimate the water use of a crop. Crop coefficients are empirical ratios of crop evapotranspiration to reference evapotranspiration and are derived from experimental data [81WR1].

Since a "living" reference crop is difficult to reproduce over a range of locations [94AL1], in May 1990, the FAO changed the concept of reference evapotranspiration and revised calculation procedures. A hypothetical reference crop, which is described by an appropriate Penman-Monteith equation has been substituted for a living reference crop as described by Allen [94AL1]. The evapotranspiration rate of this hypothetical canopy is referred to as the "Grass Reference Evapotranspiration" and is then used to calibrate empirical grass reference evapotranspiration equations as a basis for determining crop coefficients where reference evapotranspiration is not simultaneously measured with crop evapotranspiration for a certain location.

A.1 FUNDAMENTAL DEFINITIONS, SYMBOLS AND DERIVATIONS RELATING TO ATMOSPHERIC OR MOIST AIR

A.1.1. Humidity ratio, w

The humidity ratio, w, is defined as the mass of water vapor per unit mass of dry air.

$$w = \frac{\text{kg of water vapor}}{\text{kg of dry air}}, \text{ kg/kg da} \qquad (A.1)$$

Atmospheric may be considered as a mixture of two perfect gases, dry air and water vapor, obeying Dalton's Law of Partial Pressures [02CE1]. The air and water vapor are each at a partial pressure of p_a and p_v respectively. Equation (A.1) may be written as

$$w = \frac{p_v V/R_v T}{p_a V/R_a T} = \frac{p_v R_v}{p_a R_a} = \frac{p_v}{p_a}\left(\frac{461.52}{287.08}\right) = 0.622\left(\frac{p_v}{p_a}\right), \text{ kg/kg da} \quad (A.2)$$

where V is an arbitrary volume, R_v=461.52 J/kgK for water vapor and R_a=287. /kgK for air.

The total mixture pressure, $p_{atm} = p_a + p_v$ (A.3)

Substituting equation (A.3) into (A.2), find

$$w = \frac{0.622 p_v}{p_{atm} - p_a}, \text{ kg/kg da} \quad (A.4)$$

A.1.2. Specific humidity, q

The specific humidity, q, is defined as the mass of water vapor per unit mass of moist or atmospheric air.

$q = w/(1+w)$, kg/kg air (A.5)

A.1.3. Absolute humidity, χ

The absolute humidity, χ, or vapor density, is defined as the mass of water vapor per unit volume of moist air.

$\chi = w/v$, kg/m^3 (A.6)

A.1.4. Density, ρ

The density, ρ, is defined as the mass of moist air per unit volume of moist air.

$\rho = (1+w)/v$, kg/m^3 (A.7)

A.1.5. Specific volume of moist air, v

Applying Dalton's Law of Partial Pressures to the dry air component, find

$$v = \frac{R_a T}{p_a}, \text{ m}^3/\text{ kg da} \quad (A.8)$$

A.1.6. The slope of the saturated vapor pressure line, Δ

The slope of the saturated vapor pressure line is given by the Clausius-Clapeyron equation

$$\Delta = \left(\frac{dp}{dT}\right)_{sat} = \frac{i_{fg}}{T v_{fg}}, \text{ Pa/K} \quad (A.9)$$

Since $v_{fg} = v_g - v_f$ and $v_f << v_g$

$$\left(\frac{dp}{dT}\right)_{sat} \approx \frac{i_{fg}}{T v_g} \quad (A.10)$$

Applying the equation of state to the water vapor as a perfect gas, and substituting into equation (A.10), find

$$\left(\frac{dp}{dT}\right)_{sat} \approx \frac{i_{fg} p_{sat}(T)}{T^2 R_v} \equiv \Delta \quad (A.11)$$

where R_v is the gas constant for water vapor and $p_{sat}(T)$ is the saturation pressure of water vapor at temperature T.

A.1.7. Adiabatic saturation and the psychrometric constant

Adiabatic saturation takes place when a stream of unsaturated air is adiabatically being exposed to a fine spray of water which is continuously being recirculated. In the ideal situation it is assumed that the air becomes saturated and reaches the temperature of the recirculating water.

Shown below is a schematic diagram of such a process.

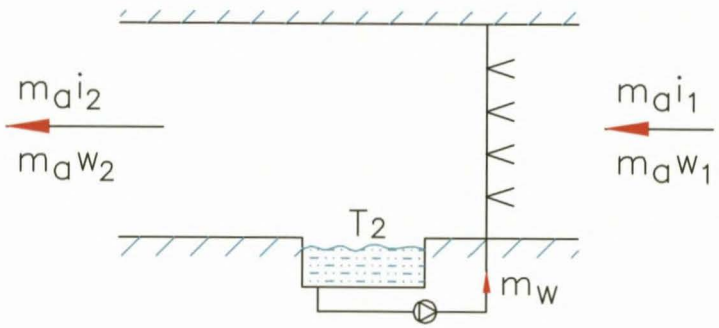

Figure A.1: Schematic adiabatic saturation process.

For a steady flow situation the following apply.

Water mass balance: $m_a w_1 + m_w = m_a w_2$ (A.12)

where m_a is the mass flowrate of dry air, and w is the specific humidity of the air

Energy balance $m_a i_1 + m_w i_f = m_a i_2$ (A.13)

where m_w is the mass flowrate of the water, and i and i_f are the specific enthalpy of the atmospheric air and the water respectively.

Consider the process schematically on the psychrometric chart as shown in Figure A.2

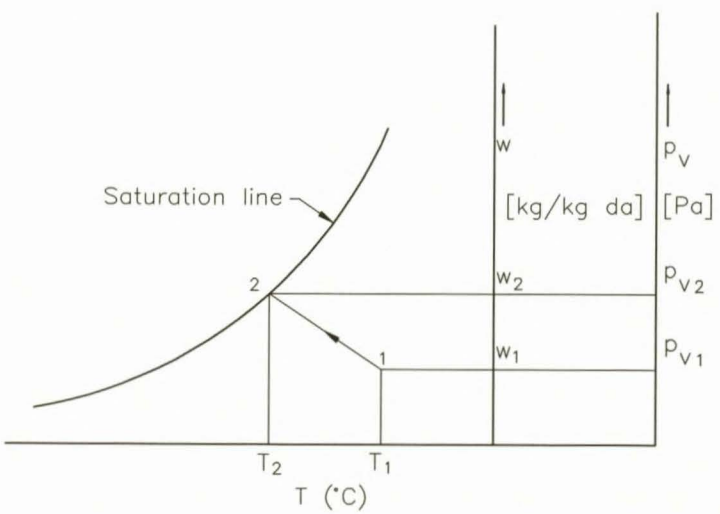

Figure A.2: Adiabatic saturation.

The enthalpy of the atmospheric air per kilogram of dry air may be expressed as

$$i = c_{pa}T + w\left(i_{wfg@0°C} + c_{pv}T\right), \text{ J/kg da, the temperature being in } ^\circ \text{ C} \qquad \text{(A.14)}$$

The reference state for zero enthalpy is 0 °C and 0 % relative humidity

Substituting equations (A.14) and (A.12) into (A.13, collecting terms and simplifiying, find

$$\left(c_{pa} + w_1 c_{pv}\right)\left(T_1 - T_2\right) = \left(w_2 - w_1\right)\left(i_{fg@0°C} + c_{pv}T_2 - c_{pw}T_w\right) \qquad \text{(A.15)}$$

Furthermore

$$i_{v_2} = i_{fg@0°C} + c_{pv}T_2 \equiv c_{pw}T_2 + i_{fg@T_2} \qquad \text{(A.16)}$$

Substitute (A.16) into (A.15) and find

$$\left(c_{pa} + w_1 c_s\right)\left(T_1 - T_2\right) = \left(w_2 - w_1\right)\left(c_{pw}T_2 - c_{pw}T_w + i_{fg@T_2}\right) \qquad \text{(A.17)}$$

But with recirculation $t_w \approx t_2$. If the air outlet state is assumed saturated at the temperature of the water the equation then simplifies to

$$\left(c_{pa} + w_1 c_s\right)\left(T_1 - T_2\right) = \left(w_2 - w_1\right) i_{fg@T_2} \qquad \text{(A.18)}$$

Rearranging, find the slope of the line of adiabatic saturation as

$$\frac{w_2 - w_1}{T_1 - T_2} = \frac{c_{pa} + w_1 c_{pv_1}}{i_{fg@T_2}} = \frac{c_{pma1}}{i_{fg@T_2}} \text{ kg vapor/kg da K} \qquad \text{(A. 19)}$$

where c_{pma1} is the specific heat of the moist or atmospheric air before saturation.

Furthermore, from equation (A.4)

$$w_1 = \frac{0.622 p_{v_1}}{p_{atm} - p_{v_1}}$$

$$w_2 = \frac{0.622 p_{v_2}}{p_{atm} - p_{v_2}} \text{ kg/kg da}$$

$p_v <<< p_{atm}$, so that

$$w_2 - w_1 \approx \frac{0.622\left(p_{v_2} - p_{v_1}\right)}{p_{atm}} \qquad \text{(A.20)}$$

Substituting (A.20) into (A.19) and rearranging, find

$$\frac{p_{v_2} - p_{v_1}}{T_1 - T_2} = \frac{c_{pma1} p_{atm}}{0.622\, i_{fg@T_2}} \text{ Pa/K} \qquad \text{(A.21)}$$

The above relationship gives the slope of the line of adiabatic saturation on the psychrometric chart. This relationship is also known as the psychrometric "constant", γ, where

$$\gamma = \frac{c_{pma1} p_{atm}}{0.622 i_{fg_2}} \equiv \frac{p_{v_2} - p_{v_1}}{T_1 - T_2} \text{ Pa/K} \qquad \text{(A.22)}$$

The psychrometric "constant" is a very weak function of temperature and varies from 66 Pa/K at 0 °C to 68 Pa/K at 40 °C and atmospheric pressure 101325 Pa and is therefore referred to as a "constant". For the range in which it is applied in this thesis, a single value is used throughout.

A.1.8. Wetbulb process

Considering the wetbulb process, the slope of the wetbulb temperature line on the psychrometric chart may be derived.

When the wetbulb temperature has been reached there is an equilibrium state in which all the energy needed for the evaporation of the water in the wick of the wetbulb thermometer is received by convection from the surrounding air. The process is represented in Figure A.3

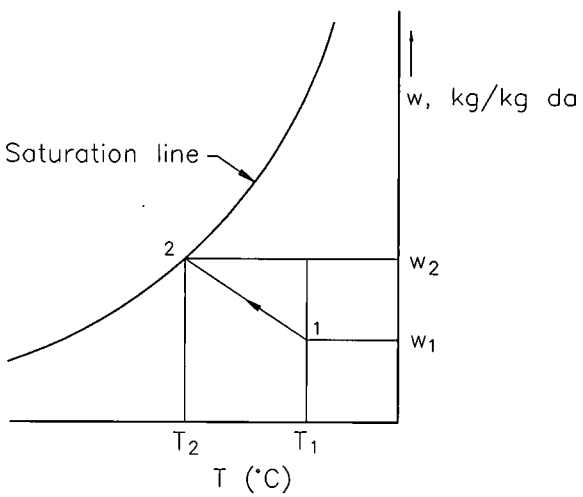

Figure A.3: Wetbulb process.

Referring to Figure A.3, the process 1-2 is the change in state of the micro-atmosphere surrounding the wick of the wetbulb thermometer at equilibrium. The mass conservation equation for this equilibrium state is

$$m_v = m_a(w_2 - w_1) \qquad \text{(A.23)}$$

where m_v is the mass of water evaporated from the surface of the wick and w is the specific humidity of the air flowing over the wick. All the heat needed for evaporating the water from the surface of the wick comes from the air with which it comes into contact.

The convective heat transfer equation over the area of evaporation is given by

$$Q_c = h_c A(T_1 - T_2) \qquad \text{(A.24)}$$

where h_c is the transfer coefficient for convective heat and A is the transfer surface for the water vapor, T_1 is the temperature of the surrounding air and T_2 is the equilibrium temperature of the wetbulb wick.

From Fick's Law for diffusion

$$m_v = h_D A(\chi_2 - \chi_1) \tag{A.25}$$

where h_D is the mass transfer coefficient, and χ_2 and χ_1 the vapor concentration or vapor density at the surface and the free stream air respectively.

The energy needed for evaporation per unit area

$$\frac{Q_{Latent}}{A} = \frac{m_v i_{fg}}{A} = h_D(\chi_2 - \chi_1) i_{fg} \tag{A.26}$$

where i_{fg} is the latent heat of evaporation.

Equations (A.24) and (A.26) may be rewritten in terms of a potential and a resistance.

Defining r_H and r_V the resistances for heat and mass transfer respectively as

$$r_H \equiv \frac{c_{pma}\rho}{h_c}, \text{ s/m for heat transfer and} \tag{A.27}$$

$$r_v \equiv 1/h_D, \text{ s/m for mass transfer} \tag{A.28}$$

where c_{pma} is the specific heat and ρ the density of atmospheric air.

Substituting equation (A.27) into (A.24) and (A.28) into (A.25), find

$$Q_c / A = c_{pma}\rho(T_1 - T_2)/r_H \tag{A.29}$$

$$Q_{latent} / A = (\chi_2 - \chi_1) i_{fg} / r_V \tag{A.30}$$

Applying the equations (A.5), (A.6), and (A.7) find

$$\chi = \rho q \tag{A.31}$$

Inserting (A.31) into (A.30) find

$$Q_{latent} / A = \rho(q_2 - q_1) i_{fg} / r_V \tag{A.32}$$

A useful expression for the specific humidity, q, may be obtained in the following way:

From the definition of the density, ρ, i.e.

$$\rho = \frac{1+w}{v} \text{ kg moist air per unit volume} \tag{A.7}$$

which can be rewritten as

$$\rho = = \frac{1}{v} + \frac{w}{v} \tag{A.33}$$

Since the air may be viewed as a perfect gas

$$p_a v = R_a T \text{ or } 1/v = p_a M_a / R_u T \tag{A.34}$$

where R_u is the universal gas constant, 8.314 kJ/kmole.

Similarly for the water vapor

$$p_v v = wR_v T \text{ or } w/v = p_v M_v / R_u T \tag{A.35}$$

Inserting (A.34) and (A.35) into (A.33), find

$$\rho = \frac{1}{R_u T}[p_a M_a + p_v M_v] \tag{A.36}$$

Since $p_{atm} = p_a + p_v$ (A.3)

Inserting and rearranging, find

$$\rho = \frac{1}{R_u T}[(p_{atm} - p_v) M_a + p_v M_v]$$

$$\rho = \frac{1}{R_u T}[(p_{atm} - p_v) M_a + p_v M_v] = \frac{M_a}{R_u T}\left[(p_{atm} - p_v) + \frac{M_v}{M_a} p_v\right]$$

$$= \frac{M_a}{R_u T}\left[\left(p_{atm} - p_v\left(1 - \frac{M_v}{M_a}\right)\right)\right] = \frac{M_a}{R_u T}[p_{atm} - p_v(0.378)] \text{ since } M_v/M_a = 0.622 \tag{A.37}$$

$p_v << p_{atm}$, then $0.378 p_v$ is even smaller than the total pressure, therefore find

$$\rho \approx \frac{M_a}{R_u T} p_{atm}, \tag{A.38}$$

Substituting equation (A.35) into (A.6), and (A.38) into (A.31) equating and rearranging, find

$$q = \frac{p_v M_v}{p_{atm} M_a} = 0.622 \frac{p_v}{p_{atm}} \tag{A.39}$$

Substituting equation (A.39) into equation (A.32) find

$$Q_{latent}/A = \frac{0.622\, i_{fg} \rho}{p_{atm} r_V}(p_{v2} - p_{v1}) \tag{A.40}$$

with p_{v2} and p_{v1} the partial vapor pressures at the surface and the free stream air respectively.

Since $\frac{c_{pma} p_{atm}}{0.622 i_{fg}} = \gamma$ from (A.22). Substituting into the above equation find

$$Q_{latent}/A = \frac{c_{pma} \rho}{\gamma\, r_V}(p_{v2} - p_{v1}) \tag{A.41}$$

This is a function involving the resistance to mass transfer.

Defining a new psychrometric "constant", γ^* where

$$\gamma^* = \gamma\, r_V / r_H \tag{A.42}$$

or $\gamma = \gamma^* r_H / r_V$ (A.43)

Substituting equation (A.43) into equation (A.41), find

$$Q_{latent} / A = \frac{c_{pma}\rho}{\gamma^* r_H}(p_{v2} - p_{v1}) \qquad (A\ 44)$$

At equilibrium the gain in convective heat is equal to the loss by evaporation (or latent heat) so that equation (A.29) equals equation (A.44), i.e.

$$\frac{c_{pma}\rho}{\gamma^* r_H}(p_{v2} - p_{v1}) = \frac{c_{pma}\rho(T_1 - T_2)}{r_H} \qquad (A.45)$$

Simplifying and defining the slope of the wetbulb line as γ^*, find,

$$\frac{p_{v2} - p_{v1}}{T_1 - T_2} = \gamma^* \qquad (A.46)$$

For fully developed turbulent flow over a flat plate where heat and mass transfer areas are the same, Monteith [90MO1] gives $r_v / r_H = (Le)^{0.67}$, where Le is the Lewis number.

Since $Le_{25\,°C}$ =0.8519 [89HO1], find $\frac{r_v}{r_H} = 0.8982 \approx 0.9$ (A.47)

for an air-water interface at 25°

Consequently equations (A.47) and (A.22) show that the process of adiabatic saturation proceeds more or less along the line of constant wetbulb temperature. The adiabatic saturation temperature and the wetbulb temperature are approximately equal to each other and for micrometeorological purposes this is sufficiently accurate.

$$\frac{r_v}{r_H} = Le^{-0.33} Le = Le^{0.67} \qquad (A.\ 48)$$

Equation (A.48) shows that the resistance to vapor transfer and convective heat transfer are nearly equal for fully developed turbulent flow over a flat surface. A single leaf may be approximated by a flat surface, however, applying this relationship to a canopy of leaves leads to error since the canopy or stomatal resistance needs to be taken into account.

A.1.9. Vapor Pressure Depression (vpd)

The vapor pressure depression is a term denoting the difference in the partial vapor pressure of saturated atmospheric air at a given drybulb temperature and the vapor pressure of unsaturated atmospheric air at the same drybulb temperature.

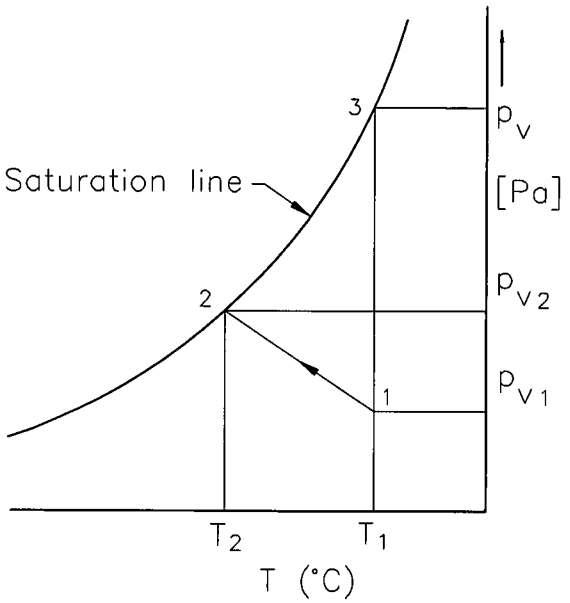

Figure A.4: Vapor pressure depression.

Per definition the vapor pressure depression at a given drybulb temperature, T_1, may be written as

$$vpd = p_{v3} - p_{v1} \tag{A.49}$$

Rewriting

$$vpd = p_{v3} - p_{v1} = (p_{v3} - p_{v2}) + (p_{v2} - p_{v1}) \tag{A.50}$$

From equation (A.46), find

$$p_{v2} - p_{v1} = \gamma^* (T_1 - T_2) \tag{A.51}$$

where T_1 is the drybulb- and T_2 the wetbulb temperature of the air.

Viewing the saturation vapor pressure line as a straight line from states 2 to 3, (which, for a small temperature difference of about 10 K, is a reasonable approximation) and applying equation (A.11), find

$$p_{v3} - p_{v2} = \Delta(T_1 - T_2) \tag{A.52}$$

Inserting equations (A.51) and (A.52) into (A.50) and collecting terms, find

$$vpd = (\Delta + \gamma^*)(T_1 - T_2) = p_3 - p_1 = p_{sat}(T_1) - p_v(T_1) \tag{A.53}$$

where Δ is evaluated at $(T_1 + T_2)/2$ for the temperature range under consideration.

A.2 PSYCHROMETRIC PRINCIPLES FOR DIABATIC HEAT AND MASS TRANSFER FOR A WETTED SURFACE-THE DERIVATION OF THE PENMAN EQUATION

When air is flowing over a heated wetted surface, it may be assumed that this micro-atmosphere directly in contact with the surface is saturated and at the same temperature as that of the surface.

Referring to Figure A.5 consider the following:

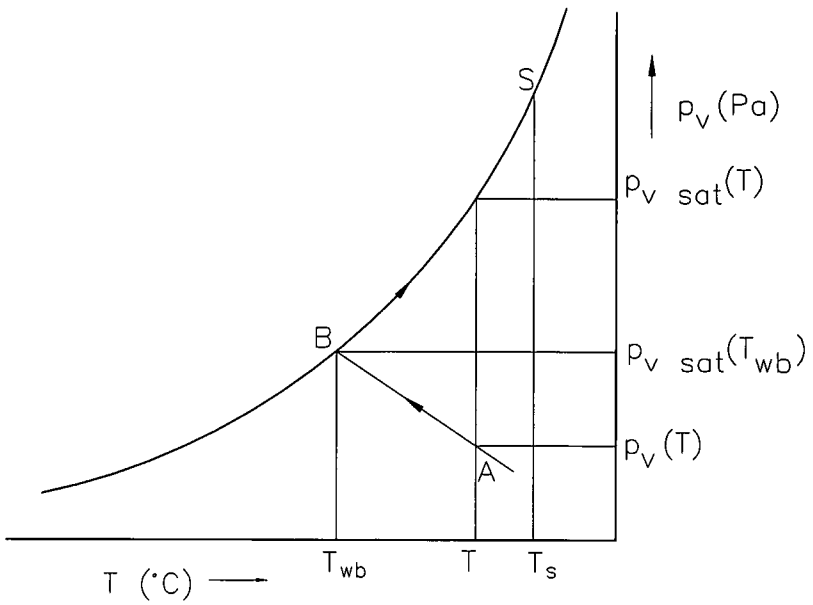

Figure A. 5: Adiabatic and diabatic heat and mass transfer

The atmospheric air flowing over the heated wetted surface is at state A and drybulb temperature T. As a consequence of this unsaturated air flowing over the surface, together with heat and mass transfer, an equilibrium surface temperature T_S is reached. The micro-atmosphere in contact with the wetted surface can be viewed as having undergone an adiabatic saturation process, A-B, whereby the temperature changes from T to the wetbulb temperature, T_{wb}; this is the adiabatic temperature change, and then a process B-S whereby the temperature changes from the wetbulb temperature, T_{wb}, to the final surface temperature T_S; this is the diabatic temperature change.

For the adiabatic process A-B, which proceeds approximately along the wetbulb temperature line, and applying equation (A.53), find the temperature difference between the dry and wetbulb temperatures to be

$$T - T_{wb} = \frac{vpd}{\Delta + \gamma^*} \qquad (A.54)$$

For an adiabatic process the latent heat gain is equal to the sensible heat loss. Applying equation (A.29), find

$$Q_{Latent} / A = Q_c / A = c_{pma} \rho (T - T_{wb}) / r_H \qquad (A.55)$$

Substituting equation (A.54) into equation (A.55), find

$$Q_{Latent} / A = \frac{c_{pma} \rho \, vpd}{(\Delta + \gamma^*)/r_H} \qquad (A.56)$$

The latent heat is equal to the amount of water evaporated times the enthalpy of evaporation, i.e.

$$Q_{Latent} / A = \frac{m_w}{A} i_{fg} \qquad (A.57)$$

Equating equations (A.56) and (A.57), and including the definition of the vapor pressure depression, find

$$Q_{Latent} / A = \frac{m_w}{A} i_{fg} = \frac{c_{pma}\ \rho}{r_H} \left\{ \frac{p_{vSat}(T) - p_v(T)}{\Delta + \gamma^*} \right\} \qquad (A.58)$$

The above result is for adiabatic saturation between a wetted surface and the air flowing over it. However, when radiant heat, I_{net}, is added, this will result in an additional sensible heat transfer, $\frac{\dot{Q}_c}{A}$, and latent heat transfer, $\frac{\dot{m}_w}{A} i_{fg}$, from the surface, now at a temperature T_s, to the air so that

$$I_{net} = \frac{\dot{Q}_c}{A} + \frac{\dot{m}_w}{A} i_{fg} = \frac{c_{pma}\ \rho\ (T_S - T_{wb})}{r_H} + \frac{\dot{m}_w}{A} i_{fg} \qquad (A.59)$$

where the accented terms refer to additional convective and latent heat terms as a result of the heat added.

An expression must be derived for the diabatic temperature change from the wetbulb temperature to the surface temperature as a result of the radiant heat input.

Referring to the Figure below, the following geometrical relationships may be visualized:

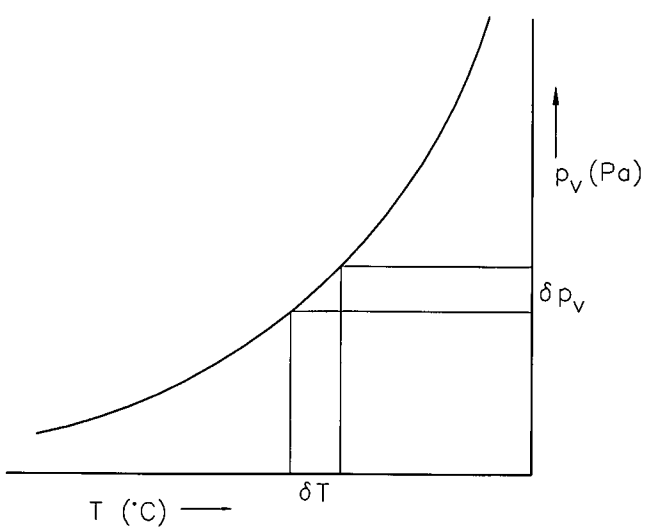

Figure A. 6: Relationships along the saturated vapor curve.

Consider a process along the saturation vapor curve where the curve is viewed as a having a constant slope for a small temperature difference δT.

Applying equations (A.29) and (A.44) the sensible heat (S.H.) and latent heat (L.H.) of saturated air per unit area increases as follows:

$$\text{S.H. increase} = \frac{c_{pma}\ \rho\ \delta T}{r_H} \qquad (A.60)$$

$$\text{L.H. increase} = \frac{c_{pma}\,\rho}{\gamma^{*} r_H}\delta p_v \tag{A.61}$$

Utilizing equation (A.11) find,

$$\text{L.H. increase} = \frac{c_{pm}\,\rho}{\gamma^{*} r_H}\Delta\,\delta T \tag{A.62}$$

Dividing equation (A.62) by equation (A.60), find

$$\frac{\text{L.H.}}{\text{S.H.}} = \frac{\Delta}{\gamma^{*}} \tag{A.63}$$

The total heat increase of the air is the sum of the latent and sensible heat increases,

$$TH = SH + LH \tag{A.64}$$

From equations (A.63) and (A.64), rearranging, find

$$\text{L.H.} = \left(\frac{\Delta}{\Delta + \gamma^{*}}\right)\text{T.H.} \tag{A.65}$$

Similarly

$$\text{S.H.} = \left(\frac{\gamma^{*}}{\Delta + \gamma^{*}}\right)\text{T.H.} \tag{A.66}$$

For a diabatic process along the saturated vapor pressure line the latent heat increase of the atmospheric air will be $\left[\frac{\Delta}{\Delta + \gamma^{*}}\right]$ times the heat added.

When a surface receives additional heat by radiation, I_{net}, the latent heat flux from the surface to the air in contact with it increases by

$$\text{L.H.} = \frac{\Delta}{\Delta + \gamma^{*}} I_{net} \tag{A.67}$$

Where Δ is evaluated at the average of the wetbulb temperature of the air and the surface temperature.

Adding equation (A.67) to (A.58), find

$$(m_v / A)_{total}\, i_{fg} = \frac{c_{pma}\,\rho}{r_H}\left\{\frac{vpd}{\Delta + \gamma^{*}}\right\} + \frac{\Delta I_{net}}{\Delta + \gamma^{*}} \tag{A.68}$$

Substituting $c_{pma}\,\rho / r_H = h_c$ from equation (A.27), find

$$(m_v / A)_{total}\, i_{fg} = h_c\left\{\frac{vpd}{\Delta + \gamma^{*}}\right\} + \frac{\Delta I_{net}}{\Delta + \gamma^{*}} = \frac{h_c\,(vpd) + \Delta I_{net}}{\Delta + \gamma^{*}} \tag{A.69}$$

The areas for convective heat transfer and area receiving radiation are probably not the same since the area for convective heat transfer and hence evapotranspiration due to convective heat transfer could be larger than the leaf area exposed to

radiation: it would be more correct to define the above equation in the following way i.e.

$$(m_v / A)_{total} i_{fg} = \frac{h_c A_e / A\ (vpd) + \Delta I_{net}}{\Delta + \gamma^*} \qquad (A.70)$$

In the application of the above equation in the small tunnel analysis, the subscript "c" of the effective convective heat transfer coefficient will be changed to "cgF" indicating heat transfer between the grass surface, g, and the air or fluid, F.

A_e/A is the ratio of the area for convective heat transfer to the projected horizontal area. Considering that this is an unknown ratio, as a fist approximation the ratio will be considered to be equal to 1.

Since Δ is a function of temperature, the value of Δ in the first term on the right hand side of equation (A.69) is not exactly the same as in the second term. The slope of the saturated vapor curve is for the first term evaluated at the average of the wetbulb and drybulb temperatures, the second at the average of the wetbulb and surface temperatures. Since the Penman equation is to be used when the surface temperature is unknown and since the temperature difference between drybulb - and surface temperatures is, for the application areas of this equation, usually less than 10 K, the average of the known wet- and drybulb temperatures is used for evaluating Δ.

This is the total latent heat flux from an evaporating surface and the equation above is known as the Penman equation. This equation was developed by Penman for evaporation from a water surface whereas the equation developed by Monteith was for evaporation from a canopy of leaves [81MO1] and known as the Penman-Monteith equation. Monteith included the canopy or stomatal resistance in addition to the surface or boundary layer resistance to vapor transfer. However, the Penman equation would apply for a water surface or a water wetted surface such as thoroughly wetted leaf.

By definition $\gamma^* = \gamma\, r_V / r_H \qquad (A.42)$

r_V being the resistance to vapor transfer.

Monteith defined the total resistance to vapor transfer analogous to a situation in an electrical circuit, as the boundary layer and stomatal resistances acting in series so that

$$r_V = r_a + r_s \qquad (A.71)$$

where $r_a \approx r_H$, considering the boundary layer resistance to vapor transfer, r_a, to have the same value as the resistance to heat transfer, r_H.

r_s is the stomatal resistance.

Applying the Monteith approach, find

$$\gamma^* = \left(\frac{r_s + r_H}{r_H}\right)\gamma = (1 + r_s / r_H)\gamma\,. \qquad (A.72)$$

The above formula would apply for vegetation as opposed to that for a water surface. Another difference between evaporation from grass and open water lies in the amounts of short wave radiation reflected. Vegetation has an albedo or reflectivity of about 23 % and water about 5 % so that less energy is available for producing

evaporation from vegetation than from open water. However, on the other hand, for wind blowing across a smooth water surface the convective heat transfer coefficient would be lower than that for the rougher vegetation surface, so that the two effects may counteract one another to a certain extent leading to similar rates of evapotranspiration under the same weather conditions for both surfaces.

A.3 SURFACE TEMPERATURE

An expression for the approximate temperature of a wetted surface may be derived by applying the Penman equation and psychrometric principles to the atmospheric air-wetted surface interaction when the surface is subject to radiation and convection. It is assumed that the air in direct contact with the wetted surface is not only saturated but also at the equilibrium surface temperature [90MO1].

Sensible heat exchange results in a change in the drybulb temperature of the air in direct contact with the wetted surface. Refer to Figure A.7 below and consider the sensible heat exchange for the entire process A-C-S. During the adiabatic process, A-C, there is a loss of sensible heat from the air with a resulting drop in drybulb temperature from A to C. The process A-C may be viewed as two separate processes namely a decrease in sensible heat only followed by an increase in latent heat. The diabatic process, C-S, may be viewed as a gain in sensible heat, process C-D, by the air resulting in a rise in drybulb temperature from T_C to T_D (or T_S), followed by a rise in the latent heat, process D-S.

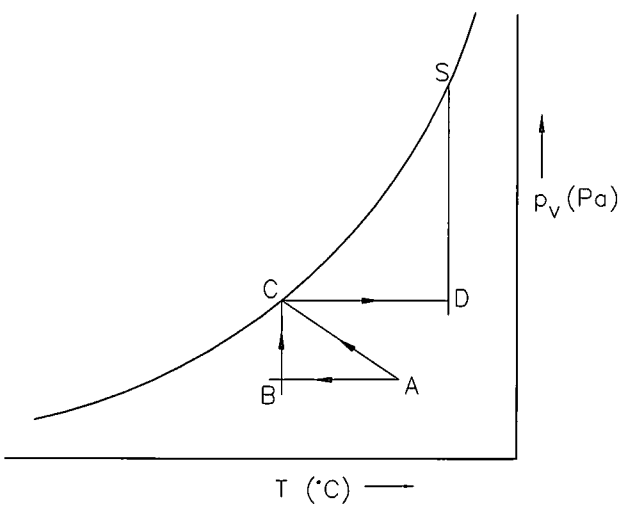

Figure A. 7: Temperature relationships

For the adiabatic saturation process the sensible (or convective) heat loss by the air is equal to the latent heat gain, so that the following may be written viz.

$$\frac{Q_{\text{sensible A-B}}}{A} = \frac{Q_{\text{Latent B-C}}}{A} = (m_v / A)\, i_{fg}\text{, or} \qquad \text{(A.73)}$$

Applying equation (A.29) and writing the temperature difference in terms of the vapor pressure depression according to equation (A.53), find

$$\frac{Q_{\text{sensible A-B}}}{A} = \frac{Q_c}{A} = \frac{c_{pma}\rho}{r_H}\left\{\frac{vpd}{\Delta + \gamma^*}\right\} \qquad \text{(A.74)}$$

During the diabatic process because of the radiant heat, I_{net}, the sensible heat gain according to equation (A.66) is given by

$$S.H. = \left(\frac{\gamma^*}{\Delta + \gamma^*}\right) I_{net} \tag{A.75}$$

Subtracting (A.74) from (A.75), find the net sensible heat gain resulting in a net temperature change from T_A to T_s.

$$Q_c / A = \left\{\frac{\gamma^*}{\Delta + \gamma^*} - \right\} I_{net} - \frac{c_{pma}\rho}{r_H}\left\{\frac{vpd}{\Delta + \gamma^*}\right\} = \frac{\gamma^* I_{net} + (c_{pma}\rho / r_H)\, vpd}{\Delta + \gamma^*} \tag{A.76}$$

assuming an average value for the specific heat and density of the air for the temperature range considered.

Applying equation (A.29) to the sensible heat transfer between the surface at T_S and the air at temperature T_A , find

$$Q_c / A = c_{pma}\rho\ (T_s - T_A)/r_H \tag{A.77}$$

Equating equations (A.76) and (A.77) and simplifying, find an expression for the surface temperature, T_S

$$T_S = T_A + \frac{(\gamma^* r_H / c_{pma}\rho)\, I_{net}}{\Delta + \gamma^*} - \left\{\frac{vpd}{\Delta + \gamma^*}\right\} \tag{A.78}$$

Substituting for the vapor pressure depression equation (A.53) into (A.78), find

$$T_s = T_A + \frac{(\gamma^* r_H / c_{pm}\rho\ )I_{nett}}{\gamma^* + \Delta} - (T_A - T_B) = T_B + \frac{(\gamma^* r_H / c_{pm}\rho\ )I_{nett}}{\gamma^* + \Delta} \tag{A.79}$$

T_A is the drybulb temperature and T_B is the equilibrium temperature reached by the surface for adiabatic saturation. Where the Lewis number is close to unity, T_B would be the wetbulb temperature of the air.

Inserting equation (A.27) into equation (A.79), find

$$T_s = T_B + \frac{\gamma^* I_{nett}}{h_c(\gamma^* + \Delta)} \tag{A.80}$$

I_{net} is the net radiation absorbed by the surface per square meter, and h_c is the effective convective heat transfer coefficient.

Several conclusions follow from the equations (A.78) and (A.80):

- Equation (A.80) shows that the surface temperature will always be above the wetbulb temperature of the air, T_B, when there is solar radiation impinging on the surface.
- This equation also shows that the larger the convective heat transfer coefficient, the smaller will be the temperature rise above the wetbulb temperature for the same level of radiation.

- Note too that the temperature T_B is the wetbulb temperature only for the situation where the resistance of vapor to heat transfer is close to unity i.e. $\gamma^* \approx \gamma$, for $r_v / r_H \approx 1$, since γ is the slope of the wetbulb temperature line.
- When the additional stomatal resistance is taken into account, the adiabatic saturation equilibrium surface temperature, T_B, will be higher than the wetbulb temperature since $\gamma\left(1+\frac{r_s}{r_H}\right) > \gamma$.
- Rewriting equation (A.78) as

$$T_S = T_A + \frac{1}{(\Delta+\gamma^*)}\left(\frac{\gamma^* I_{net}}{h_c} - vpd\right) \qquad (A.81)$$

shows that for situations of low air humidity and hence a high vapor pressure depression, the surface temperature may be below the surrounding air drybulb temperature. During the experiments it was found that at times of low humidity the drybulb temperature of the air at the outlet of the tunnel was indeed lower than at the inlet indicating contact with a surface at a temperature lower than that of the inlet air.

In the application of equation (A.81) to the specific experimental set – up the following symbols are used

$$T_g = T_F + \frac{1}{(\Delta+\gamma^*)}\left(\frac{\gamma^* I_{net}}{h_{cgF}} - vpd\right)$$

A.4 INFRARED HEAT EXCHANGE AND HEAT LOSS TO SOIL

In calculating the net heat energy added to the surface, the heat transfer by longwave or infrared radiation exchange between the surface and, in this case, the glass roof as well as the heat loss to the soil must be taken into account

$$I_{net} = I_{solar} - I_{longwave} - Q_{soil}/A \quad W/m^2 \text{ where} \qquad (A.82)$$

$$I_{longwave}/A = \frac{\sigma\left(T_g^4 - T_R^4\right)}{\frac{1}{\varepsilon_g} + \frac{1}{\varepsilon_R} - 1} \qquad (A.83)$$

The subscripts g and R refer to the grass and glass roof respectively.

The energy lost to the soil (when the grass temperature is higher than the soil temperature; a condition which occurs during daylight except for early morning, is given for hourly or shorter periods by the FAO [04FA1].

$$Q_{soil}/A = 0.1 I_{net} \qquad (A.84)$$

For day or 10 day periods the heat flux to the soil is insignificantly small and then

$$Q_{soil}/A \approx 0 \qquad (A.85)$$

These values are assuming a constant soil heat capacity of 2.1×10^6 J/m^3K. The soil heat capacity is dependent on the moisture content and, as this changes during the day, unless this is monitored, this is the approximation which will be used.

APPENDIX B

LITERATURE STUDY: SOLAR RADIATION AND RADIANT ENERGY EXCHANGED BETWEEN SURFACES

B.0 INTRODUCTION

Most of the energy utilized on earth has as its prime source, solar energy. In order to establish the amount of radiation reaching a vegetated surface under glass, the effect of all the intervening layers must be established.

The *Solar Constant*, I_{sc}, is the earth's energy from the sun per unit time, received outside the atmosphere on a unit area of surface perpendicular to the direction of propagation. This value is 1367 W/m^2 as determined by the World Radiation Centre [91DU1]. Due to the influence of the atmosphere all this energy does not reach the surface of the earth. Solar radiation which eventually reaches the surface of the earth is determined by the interaction with the earth's atmosphere. Scattering and absorption of solar radiation by atmospheric gases on a cloudless day with the sun directly overhead lead to about 1000 W/m^2 reaching the earth's surface [74 NO]. The Solar Constant varies slightly in that the radiation itself emitted by the sun varies (±1.5 %). I_{on}, the extraterrestrial radiation, measured on the plane normal to the radiation, varies according to the day of the year and is given by the following equation.

$$I_{on} = I_{sc}\left(1 + 0.033\cos\frac{360n}{365}\right) \qquad (B.1)$$

where n is the day of the year.

Table B.1 shows the representative "day of the year" for every month.

Table B.1: Representative "Day of the Year" for each month.

Date	N	Date	n
Jan	17	July	198
Feb	47	Aug	228
Mar	75	Sept	258
Apr	105	Oct	288
May	135	Nov	318
June	162	Dec	344

B.1 THE CALCULATION OF THE ZENITH ANGLE, θ_z [91DU1]

For horizontal surfaces, the angle of incidence θ_z, which is also the zenith angle of the sun (i.e. the angle between the beam radiation on a surface and the normal to that surface) is related to the other solar angles by

$$\cos\theta_z = \cos\phi\cos\delta\cos\omega + \sin\phi\sin\delta \qquad (B.2)$$

ϕ is the latitude angle. For Stellenbosch ϕ = 33.93 ° S

δ is the declination, the angular position of the sun at solar noon with respect to the plane of the equator, South negative.

$$\delta = -\left[23.45\sin(360\times\frac{284+n}{368}\right]^{\circ} \quad \text{(B.3)}$$

where n is the Day of the Year (DOY)

ω is the hour angle, the angular displacement of the sun east or west of the local meridian because of earth's rotation at 15 ° per hour, morning negative, afternoon positive.

This is given by the following equation

$$\omega = 15\left[\psi - 12 - \frac{4(L\phi_m - L\phi_l) - EOT}{60}\right]^{\circ} \quad \text{(B.4)}$$

where ψ is the decimal hour after midnight (local time)

$L\phi_m$ the standard meridian for the time zone applicable (30 °E for South Africa) [52NB].

$L\phi_l$ the longitude angle of the geographical location (18.85 °E for Stellenbosch).

B.2 CONVERSION OF LOCAL TIME TO SOLAR TIME

All solar relationships are related to the solar hour and therefore local time needs to be converted to solar time in order to apply the relationships. The following corrections need to be made. Firstly a correction for the difference in longitude between the observer's meridian and the meridian (or longitude) on which the local standard time is based. In South Africa the standard meridian is 30 °E and Stellenbosch is 18.85 °E and the time correction for this is

$$\text{Longitude time correction} = 4(L\phi_m - L\phi)_l = 4(30 - 18.85) = 44.6^{\circ} \text{ [52NB]} \quad \text{(B.5)}$$

The second correction is the Equation of Time, EOT, (in minutes) which varies from day to day and is due to non-uniformity in the movement of the earth along its orbit around the sun.

$$EOT = 2.292\ (0.0075 + 0.18\cos B - 3{,}2077\sin B - 1.4615\cos 2B - 4.089\sin 2B) \quad \text{(B.6)}$$

$$\text{where } B = (n-1)\frac{360}{365} \quad \text{(B.7)}$$

n = day of the year (from Table B.1)

Putting both corrections together, find for Cape Town (Stellenbosch),

$$\text{Solar time} = \text{local time} - 44.6 + EOT \quad \text{(B.8)}$$

B.3 OPTICAL PROPERTIES OF GLAZING

B.3.1 Introduction

The solar characteristics of the glass roof need to be determined in order to ascertain how much of the solar radiation striking the glass roof is absorbed by the grass. In

determining the transmissivity, reflectivity, and absorptivity of solar radiation by glass, all properties will be assumed to be independent of wavelength. According to Duffie [91DU1] this is a reasonable assumption for glass.

B.3.2 Reflection of radiation

Fresnel's equations predict the reflectivity of radiation passing from one medium, with refractive index n_1, to another medium with refractive index n_2 where:

$$\frac{n_1}{n_2} = \frac{\sin\theta_2}{\sin\theta_1} \tag{B.9}$$

where θ_1 and θ_2 are the angles of incidence and refraction respectively.

Note that for a horizontal surface receiving beam radiation the angle of incidence is also equal to the zenith angle, i.e. $\theta_1 = \theta_z$.

For air the refraction index is nearly unity, and for glass the index is 1.526

n_1 = 1 if medium 1 is air and

n_2 = 1.526 for glass as the second medium

so that

$$\sin\theta_2 = \frac{\sin\theta_1}{1.526} = 0.6553\sin\theta_1 \tag{B.10}$$

The reflectivity for radiation is given by

$$r_\perp = \frac{\sin^2(\theta_2 - \theta_1)}{\sin^2(\theta_2 + \theta_1)} \tag{B 11}$$

$$r_{11} = \frac{\tan^2(\theta_2 - \theta_1)}{\tan^2(\theta_2 + \theta_1)} \tag{B.12}$$

For unpolarized light the reflectivity is given by the average of the perpendicular $(r_\perp)$ and parallel $(r_{||})$ components.

$$\rho_b = \frac{I_r}{I_i} = 1/2(r_\perp + r_{11}) \tag{B.13}$$

For a wide range of conditions beam radiation incident at an angle of 60° has the same transmissivity and reflectivity as isotropic diffuse radiation and the equations in the previous paragraph may be applied to diffuse radiation by inserting an angle of 60° for θ_1.

The reflectivity for diffuse radiation may be obtained by setting $\theta_1 = 60°$

Inserting the relevant values into the above equations, find

$$\sin\theta_2 = \frac{\sin\theta_1}{1.526} = 0.6553\sin 60 = 0.5675 \text{ so that}$$

$$\theta_2 = 34.6° \text{ and } \rho_d = 0.0935 \tag{B.14}$$

B.3.3 Transmittance of radiation by glass

Bouguer's Law [91DU1] gives the value of incident radiation transmitted when the absorptivity of the glass has been taken into account as

$$\tau_a = \frac{I_{transmitted}}{I_{incident}} = e^{-\frac{kL}{\cos\theta_2}} \qquad (B.15)$$

where k varies from 4 m^{-1} for water white glass to 32 m^{-1} for green edge of glass. L is the thickness of the glass. From experimentation by Lombard [02LO1], the value of k for the glass used is 13 m^{-1}.

B.3.4 Effective optical properties of glazing

The effective optical properties of glazing are determined when both reflectivity and absorptivity of the glass are taken into account.

The following diagram illustrates the principles involved into deducing an expression for the properties of a glass sheet (diathermous material) of finite thickness where the reflectivity, transmissivity and absorptivity of the glass which has air on both sides are taken into account.

There are two interfaces which cause reflection losses and a portion of the wave striking the second interface is rereflected to the first interface. Figure B.1 shows the effect of reflectivity and transmissivity in a thick semitransparent sheet.

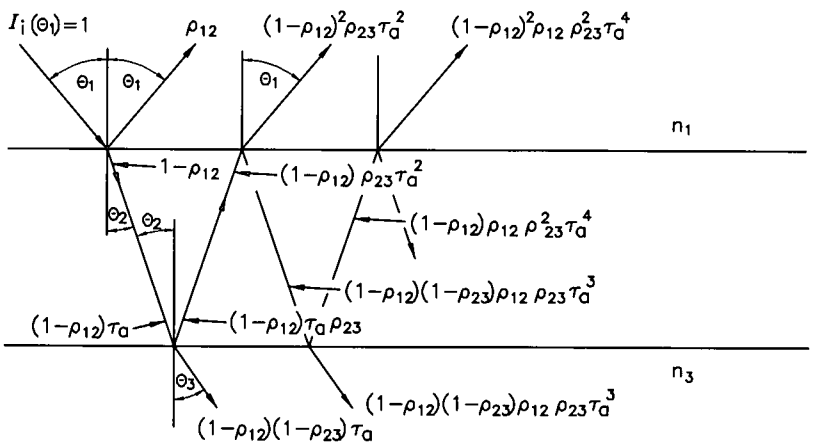

Figure B.1:

Reflectivity and transmissivity of a thick semitransparent sheet (Reproduced from Modest [93 MO1])

Referring to figure B.1 and considering the case for air on both sides of the slab, the following applies:

$n_3 = n_1$

$\theta_3 = \theta_1$

$\rho_{12} = \rho_{23} = \rho$

Defining the effective glass or slab transmissivity for beam radiation as $\tau_{glass,b}$, this can be calculated by summarizing over all the contributions i.e.

$$\tau_{glass,b} = (1-\rho)^2 \tau_a \left[1 + \rho^2 \tau_a{}^2 + \left(\rho^2 \tau_a{}^2\right)^2 + \ldots\ldots\ldots\ldots\ldots\right] = \frac{(1-\rho)^2 \tau_a}{1-\rho^2 \tau_a{}^2} \qquad \text{(B.16)}$$

where τ_a is the transmissivity of glass when absorptivity is taken into account and $\rho^2 \tau_a{}^2 << 1$

The effective reflectivity of the glass for beam radiation, $\rho_{glass,b}$ is similarly given by the expression

$$\begin{aligned} \rho_{glass,b} &= \rho + \rho(1-\rho)^2 \tau_a{}^2 \left[1 + \rho^2 \tau_a{}^2 + \left(\rho^2 \tau_a{}^2\right)^2 + \ldots\ldots\right] \\ &= \rho + \frac{\rho(1-\rho)^2 \tau_a{}^2}{1-\rho^2 \tau_a{}^2} = \rho\left[1 + \frac{(1-\rho)^2 \tau_a{}^2}{1-\rho^2 \tau_a{}^2}\right] \\ &= 0.0935\left[1 + \frac{(1-0.09346)^2 (0.93879)^2}{1-0.0935^2 (0.93879)^2}\right] = 0.16168 \end{aligned} \qquad \text{(B.17)}$$

The glass absorptivity is deduced from the conservation of energy

$$\alpha_{glass,b} + \rho_{glass,b} + \tau_{glass,b} = 1 \qquad \text{(B.18)}$$

Inserting (B.16) and (B.17) into (B.18), find

$$\alpha_{glass,b} = \frac{(1-\rho)(1-\tau_a)}{1-\rho\tau_a} \qquad \text{(B.19)}$$

The effective transmissivity of glass for diffuse radiation may be determined by using equations for beam radiation, but for an angle of incidence of 60°.

$$\tau_a = \frac{I_{transmitted}}{I_{incident}} = e^{-\frac{kL}{\cos\theta_2}}$$

$$\tau_{a,diffuse} = e^{\frac{-13(0.004)}{\cos 34.6}} = 0.9387 \qquad \text{(B.20)}$$

$$\rho_{diffuse} = 0.0935 \text{ so that} \qquad \text{(B.21)}$$

$$\tau_{glass,d} = \frac{(1-\rho)^2 \tau_a}{1-\rho^2 \tau_a{}^2} = \frac{(1-0.0935)^2 0.9387}{1-0.0935^2 0.9387^2} = 0.7775 \qquad \text{(B.22)}$$

The above are all for glass with air on either side.

B.3.5 The effective transmittance-absorptance product, ($\tau\alpha$)

The amount of solar radiation absorbed by the grass is dependent not only on the radiation transmitted through the glass, but also on the absorptivity and reflectivity of the grass.

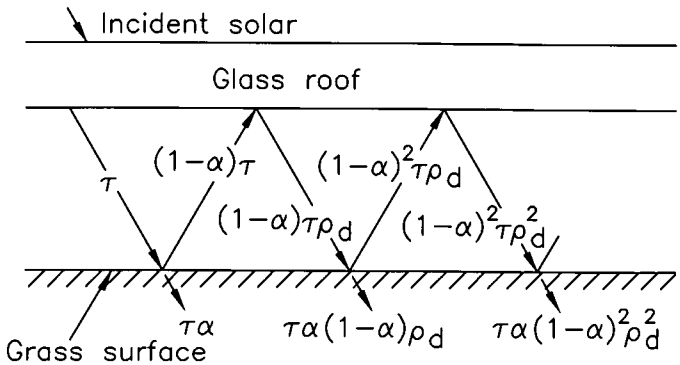

Figure B.2: Absorption of solar radiation by grass surface under glass roof [91DU1].

According to Duffie [91 DU1] and referring to figure B.2, the effective transmissivity-absorptivity product, $(\tau\alpha)$, is given by

$$(\tau\alpha) = \alpha\left[\frac{\tau}{1-(1-\alpha)\rho_d}\right] \tag{B.23}$$

where α is the absorptivity of the lower absorbing surface and ρ is the reflectivity of the upper surface and where ρ_d is the diffuse reflectivity of the upper glass surface.

Substituting equation (B.16) into (B.23), find

$$(\tau\alpha) = \left[\frac{\alpha}{1-(1-\alpha)\rho_d}\right]\left[\frac{(1-\rho^2)\tau_a}{1-\rho^2\tau_a{}^2}\right] \tag{B.24}$$

The absorptivity of the grass is dependent on the albedo of the grass. This is a function of the angle of the radiation striking the grass surface.

For a horizontal surface the angle, θ, (degrees) at which the solar radiation will strike the surface can be written in terms of the zenith angle, namely

$$\theta = 1-\theta_z \tag{B.25}$$

In this application the absorbing surface is the grass and the albedo of grass is given by Dong [92DO1] as

$$\lambda = 0.00158\theta + 0.386\exp(-0.0188\theta) \tag{B.26}$$

The absorptivity of the grass, assuming the transmissivity to be zero, is therefore given by

$$\alpha_g = 1-\lambda \tag{B.27}$$

The above are applicable for beam and diffuse radiation and found by inserting the appropriate angular values so that the total radiation absorbed by the grass is given by

$$I_{absorbed} = [(\tau\alpha)_b + (\tau\alpha)_d]\, I_{transmitted\ through\ glass} \tag{B.28}$$

B.4 INFRARED RADIATION EXCHANGE BETWEEN GREY SURFACES

The radiation exchange between the vegetation and the glass roof is equivalent to that between two infinite parallel plates and is given by

$$q_{rgR} = \frac{\sigma\left(T_2^4 - T_1^4\right)}{\frac{1}{\varepsilon_1} + \frac{1}{\varepsilon_2} - 1} \qquad \text{(B.29)}$$

where ε_1 and ε_2 are the emissivities of the plates (the vegetated surface and glass roof respectively).

For the set-up in the solar tunnel, [63 HS 1], [68 GA 1]

$$\varepsilon_{roof} = 0.9 \text{ to } 0.95 \qquad \text{(B.30)}$$

$$\varepsilon_{grass} = 0.95 \qquad \text{(B.31)}$$

APPENDIX C

LITERATURE STUDY: PLANT PHYSIOLOGY

C.0 INTRODUCTION

In this thesis the evapotranspiration of grass is investigated. Grasses are classified as flowering plants called Angiosperms, and of the branch, monocots.

C.1 DEFINITIONS

C.1.1 PHOTOSYNTHESIS

Photosynthesis is the process whereby light energy is converted into chemical energy. Carbon is fixed into organic compounds. In plants the carbon is stored in the form of carbohydrates and is necessary for almost all life on earth. The carbon comes mainly from the carbon dioxide in the atmosphere. The photosynthetic process may be written as

Carbon dioxide + water+ light = carbohydrate + oxygen

According to Nobel [74NO1] the entire atmospheric content of oxygen is evolved by photosynthesis every few thousand years.

C.1.2 RESPIRATION

Respiration is an energy releasing process during which carbohydrates are oxidized to carbon dioxide. This process may be written as

Carbohydrate + oxygen = carbon dioxide + water + energy

C.1.3 PHOTORESPIRATION

Photorespiration is the process whereby plants start fixing oxygen in the presence of light, causing the plant to lose carbon. As much as 50 % of the carbon fixed is re-oxidized and lost as carbon dioxide. Photorespiration undoes photosynthesis. This process commences when CO_2 drops below a certain concentration level.

C.1.4 TRANSPIRATION

Transpiration is the loss of water vapor mainly through the leaves and stems of plants.

C.2 STRUCTURE AND FUNCTION OF SOME PLANT COMPONENTS

Cells consist of a cell wall that surrounds a plasma membrane which encloses many smaller parts called organelles. Each organelle has its own set of functions. Leaf cells have organelles called chloroplasts which contain, amongst other substances, the chlorophylls which absorb light energy.

The epidermis is the outermost surface of the plant. It has several functions, one of which is gaseous exchange by way of the stomata. The stomata are the only intercellular spaces or pores in the epidermis. Each stoma (Greek – "mouth") is surrounded by two guard cells. Stomata are most abundant on the undersides of leaves. They usually cover less than 1 % of the epidermal surface and yet are very numerous. The leaves of most plants have 10000 to 80000 stomata per square centimeter. When wide open, stomatal pores are usually 3×10^{-6} to 12×10^{-6} m wide

and 10×10^{-6} m to 40×10^{-6} m long [95MO1]. A water molecule has a diameter of 0.00025×10^{-6} m and consequently several thousand water molecules will easily pass even through closed stomata (a closed stoma has a diameter of about 1×10^{6} m). The guard cells around the stomata regulate gas exchange by opening and closing the stomata. The diffusion of carbon dioxide into the leaf for photosynthesis and water loss or transpiration is determined by the stomatal aperture. For every gram of carbon fixed during photosynthesis, the plant loses between 250 g and 600 g of water. Nobel [74NO1] gives 150 g water lost per gram carbon dioxide fixed. The stomata of grasses are dumbbell shaped and as they fill up with water (become turgid) their variable elastic cell walls cause them to change in shape in such a way as to open the stomata.

C.3 MOVEMENT OF WATER IN PLANTS

Plants lose water mainly by transpiration from the leaves. When leaves transpire, water evaporates from the cell walls and escapes to the atmosphere by diffusing into sub-stomatal cavities, through the stomatal pores, through the leaf boundary layer and into the free air stream. Leaves are supplied by an elaborate plumbing system, from the root to the tip of the plant and assembled in such a way that evaporation from cell walls keeps the air spaces between them almost saturated with water vapor even when the leaf is transpiring.

The transpiration-cohesion hypothesis [95MO1] states that water moves from the roots to the top of the plant in an unbroken column in order to replace the water evaporating from the leaves. This loss of water from the cells exposed to the atmosphere by way of the stomata is replaced by that from adjoining cells. Since water is a polar molecule, and coheres, this cohesion produces a high tensile strength ensuring that the water column remains intact. Adhesion to the cell wall prevents gravity from draining the water from the water conducting elements in the plant.

C.4 THE PHOTOSYNTHESIS-TRANSPIRATION COMPROMISE [95MO1]

Land plants are faced with the dilemma of competing demands to take up carbon dioxide for photosynthesis while limiting water loss. Stomatal control couples leaf transpiration to leaf photosynthesis. The chemical reaction of photosynthesis is light driven; so too are the light sensitive guard cells controlling the stomatal apertures. At night when no photosynthesis takes place and therefore no demand for carbon dioxide is made, the stomatal apertures are kept small by the increased turgidity of the guard cells in response to the absence of light. This prevents undue loss of water. When an adequate water supply is available and the solar radiation incident on the leaf favours high photosynthetic activity, the demand for carbon dioxide inside the leaf is large. The stomatal pores are wide open and water loss by transpiration is then substantial. When the stomata are open, water is transported from the soil to the atmosphere purely in response to physical forces.

As far as botanists can ascertain, transpiration does not seem to be essential for plant growth. The water column throughout the plant can remain intact, as it does when the stomata are closed, without transpiration. Minerals can move independently of transpiration. Most botanists today regard transpiration as an "unavoidable evil - unavoidable because of leaf structure, and evil because it desiccates and often injures leaves" [95MO1].

C.5 LIGHT, LEAVES AND PHOTOSYNTHESIS

The absorption of light by molecules proceeds in the following way: only light that is actually absorbed can be effective in producing a chemical change (Grotthus–Draper Law of Photochemistry). Each absorbed photon activates a single molecule (Stark–Einstein Law), and, according to Einstein, all the energy of a light quantum is transferred to a single electron during the absorption event. This electron then moves to a higher energy state. The movement of an electron from one energy state to another can occur only in discrete steps: i.e. the energy state can only have certain specific values. Only light of certain wavelengths will therefore have the proper quantum energy to cause a specific electron to move from one "allowed" state to another. These allowed states are determined by quantum mechanics.

The photosynthetic process is that by which plants utilize the energy of the visible part of the solar spectrum by means of the chlorophylls. Because of the nature of the chlorophylls, one of the chlorophylls absorbs predominantly in the red (wavelength approximately 680 nm) and blue portions (wavelength about 430 nm) of the spectrum. Between 700 nm and 1200 nm the absorption by the leaf is very low and this is important for minimizing the energy input into a leaf, since much global radiation occurs in this interval of the infrared. Beyond 2000 nm the absorption of solar radiation is again high but since very little radiant emission from the sun occurs beyond 2000 nm, this does not result in excessive heating of the leaf. This absorption of solar energy only in specific wavelengths reduces energy input into the leaf and prevents undue rise in leaf temperature. Only about 4 % of the annual solar energy incident on the earth's atmosphere is absorbed by chlorophyll and other photosynthetic pigments. Of this only about 1 % ends up stored by plant cells [74NO1]. Since only a portion of the visible spectrum can be absorbed by the chlorophylls most of the incident energy gets wasted as heat.

C.6 A CLOSER LOOK AT THE TRANSPIRATION OR EVAPORATIVE PROCESS FOR LEAVES

Water vapor moves from the leaf to the atmosphere by diffusion through the stomata. Evaporation of water from a wetted surface, and therefore also transpiration from the leaf, depends on two factors viz.

1. The difference in water vapor concentration between the wetted surface or the leaf air spaces and the external air, and
2. The diffusional resistance of this pathway. In a leaf this consists mainly of the resistance of the stomatal pore r_s and the boundary layer r_a of the air at the surface of the leaf.

The volume of air space inside the leaf is small, whereas the wet surface from which water evaporates within the leaf may be 7 to 30 times the external leaf area [98TZ]. This high ratio of surface area to volume makes for rapid vapor equilibrium inside the leaf. The air spaces of living leaves therefore have a high relative humidity (0.99 for the inner spaces at 25 °C and 0.95 just inside the stomatal pore if the bulk air is at 20 °C and relative humidity of 50 % [74NO1]) and can be viewed without too much error as being saturated. Therefore the water vapor concentration within the leaf spaces, or more correctly in the stomatal pore space, is solely dependent on leaf temperature. The vapor pressure difference between the saturated vapor pressure of water at the leaf temperature and that of the unsaturated surrounding air is the driving potential for transpiration.

Apart from the vapor pressure difference as the driving potential for mass transfer, the amount of mass or water vapor transfer is dependent on the mass transfer coefficient. This in turn is dependent on the resistances of the stomata and the boundary layer. When the wind velocity is high the boundary layer resistance is very much smaller than the stomatal resistance, consequently the stomatal resistance has the greatest control over water loss by the leaf. Meidner [68ME1] confirms this theory by stating that only in still air is this boundary layer resistance significant. The stomatal resistance depends on the geometry, size and spacing of the stomata. The boundary layer resistance will be a function of the leaf dimensions as well as the velocity of the air flowing over it (as reflected by the Reynold's number) [68ME1]. The value for the stomatal resistance to the diffusion of water vapor is calculated by Nobel [74NO1] to be of the order of 30 s/m for a typical grass leaf when the stomata are fully opened as they are in response to sunlight rather than higher temperatures. Nobel gives the range of 50 to 500 s/m stomatal resistance for most mesophytes. Instead of viewing a leaf on its own, Monteith [90MO1] views the entire canopy of leaves and his "short grass" reference crop is based on a bulk canopy stomatal resistance of 70 s/m. The effective convective heat transfer coefficient is linked to this resistance as explained in Appendix D. This bulk canopy stomatal resistance is for unstressed grass exposed to the atmosphere. In the experimental tunnel the resistance should be of the same order except when the grass temperature may rise above 35 °C in which case stomatal closure may be experienced with the accompanying rise in canopy resistance. High air temperatures may have the same effect and when the soil water is depleted, as can happen during the afternoon in the small tunnel, it is expected that the canopy resistance will increase.

APPENDIX D

LITERATURE STUDY: VISCOUS FLUID FLOW AND CONVECTIVE HEAT TRANSFER

D.0 INTRODUCTION

Prandtl in 1904 divided general viscous fluid flow into two regions viz.

1. A boundary layer where viscous effects prevail.
2. Flow outside the boundary layer which is then viewed as inviscid

Viscous effects are confined to a relatively thin layer along a solid surface in which the velocity varies from the free stream value to zero on the body surface. All momentum, heat and mass transfer to or from the surface takes place through this layer. Expressions for the effective convective heat transfer coefficients, firstly between the grass surface and the air flowing over it and secondly between the glass roof and the air, need to be found. There are many analytical expressions for the transfer coefficients for laminar plate and pipe flow and semi-empirical and empirical equations for turbulent flow. These are applicable to the glass roof-air interaction since the glass is viewed as a smooth surface. The heat transfer coefficient between the grass surface and the air however is always problematic as is shown by the large amount of research on the subject [48PE1], [83FR1], [89DJ1], [90MO2], [94AL1], [94AL2] [00SA1], [04FA1]. Various options are investigated and the one chosen which best agrees with the measured data.

In this particular study the flow at the entrance to the tunnel could be viewed as flow over a flat plate, both under the upper glass roof, which is a smooth surface, and over the lower grass surface, which is a rough surface. The flow will begin as laminar changing to turbulent if the tunnel is long enough until the two boundary layers converge and thereafter the flow can be viewed as fully developed duct flow or flow between parallel plates.

D.1 LAMINAR FLOW RELATIONSHIPS OVER A FLAT PLATE

D.1.1 Laminar velocity distribution

The laminar velocity distribution in the boundary layer for flow over a flat plate [89HO1] is given by

$$\frac{u}{u_\infty} = \frac{1}{2}\frac{y}{\delta} - \frac{1}{2}\left(\frac{y}{\delta}\right)^3 \qquad (D.1)$$

where u_∞ is the free stream velocity and u is the velocity at a vertical distance y from the wall.

D.1.2 The boundary layer thickness

The boundary layer thickness, δ, at position x from the leading edge [61RO1] is given by

$$\frac{\delta}{x} = \frac{5}{Re_x^{0.5}} \qquad (D.2)$$

where the local Reynolds number is given by

$$Re_x = \frac{\rho u_\infty x}{\mu} \tag{D.3}$$

D.1.3 The convective heat transfer coefficient

When a fluid flows over a surface at a fluid temperature different from the wall temperature with which it is in contact, heat is transferred by conduction from the wall to the fluid. The local heat flux is given by Fourier's equation i.e.

$$q = -k\frac{\partial T}{\partial y}\Big|_{wall} \tag{D.4}$$

From Newton's Law of cooling

$$q = h_c(T_w - T_\infty) \tag{D.5}$$

where h_c is the convection heat transfer coefficient. T_w and T_∞ are the surface or wall and free-stream temperatures respectively.

Since the heat transferred must be equal, find

$$h_c = \frac{-k(\partial T/\partial y)}{T_w - T_\infty} \tag{D.6}$$

The temperature profile may be obtained from the energy equation applied to boundary layer flow for incompressible fluids [89 HO1].

$$\frac{T - T_w}{T_\infty - T_w} = \frac{3}{2}\frac{y}{\delta_t} - \frac{1}{2}\left(\frac{y}{\delta_t}\right)^3 \tag{D.7}$$

δ_t is the thermal boundary layer thickness.

The hydrodynamic and thermal boundary layer thicknesses are related to each other through the Prandtl number [89HO1] as follows

$$\frac{\delta_t}{\delta} = \frac{1}{1.026}Pr^{-1/3} \tag{D. 8}$$

Substitute (D.8) into (D.7), differentiate this equation with respect to temperature and insert into (D.6). Integrate over the boundary layer thickness at a position x, along the plate and find the local convective heat transfer coefficient to be

$$h_x = 0.332\, k\, Pr^{1/3}\left(\frac{\rho u_\infty}{\mu x}\right)^{1/2} \tag{D.9}$$

The above equation can be non-dimensionalized by multiplying both sides by x/k. Defining the local dimensionless Nusselt number, $Nu_x = \frac{h_x x}{k}$, find

$$\frac{h_x x}{k} = Nu_x = 0.332\, Pr^{1/3}\left(\frac{\rho u_\infty x}{\mu}\right)_x^{1/2} = 0.332\, Pr^{1/3}(Re)_x^{1/2} \tag{D.10}$$

D.1.4 The relation between fluid friction and heat transfer for laminar flow over a flat plate

Stress, τ_w, at a wall may be expressed in terms of the Fanning friction factor, f.

$$\tau_w = f\frac{\rho u_\infty^{\ 2}}{2} \tag{D.11}$$

or employing the Darcy friction factor

$$\tau_w = \frac{f_D}{4}\left(\frac{\rho u_\infty^{\ 2}}{2}\right)$$

Shear stress in laminar flow is expressed by

$$\tau_w = \mu\frac{\partial u}{\partial y}\Big|_{wall} \tag{D.12}$$

Differentiate the equation for the laminar velocity distribution, equation (D.1), substitute into the above equation and integrate over the boundary layer thickness to find

$$\tau_w = \frac{3}{2}\frac{\mu u_\infty}{\delta} \tag{D.13}$$

The boundary layer thickness at a distance, x, from the leading edge is given by equation (D.2). Inserting this equation into equation (D.13) and then into (D.11) find

$$\frac{f}{2} = \frac{0.323}{Re_x^{\,1/2}} \tag{D.14}$$

Utilizing equation (D.10) find,

$$\frac{Nu_x}{Re_x\,Pr} = St = \frac{h_x}{\rho\, c_p\, u_\infty} = 0.332\,Pr^{-2/3}\,Re^{-1/2} \tag{D.15}$$

Therefore,

$$St_x\,Pr^{2/3} = \frac{0.332}{Re^{1/2}} \tag{D.16}$$

But

$$\frac{f}{2} = \frac{0.323}{Re^{1/2}} \equiv \frac{f_D}{8}$$

so that

$$St_x\,Pr^{2/3} \approx \frac{f}{2} \tag{D.17}$$

This is known as the "Reynolds–Colburn Analogy" expressing the relationship between fluid friction and the heat transfer coefficient for laminar flow over a flat plate. The same relationship is valid for turbulent flow over a flat plate, but needs some modification for pipe flow.

All properties are to be evaluated at the arithmetic mean temperature of the wall and the fluid.

D.2 TURBULENT FLOW OVER A FLAT PLATE

D.2.1 Velocity distribution in turbulent flow

From the application of the Logarithmic-Overlap Law [91WH], find the velocity distribution for turbulent flow to be

$$\frac{u}{u^*} = \frac{1}{\kappa}\ln\frac{yu^*}{\nu} + B \qquad \text{(D.18)}$$

The value of κ and B were found by experimentation to be 0.41, the von Kármán constant, and 5.0 respectively. The above equation is known as "The Logarithmic-Overlap law" and approximates nearly the entire velocity profile for a decreasing pressure.

D.2.2 Thickness of the turbulent boundary layer

The boundary layer thickness for turbulent flow may be obtained from the velocity profile outside the laminar sublayer. The difficulty of evaluating the boundary layer thickness is overcome by application of Prandtl's "Seventh Power Law' profile (1921) as quoted by White [91WH1] where by analogy with pipe flow data he suggested

$$\frac{u}{u_\infty} \approx \left[\frac{y}{\delta}\right]^{1/7} \qquad \text{(D.19)}$$

The thickness of the turbulent portion of the boundary layer as found from the expression above is equivalent to the thickness of the entire boundary layer since the laminar sublayer is so thin. The laminar sublayer extends over less than 2% of the profile.

When the boundary layer follows a laminar growth pattern up to the critical Reynolds number of 5.0×10^5 and beyond, the thickness is given by

$$\frac{\delta}{x} = 0.381\,Re_x^{-1/5} - 10256\,Re^{-1}, \text{ for } Re_{crit} \le Re \le 10^7 \qquad \text{(D.20)}$$

White [91 WH 1] gives the Prandtl equation (1921) for the thickness of the turbulent boundary layer as

$$\frac{\delta}{x} \approx \frac{0.16}{Re_x^{1/7}} \qquad \text{(D.21)}$$

D.2.3 Turbulent heat transfer for flow over a flat plate based on fluid-friction analogy

Turbulent heat transfer is analogous to turbulent momentum transfer just as in the case of laminar flow. For turbulent flow over flat plates Schlichting [89HO1], gives the local skin-friction coefficient a distance x from the beginning of the plate as

$$f_x = 0.0592\,Re_x^{-1/5} \text{ for } 5\times10^5 \le Re \le 10^7 \qquad \text{(D.22)}$$

The average friction coefficient for a flat plate with a laminar boundary layer up to the critical Reynolds number [89HO1] is given by

$$\bar{f} = \left(\frac{0.074}{Re_L^{1/5}}\right) - \frac{A}{Re_L} \quad \text{for} \quad Re_{crit} < Re_L < 10^7$$

$$A = 1050 \quad \text{for} \quad Re_{critical} = 3.0 \times 10^5 \qquad \text{(D.23)}$$
$$A = 1700 \quad \text{for} \quad Re_{critical} = 5.0 \times 10^5$$

For the turbulent boundary layer on a flat plate Prandtl in 1927 [89HO1] gave

$$f_x = \frac{0.027}{Re_x^{1/7}} \qquad \text{(D.24)}$$

An alternative was provided by Kestin and Petersen in 1962 [94WH1] viz.

$$f_x \approx \frac{0.455}{\ln^2(0.06\,Re_x)} \qquad \text{(D.25)}$$

Schlichting (1979) [91WH 1] recommends the following curve-fit relationship for the friction coefficient for flow past a rough plate.

$$f_x \approx \left[2.87 + 1.58 \log_{10}\left(\frac{x}{\varepsilon}\right)\right]^{-2.5} \qquad \text{(D.26)}$$

where ε is the average roughness height.

Applying the fluid-friction analogy, from equation (D.27) find

$$St_x\, Pr^{2/3} = \frac{f}{2} = 0.0296 Re_x^{-1/5} \quad \text{for} \quad 5 \times 10^5 < Re_x < 10^7 \qquad \text{(D.27)}$$

Over the entire laminar-turbulent boundary layer Holman [89HO1] gives the average Nusselt number and therefore the convective heat transfer coefficient as

$$\overline{Nu_L} = \frac{\overline{hL}}{k} = Pr^{1/3}\left(0.037 Re_L^{0.8}\right) - 850 \qquad \text{(D.28)}$$

For constant heat flux the local Nusselt number is about 4% higher than that for the isothermal surface [89HO1] so that

$$Nu_x = 1.04 Nu_x \Big|_{T_w = constant} \qquad \text{(D.29)}$$

The flow in the tunnel starts off as flow over a flat plate until the boundary layers above the grass and below the glass meet each other and thereafter it can be viewed as flow in a tube. In this investigation the pressure drop over the tunnel was measured and a friction factor determined.

The pressure drop over the tunnel is measured for various air velocities and the Darcy friction factor determined. The method is not strictly accurate since the flow is not adiabatic but is the best under the circumstances. Nobel [74NO1] gives a value of between 30 s/m and 100 s/m as the boundary layer resistance for a leaf. When the effective convective heat transfer coefficients are determined, the boundary layer resistance may be calculated, and compared with the values of Nobel as a guideline to judge whether the values are reasonable.

For turbulent flow in smooth pipes where ε/d is very small Haaland [83HA1] proposes

$$f_D = 2.7778\left[\log_{10}\left\{\frac{7.7}{Re}\right\}^3 + \left\{\frac{\varepsilon/d}{3.75}\right\}^{3.33}\right]^{-2}$$

Where roughness influences the friction factor significantly, Haaland gives an equation to fit data for the transition through to fully turbulent pipe or duct flow

$$1/\sqrt{f_D} = -1.8\log\left[\frac{6.9}{Re_d} + \left(\frac{\varepsilon/d}{3.7}\right)^{1.11}\right] \qquad (D.30)$$

D.3 EMPIRICAL EFFECTIVE CONVECTIVE HEAT TRANSFER COEFFICIENT

The theoretical and experimental work of Burger and Kröger [06BU1] for determining the convective heat transfer coefficient between a smooth horizontal surface and the natural environment has led to the following dimensionless expression for a surface subject to a uniform heat flux. The expression takes both the wind velocity, v_w, and the friction factor into account. For a surface temperature greater than the air temperature the following correlation applies to a heated surface facing upward and subject to a uniform heat flux:

$$h_{cgF}\left[\frac{\mu T}{g(T_{oq}-T_a)c_p k^2 \rho^2}\right]^{1/3} = 0.2106 + v_w(C_f/2)\left[\frac{\rho T}{\mu g(T_{oq}-T_a)}\right]^{1/3} \qquad (D.31)$$

Alternately,

$$h_{cgF} = \frac{0.2106 + v_w C_f/2\,(\rho T/\mu g \Delta T)^{1/3}}{(\mu T/g\Delta T c_p k^2 \rho^2)^{1/3}}\ W/m^2K \text{ for } (T_{oq} - T_a) = \Delta T \geq 4°C \text{ where} \qquad (D.32)$$

$C_f/2 = 0.0026$ for a smooth surface

h_{cq} the effective convective heat transfer coefficient

C_f the surface friction coefficient

T_{oq} and T_a the surface and air temperatures respectively, and T the average of the two

When the temperature difference is less than 4 °C, Kröger suggests

$$h_q = 3.87 + 0.0022\left(\frac{V\rho c_p}{Pr^{2/3}}\right) \qquad (D.33)$$

also for a smooth surface.

For most natural surfaces with low conductivity the uniform heat flux expression is applicable.

D.4 EXPERIMENTAL DETERMINATION OF THE FRICTION FACTOR

D.4.1 Pressure drop measurements for a single grass length at varying velocities

The pressure drop over the tunnel for a single grass length was measured for various air velocities and the Darcy friction factor determined.

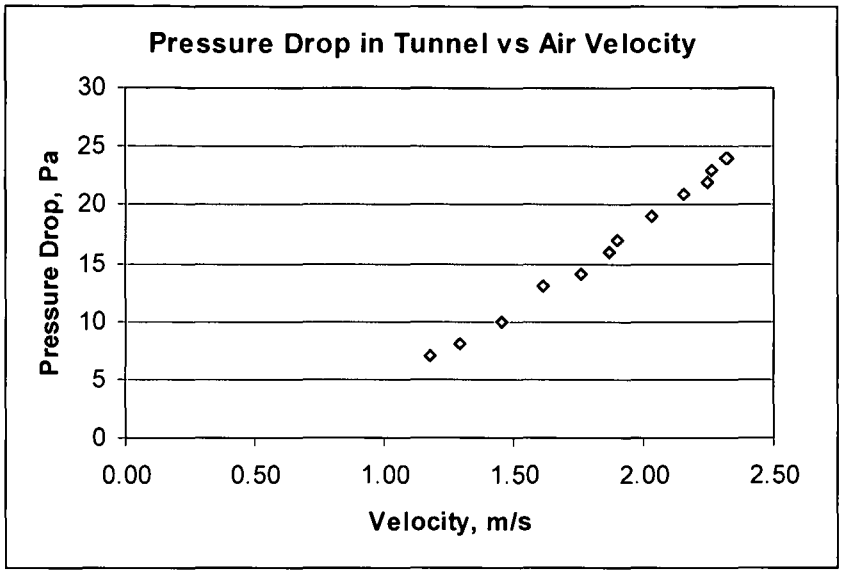

Figure D.1: Pressure drop over the tunnel vs. the velocity of the air

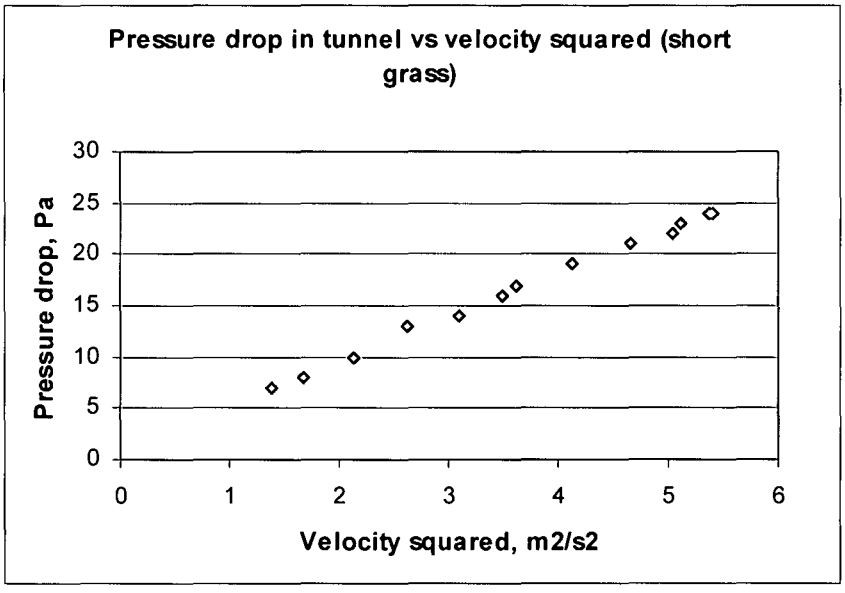

Figure D.2: Pressure drop over the tunnel vs. the velocity of the air squared

The pressure drop over the tunnel may be utilized to determine the Darcy friction coefficient. Considering the definition of the Darcy friction factor [82ST01]

$$f_D = \frac{\Delta p}{\frac{\rho V^2}{2}\frac{L}{d}} \qquad (D.34)$$

For duct flow of a non-circular section the Reynolds number is based on the hydraulic diameter defined as

$$d_e = \frac{4 \times \text{flow} \quad \text{area}}{\text{wetted} \quad \text{perimeter}} \approx 2\,H \qquad \text{(D.35)}$$

Where H is the height of the tunnel. For turbulent flow between parallel plates, the friction factor is most accurately predicted when an effective diameter, D_{eff}, equal to 0.64 times the hydraulic diameter, d_e is employed [83HA1].

The distance between the grass surface and the glass roof is about 0.15 m and the tunnel is 1m wide so that an effective diameter can be calculated:

$$D_e = \frac{4 \times 0.15}{2.3} = 0.26 \text{ m and}$$

$$D_{eff} = 0.64 \times 0.26 = 0.1664 \text{ m}$$

Utilizing this approach, find L/d = 16/0.1664 = 96.15, and from this the Darcy friction coefficient may be calculated. Table D. 1 shows the values.

Table D.1: Darcy friction factor from pressure drop measurements

Velocity in tunnel, m/s	Pressure drop in tunnel, Pa	Darcy friction factor
1.175	7	0.105633
1.292	8	0.099848
1.456	10	0.098277
1.616	13	0.103714
1.759	14	0.09427
1.867	16	0.095633
1.902	17	0.097905
2.031	19	0.095964
2.156	21	0.094123
2.244	22	0.091023
2.261	23	0.093735
2.314	24	0.093381
2.322	24	0.092739

The average Darcy friction factor is found to be $f_D = 0.095885$

The Fanning friction factor is found from

$$f_{fanning} = f_D / 4 = 0.095885 / 4 = 0.023971$$

so that

$$f_{fanning} / 2 = 0.011986$$

This value is then used in the Burger-Kröger equation in the place of the surface friction factor.

D.4.2 The effect of grass length on the pressure loss over the grass

Investigation of the pressure drop measured over the grass in the tunnel on consecutive days in February shows that the pressure drop varied by a factor 3 over a period of 11 days. On the 6th of February the pressure drop for an air velocity in the

tunnel of 2 m/s was 5 Pa whereas on the 17th of the same month the pressure drop for the same velocity was 14.7 Pa. This has implications for the computation of the effective convective heat transfer coefficient. The Darcy friction factor changed from 0.03 for shorter grass to 0.0882 for longer grass. This implied a change in value of the effective convective heat transfer coefficient for more or less the same set of circumstances from 14.83 W/m^2K to 36.08 W/m^2K. It was endeavoured to gather and use data collected when the grass was recently mowed in order to eliminate a complicating parameter. Note too that in turbulent flow, the canopy or stomatal resistance is the controlling parameter so that the effective convective heat transfer coefficient plays a smaller role in the total resistance effect.

D.5 THE FAO PENMAN-MONTEITH EQUATION APPROACH

The exchange of heat and water vapor between a stand of vegetation and the atmosphere is a much more complex process than the corresponding exchange at the surfaces of individual leaves. The value of the heat transfer coefficient is problematic. Much research has gone into even finding a model for a single leaf and several empirical equations are available.

Since a large number of empirical methods have been developed over the past 50 years, in May 1990, the FAO adopted a hypothetical reference canopy described by a Penman-Monteith equation. All calculations have been revised by Allen et al. [94AL1].

The convective heat transfer coefficient is written in terms of a resistance; r_H [90MO1], where

$$h_c = \frac{c_{pma}\rho}{r_H} \tag{D.36}$$

The FAO Penman-Monteith equation approach [04FA1] gives the aerodynamic resistance to heat transfer r_H, for a surface as

$$r_H = \frac{\ln\left[\frac{z_m - d}{z_{om}}\right]\ln\left[\frac{z_h - d}{z_{oh}}\right]}{k^2 u_z} \text{ s/m} \tag{D.37}$$

where

z_m is the height of wind measurement

z_h is the height of humidity measurement

d is the zero plane displacement height

z_{om} is the roughness length governing momentum transfer

z_{oh} is the roughness length governing heat and vapor transfer

k is von Karman's constant and equal to 0.41

u_z is the windspeed at height z

The standardized height of measurement is usually 2 m so that $z_m = z_h = 2$ m.

For the hypothetical canopy which has a fixed height of 0.12 m, find the boundary layer resistance to be

$$r_H = \frac{\ln\left[\frac{2-2/3(0.12)}{0.123(0.12)}\right]\ln\left[\frac{2-2/3(0.12)}{(0.1)0.123(0.12)}\right]}{0.41^2 u_z} = \frac{208}{u_z}\,s/m \qquad (D.38)$$

The above equation must be investigated to see whether it can be applied in this particular situation in that the average temperature, humidity and velocity are determined remote from the grass surface itself and a measurement height is therefore not applicable.

As far as the vapor transfer is concerned, Monteith defines the total resistance as the sum of the stomatal and aerodynamic or boundary layer resistance acting in series. For a grass reference crop, the FAO calculates the value of the stomatal resistance with the stomata open and the grass unstressed as approximately 70 s/m. The problem with working with a living crop is that the height of the grass differs between cuttings, the approximate LAI as defined by Allen et al. (1989) may range between 1.9 to 3.6 leading to a variation in bulk surface resistance depending on the structural characteristics and regrowth. This is evident from the variation in measured pressure drop over the grass for the same air velocity.

APPENDIX E

MASS TRANSFER FOR A WATER WETTED SURFACE

E.0 INTRODUCTION

The Concept of Enthalpy Potential

The use of the enthalpy potential between unsaturated air in contact with a water wetted surface where both sensible and latent heat or mass transfer take place simultaneously enables one to determine the direction in which the total or net heat transfer takes place in addition to calculating an approximate value thereof. The difference in dry bulb temperature between the surface and the air leads to the transfer of sensible heat, the direction being determined by the direction of the temperature difference. For the latent heat or mass transfer it can be assumed that the air directly in contact with the wetted surface will be saturated and have a partial vapor pressure equal to the saturation vapor pressure at the temperature of the water. The difference in the partial vapor pressure of the free stream air and the saturated vapor pressure at the temperature of the wetted surface leads to the transfer of mass. This transfer of mass causes a thermal energy transfer as well; either the latent heat of evaporation or that of condensation. An approximate expression for the total heat transfer can be deduced from the transfer equations and psychrometric principles.

The rate of sensible heat transfer from the water surface at temperature T_s to the air at T_a is given by

$$dQ_s = h_c dA(T_s - T_a) \qquad (E.1)$$

where h_c is the convective heat transfer coefficient. In terms of a resistance, $r_H = \frac{c_{pma}\rho}{h_c}$ (A.27) so that

$$dQ_s = \frac{c_{pma}\rho}{r_H} dA(T_s - T_a) \qquad (E.2)$$

E.1 Water wetted surfaces

For water surfaces with air flowing over them, the enthalpy potential concept may be applied in order to determine the convective heat transfer coefficient when the ratio of the resistance to vapor and heat transfer is close to unity since the only resistance to vapor transfer is the boundary layer resistance. This does not apply to leaves where the ratio of the resistance to vapor and the resistance to heat transfer is not close to unity since the stomatal resistance is included.

The rate of latent heat transfer from the saturated atmosphere at the water surface to the free stream air is from equations (A.28) and (A.30)

$$dQ_L = dA\, h_D(\chi_s - \chi_a) i_{fg}$$

Where χ is the vapor density and h_D the vapor transfer coefficient and i_{fg} the latent heat of evaporation at the wetted surface temperature.

Since $\chi = \rho q$ (A.31), $q = 0.622\frac{p_v}{p}$ (A.39) and $h_D = 1/r_v$ (A.28), find

$$dQ_L = \frac{dA\,\rho\,0.622(p_s - p_a)i_{fg}}{p r_v} \tag{E.3}$$

From equation (A.4) $w = 0.622\frac{p_v}{p_a}$ and $p_a + p_v = p$ with $p_v <<< p$, find

$$dQ_L \approx \frac{dA\,\rho(w_s - w_a)i_{fg}}{r_v} \tag{E.4}$$

The total heat, dQ_T, transferred will be

$$\frac{dQ_s + dQ_L}{dA} = \frac{dQ_T}{dA} = \frac{c_{pma}\rho}{r_H}(T_s - T_a) + \frac{\rho(w_s - w_a)i_{fg}}{r_v}$$

For fully developed turbulent flow over a flat plate, the heat and mass transfer resistances are nearly equal so that $r_H \approx r_v$ (A.48)

$$\frac{dQ_T}{dA} \approx \frac{\rho}{r_H}\left[c_{pma}(T_s - T_a) + i_{fg}(w_{,s} - w_a)\right] \tag{E.5}$$

The enthalpy of the free stream air and the saturated air at the temperature of the water surface can each be written as

$i_a = c_{pa}T_a + w_a\left(i_{wfg@0°C} + c_{pv}T_a\right)$ (A.14), and (E.6)

$$i_s = c_{pa}T_s + w_s\left(i_{wfg@0°C} + c_{pv}T_s\right). \tag{E.7}$$

Subtracting equation (E.6) from (E.7), find

$$i_s - i_a = c_{pa}T_s + w_s\left(i_{wfg@0°C} + c_{pv}T_s\right) - c_{pa}T_a - w_a\left(i_{wfg@0°C} + c_{pv}T_a\right)$$

Since $c_{pma} = c_{pa} + w\,c_{pv}$, find

$$i_s - i_a = c_{pma}(T_s - T_a) + (w_s - w_a)\left(i_{fg@0°C}\right) \tag{E.8}$$

Comparing equations (E.5) and (E.8) and noting that i_{fg} is a weak function of temperature, equation (E.5) may be approximated as

$$\frac{dQ_T}{dA} \approx \frac{\rho}{r_H}(i_s - i_a) \tag{E.9}$$

Substituting $r_H = \frac{c_{pma}\rho}{h_c}$, find

$$\frac{dQ_T}{dA} \approx (h_c / c_{pma})(i_s - i_a) \tag{E.10}$$

This equation illustrates that the total heat transfer per unit area is proportional to the difference in enthalpy between saturated air at the temperature of the water surface, and the enthalpy of the free stream air flowing over the wetted surface. This

difference in enthalpy is known as the enthalpy potential and is the driving force for total heat transfer, giving the direction and value when the convective heat transfer coefficient is known.

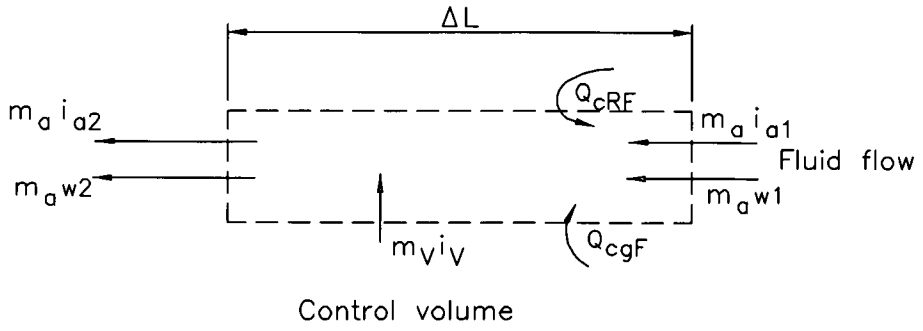

Figure E.1 Mass and heat transfer in a control volume

Consider the control volume shown in Figure E.1 and where the grass surface in the tunnel is replaced by a water surface and states 1 and 2 refer to the inlet and outlet states of the tunnel. The total energy exchanged between the fluid, air, and the water surface, Q_T, is be given by

$$Q_T + Q_{cRF} + m_a i_{a1} = m_a i_{a2}$$

or

$$Q_T = m_a(i_{a2} - i_{a1}) - Q_{cRF} \qquad \text{(E.11)}$$

Applying equation (E.10) for the entire length of the tunnel and the log mean enthalpy potential, LMPE (similar to applications for parallel flow heat exchangers where the LMTD is used), find

$$Q_T \approx A_{tunnel}(h_c / c_{pma})LMEP = A_{tunnel} h_c \frac{(i_{s1} - i_{a1}) - (i_{s2} - i_{a2})}{c_{pma} \ln[(i_{s1} - i_{a1})/(i_{s2} - i_{a2})]} \qquad \text{(E.12)}$$

From which

$$h_c \approx c_{pma} \frac{m_a(i_{a2} - i_{a1}) - Q_{cRF}}{A_{tunnel} \times LMEP}, \text{ W/m}^2\text{K} \qquad \text{(E.13)}$$

where i_a is the enthalpy of the free stream air and i_s the enthalpy of saturated air at the water surface temperature.

APPENDIX F

PROPERTIES OF FLUIDS [04KR1]

F.1 The thermophysical properties of dry air from 220 K to 380 K at standard atmospheric pressure (101325 N/m^2).

Density:

$$\rho_a = p_a/(287.08\ T),\ kg/m^3 \qquad (F.1.1)$$

Specific heat [82AN1]:

$$c_{pa} = 1.045356 \times 10^3 - 3.161783 \times 10^{-1}\ T + 7.083814 \times 10^{-4}\ T^2 - 2.705209 \times 10^{-7}\ T^3,\ J/kgK \qquad (F.1.2)$$

Dynamic viscosity [82AN1]:

$$\mu_a = 2.287973 \times 10^{-6} + 6.259793 \times 10^{-8}\ T - 3.131956 \times 10^{-11}\ T^2 + 8.15038 \times 10^{-15}\ T^3,\ kg/sm \qquad (F.1.3)$$

Thermal conductivity:

$$k_a = -4.937787 \times 10^{-4} + 1.018087 \times 10^{-4}\ T - 4.627937 \times 10^{-8}\ T^2 + 1.250603 \times 10^{-11}\ T^3,\ W/mK \qquad (F.1.4)$$

F.2 The thermophysical properties of saturated water vapor from 273.15 K to 380 K

Vapor pressure [65GO1]:

$$p_v = 10^z,\ N/m^2 \qquad (F.2.1)$$

$$z = 10.79586(1 - 273.16/T) + 5.02808\ \log_{10}(273.16/T) + 1.50474 \times 10^{-4}\ [1 - 10^{-8.29692\{(T/273.16)\ -1\}}] + 4.2873 \times 10^{-4}\ [10^{4.76955(1-273.16/T)} -1] + 2.786118312$$

Specific heat:

$$c_{pv} = 1.3605 \times 10^3 + 2.31334T - 2.46784 \times 10^{-10}T^5 + 5.91332 \times 10^{-13}T^6,\ J/kgK \qquad (F.2.2)$$

Dynamic viscosity:

$$\mu_v = 2.562435 \times 10^{-6} + 1.816683 \times 10^{-8}T + 2.579066 \times 10^{-11}T^2 - 1.067299 \times 10^{-14}T^3,\ kg/ms \qquad (F.2.3)$$

Thermal conductivity [82AN1]:

$$k_v = 1.3046 \times 10^{-2} - 3.756191 \times 10^{-5}T + 2.217964 \times 10^{-7}T^2 - 1.111562 \times 10^{-10}T^3,\ W/mK \qquad (F.2.4)$$

Vapor density [70UK1]:

$$\rho_v = -4.062329056 + 0.10277044T - 9.76300388 \times 10^{-4}T^2 + 4.475240795 \times 10^{-6}T^3 - 1.004596894 \times 10^{-8}T^4 + 8.9154895 \times 10^{-12}T^5,\ kg/m^3 \qquad (F.2.5)$$

Temperature:

$$T = 164.630366 + 1.832295 \times 10^{-3}\ p_v + 4.27215 \times 10^{-10}\ p_v^2 + 3.738954 \times 10^3 p_v^{-1} - 7.01204 \times 10^5\ p_v^{-2} + 16.161488\ \ln p_v - 1.437169 \times 10^{-4}\ p_v\ \square n\ p_v,\ [K] \qquad (F.2.6)$$

Enthalpy of saturated water vapor

$$i_v = 2.5013\times10^6 + c_{pv}(T-273.15)$$
$$= 2.5013\times10^6 + (1.3605 \times 10^3 + 2.31334T - 2.46784 \times 10^{-10}T^5 + 5.91332 \times 10^{-13}T^6)(T-273.15) \quad J/kg \qquad (F.2.7)$$

F.3 The thermophysical properties of mixtures of air and water vapor

Density [72AS1]:

$$\rho_{av} = (1 + w)\,[1 - w/(w + 0.62198)]\,p_{abs}/(287.08T), \text{ kg air-vapor/m}^3 \qquad (F.3.1)$$

Specific heat [78FA1]:

$$c_{pav} = (c_{pa} + wc_{pv})/(1 + w), \text{ J/K kg atmospheric air} \qquad (F.3.2a)$$

or the specific heat of the air-vapor mixture per unit mass of dry air

$$c_{pma} = (c_{pa} + wc_{pv}), \text{ J/K kg dry air} \qquad (F.3.2b)$$

Dynamic viscosity [54GO1]:

$$\mu_{av} = (X_a\mu_a M_a^{0.5} + X_v\mu_v M_v^{0.5})/(X_a M_a^{0.5} + X_v M_v^{0.5}), \text{ kg/ms} \qquad (F.3.3)$$

where M_a = 28.97 kg/mole, M_v = 18.016 kg/mole, $X_a = 1/(1 + 1.608\ w)$ and

$X_v = w/(w + 0.622)$

Thermal conductivity [57LE1]:

$$k_{av} = (X_a k_a M_a^{0.33} + X_v k_v M_v^{0.33})/(X_a M_a^{0.33} + X_v M_v^{0.33}), \text{ W/mK} \qquad (F.3.4)$$

Humidity ratio [82JO1]:

$$w = \left(\frac{2501.6 - 2.3263(T_{wb} - 273.15)}{2501.6 + 1.8577(T - 273.15) - 4.184(T_{wb} - 273.15)}\right)\left(\frac{0.62509p_{vwb}}{p_{abs} - 1.005p_{vwb}}\right)$$
$$-\left(\frac{1.00416(T - T_{wb})}{2501.6 + 1.8577(T - 273.15) - 4.184(T_{wb} - 273.15)}\right), \text{ kg/kg dry air} \qquad (F.3.5)$$

Enthalpy:

$$i_{av} = [c_{pa}\,(T - 273.15) + w\{i_{fgwo} + c_{pv}\,(T - 273.15)\}]/(1 + w), \text{ J/kg air-vapor} \qquad (F.3.6a)$$

or the enthalpy of the air-vapor mixture per unit mass of dry air

$$i_{ma} = c_{pa}(T - 273.15) + w[I_{fgwo} + c_{pv}(T - 273.15)], \text{ J/kg dry air} \qquad (F.3.6b)$$

where the specific heats are evaluated at (T + 273.15)/2 and the latent heat i_{fgwo} = 2.5016 x 10^6 J/kg.

The calculation of the vapor pressure given the drybulb temperature and the wetbulb temperature

$$p_v = p_{v_{sat\,@\,twb}} - \frac{(t_{db} - t_{wb})(P_{abs} - P_{v_{sat\,@\,twb}})}{1550 - 1.44t_{wb}} \qquad (F.3.7)$$

F.4 The thermophysical properties of saturated water liquid from 273.15 K to 380 K

Density:

$$\rho_w = (1.49343 \times 10^{-3} - 3.7164 \times 10^{-6}T + 7.09782 \times 10^{-9}T^2 - 1.90321 \times 10^{-20}T^6)^{-1}, \text{ kg/m}^3 \quad \text{(F.4.1)}$$

Specific heat:

$$c_{pw} = 8.15599 \times 10^3 - 2.80627 \times 10T + 5.11283 \times 10^{-2}T^2 - 2.17582 \times 10^{-13}T^6, \text{ J/kgK} \quad \text{(F.4.2)}$$

Dynamic viscosity [82AN1]:

$$\mu_w = 2.414 \times 10^{-5} \times 10^{247.8/(T - 140)}, \text{ kg/ms} \quad \text{(F.4.3)}$$

Thermal conductivity:

$$k_w = -6.14255 \times 10^{-1} + 6.9962 \times 10^{-3}T - 1.01075 \times 10^{-5}T^2 + 4.74739\ 10^{-12}T^4, \text{ W/mK} \quad \text{(F.4.4)}$$

Latent heat of vaporization:

$$i_{fgw} = 3.4831814 \times 10^6 - 5.8627703 \times 10^3T + 12.139568T^2 - 1.40290431\ 10^{-2}T^3, \text{ J/kg} \quad \text{(F.4.5)}$$

GLOSSARY

ALBEDO - the reflection coefficient of a natural surface for the whole solar spectrum.

EVAPOTRANSPIRATION AND TRANSPIRATION. The first term refers to evaporation from both the vegetation and from the soil; transpiration refers to evaporation from plants or vegetation only.

LEAF AREA INDEX - the plan area of leaves per unit ground area – for grasses this value is about 7.5 [74NO1].

MICROMETEOROLOGY. This is the measurement and analysis of the state of the atmosphere near the surface of the earth. The main objective is to provide a quantitative framework for describing processes such as heat and mass transfer in terms of mechanisms such as radiative exchange, turbulent diffusion, and the conduction of heat in soil [75MO1].

REFERENCE TOTAL EVAPORATION, E_0, as defined by Doorenbos and Pruitt (1977) The rate of total evaporation of an extended surface of an 80 mm-150 mm tall grass cover of uniform height actively growing, completely shading the ground and not deficient in water or nutrients [88DJ].

MAXIMAL TOTAL EVAPORATION, E_m, as defined by Bouchet and Robelin (1969) and later endorsed by Wright (1981) as the rate of evapotranspiration from an incomplete actively growing vegetative cover under which the root zone soil water content corresponds to field capacity or greater and the soil surface is saturated. According to Rosenberg evapotranspiration et al. (1983) this is governed entirely by atmospheric driving forces.

BASAL PLANT EVAPORATION E_{vm}, [Wright, 1981] differs from the above in that the soil surface is so dry that comparatively insignificant soil evaporation occurs. This is thus evaporation only from the vegetated surface.

CROP COEFFICIENT CONCEPT (Doorenbos and Kassam, 1979) relate maximum total evaporation to reference total evaporation

$$k_m = E_m / E_0$$

BASAL CROP COEFFICIENT (Wright, 1981)

$$k_{vm} = E_{vm} / E_0$$

ATMOSPHERIC EVAPORATION DEMAND, (AED) [88 DJ] defined by de Jager in 1988

The upper limit of the atmospheric demand for water from a natural surface and is to be defined as follows

"the water vapor transfer to the atmosphere required to *sustain* the energy balance of a *given* vegetative surface (crop) in its present growth stage when the water status of its root zone permits unhindered plant evaporation and the water status of the top 150 mm of soil equals its *current* value."